

附件 4

编号	
----	--

## 江苏省成人高等教育精品资源共享课程建设

# 申报书

学 校 名 称 南京农业大学

课 程 名 称 兽医微生物学

课 程 层 次 高起专 高起本 专升本

课 程 类 型 公共基础课 专业基础课 专业课

课 程 基 础 校级精品 省级精品

所属一级学科名称 农学

所属二级学科名称 动物医学类

课程负责人 姚火春

申报日期 2016年12月08日

江苏省教育厅 制

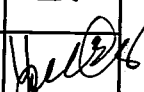
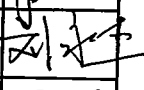
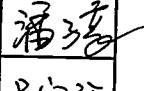
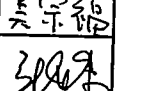
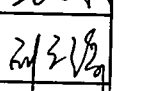
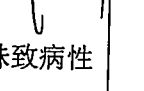
## 填写要求

1. 本表限用 A4 纸双面打印。
2. 表格文本中外文名词第一次出现时，要写清全称和缩写，再次出现时可以使用缩写。
3. 涉密内容不填写，有可能涉密和不宜大范围公开的内容，请在说明栏中注明。
4. 课程所属学科按教育部规定的方式分类：本科专业按照《普通高等学校本科专业目录》（教高〔2012〕9号）填报，专科专业按照《普通高等学校高等职业教育（专科）专业目录》（教职成〔2015〕10号）填报。
5. 本表中填写内容可以根据情况进行扩充；本表有关统计内容截止时间为 2016 年 8 月 31 日。

## 1. 课程负责人

基本信息	课程负责人	姚火春	性 别	男	出生年月	1963.02
	最终学历	博士	专业技术职务	教授		
	学 位	博士	行政职务	实验室中心主任		
	所在院系	动物医学院				
	通信地址(邮编)	210000				
	研究方向	兽医微生物与免疫学				
教学情况	近五年来讲授的					
	主要课程名称	课程类型	周学时	届数	学生总人数	
	兽医微生物学	专业基础课	3	3	63	
	现代免疫学	专业课	2	3	50	
	高级免疫学	专业课	2	3	85	
	分子免疫学	专业课	2	3	86	
承担研究生微生物以及免疫学相关课程试验设计教学指导督导工作。承担本科生课程设计和毕业论文共计 6 篇，研究生毕业论文 12 篇。						
学术研究	教学研究课题：					
	1、兽医微生物学国家精品资源共享课程建设，教育部，2013.7-2018.12					
	教学表彰/奖励：1、2013-2014 学年第二学期教学质量综合评价优秀奖					
	2、武汉回盛奖教金，2013 年					
代表性本科教学成果：						
1、2013 年国家精品资源共享课程 负责人						

## 2. 课程团队

	姓名	性别	出生年月	单位	职称	学科专业	在课程建设中承担的工作	签字
主讲教师、教学辅助人员基本信息	姚火春	男	1963.02	南京农业大学	教授	预防兽医学	主持	
	刘永杰	女	1972.03	南京农业大学	教授	预防兽医学	参与	
	潘子豪	男	1980.07	南京农业大学	讲师	预防兽医学	参与	
	吴宗福	男	1981.08	南京农业大学	副教授	预防兽医学	参与	
	张炜	男	1976.11	南京农业大学	教授	预防兽医学	参与	
	刘广锦	女	1984.08	南京农业大学	讲师	预防兽医学	参与	
教师队伍整体素质	<p>说明教师队伍知识结构、年龄结构、配置情况。</p> <p>(1) 主持南京农业大学创新性实验实践教学项目两项：“细菌性病原临床分离株致病性判定法则的应用实践”和“如何建立动物细菌病原的分子生物学鉴定系统”</p> <p>(2) 参加国家精品课程建设与教学，2009年被教育部授予国家级精品课程。</p> <p>(3) 参加国家精品资源共享课建设与教学。</p> <p>(4) 指导本科毕业论文，8-15人/年，共计12人次获优秀本科毕业论文。</p> <p>(5) 项目成员主编面向21世纪课程教材《兽医微生物学实验指导》(第二版)参编普通高等教育农业部“十二五”规划教材《兽医微生物学》第三版至第五版</p> <p>(6) 近5年指导37项SRT研究，其中1项获国家大学生实验计划资金资助、2项获江苏省大学生科技创新基金资助，其他项目均由南京农业大学专项资金资助。</p> <p>(7) 获勃林格殷格翰、恒丰强、希尔思、生泰尔、回盛、森楠等奖教金12人次。</p>							
学术研究与教学研究	<p>1. Sun M, Ma J, Wang Y, Huochun YAO et al. Genomic and epidemiological characteristics provide new insights into the phylogeographical and spatiotemporal spread of porcine epidemic diarrhea virus in Asia[J]. Journal of clinical microbiology, 2015, 53(5): 1484-1492.</p> <p>2. Ma J, Bao Y, Sun M, et al. Two functional type VI secretion systems in avian pathogenic Escherichia coli are involved in different pathogenic pathways[J]. Infection and immunity, 2014, 82(9): 3867-3879.</p> <p>3. Chen T, Huang Q, Li Z, et al. Construction and characterization of a Streptococcus suis serotype 2 recombinant expressing enhanced green fluorescent protein[J]. PloS one, 2012, 7(7): e39697.</p> <p>4. Ma J, Sun M, Bao Y, et al. Genetic diversity and features analysis of type VI secretion systems loci in avian pathogenic Escherichia coli by wide genomic scanning[J]. Infection, Genetics and Evolution, 2013, 20: 454-464.</p> <p>5. Rong J, Zhang W, Wang X, et al. Identification of candidate susceptibility and resistance genes of mice infected with Streptococcus suis type 2[J]. PloS one, 2012, 7(2): e32150.</p>							

### 3. 教学理念与课程设计

#### 3-1 教学理念

本课程在课程设计、实施过程中的教学理念。

##### 1. 教学平台积极转型和升级，实现资源共享和知识传播

根据兽医微生物课程群中不同的具体课程，本科生课程：兽医微生物学、水产微生物学和动物病原学等，以及研究生课程兽医细菌学及细菌学技术等，根据本学科的发展，追踪学科前沿，不断更新教学内容，使学生在掌握本课程基本理论体系的同时，了解学科研究进展，丰富知识体系。

##### 2. 启发学生主动学习相关知识，充分利用课堂时间与学生交流

不断强化实践教学环节，着力培养学生的课程感知与实践动手能力。在课程组织教学的过程中，指导学生预习相关教学内容，让学习带着相关问题去尝试解答相应问题。在正式上课时，与学生交流他们预习的成果，并指导他们解答不懂的部分。

##### 3. 课程设计、课程论文和自学课程安排

在兽医课程学习的不同阶段，安排内容新颖，有知识点，学生感兴趣的小课程论文 2-3 篇，如某些理论的来历和背景；或以班为单位，或自由组合，或个人完成，激励主动学习的兴趣和能力，并鼓励他们用 PPT 的方式讲解出来，通过实践提升了学生对本课程的兴趣，提高了教学效果。

##### 4. 外文文献或国外原版教材引入教学

积极开展“双语教学”一直是高等教育改革的主要内容，也是培养国内人才具有“国际竞争力”的有效手段，本课程教学中，在动医强化班实行双语教学。普通班则尽可能增加用英语对专业术语及概念的解释，积极鼓励学生选读国外原版教材的个别章节或部分，培养了学生对文献理解和对教材直接信息理解的能力，提高学生外语水平，促进学生趋近学科前沿。

##### 5. 注重实验课的教学工作

兽医微生物学这门课的教学包括理论教学和实验技术两大部分，为了适应学科高速发展和多学科交叉的趋势，理论教学部分，教学内容的组织上注意不断补充学科发展前沿内容，先后两次对教学大纲进行了修订。增加了一些的病原、新的检测方法等内容，使教学内容具有鲜明的时代性和实用性。

学生对现在的微生物学实验教学反应良好，但因为现在的微生物学实验涉及先进的分子生物学诊断技术较少，针对这种状况，先后申请了两个校级“创新性实验实践教学项目”，强化分子生物学诊断技术在兽医微生物学中的应用，促进了学生对新技术的掌握，取得了良好的效果。

##### 6. 网络课程的更新和完善

根据国家级精品资源共享课程建设的要求，对原有的教学录像进行了更新，采用了高清画面录制，并上传到相关网站，实现了资源的共享。

## 3-2 课程总体设计

### 培养方案:

本学科中与兽医微生物相关的课程较多,包括兽医微生物学、水产微生物学、动物病原学、兽医细菌学及细菌学技术等,所以课时安排不能一概而论,总体来说以总论讲述占60-70%,各论占30-40%的课时讲述。

### 第一部分 绪论

主要介绍微生物的概念、种类和特点,微生物学的发展历程以及兽医微生物学的研究内容。

### 第二部分 细菌学总论,共六章

第一章 细菌的形态及构造、第二章 细菌的生长繁殖和生态、第三章 消毒与灭菌  
第四章 细菌的感染与致病机理、第五章 细菌的遗传变异、第六章 细菌的分类与命名

这一部分主要介绍细菌的一般规律,如形态、结构、生理、致病机制、遗传变异和分类命名等。

### 第三部分 细菌学各论,包含七章

第一章 革兰氏阳性球菌、第二章 肠杆菌科、第三章 弧菌科、第四章 巴氏杆菌科及相关属  
第五章 革兰氏阴性需氧菌、第六章 革兰氏阳性无芽胞杆菌、第七章 分支杆菌属及相似属

这一部分主要在掌握细菌学一般规律基础上介绍不同种属细菌的形态染色、培养特性、生化特性、毒力因子与致病性、微生物学诊断等。

### 第四部分 其他原核细胞型微生物与真菌

这一部分主要掌握螺旋体、霉形体、立克次氏体、衣原体等原核细胞型微生物及真菌的分类、培养特性与致病特点。

### 第五部分 病毒学总论,共五章

第一章 病毒的结构、第二章 病毒的复制、第三章 病毒的遗传与进化、第四章 病毒与细胞的相互作用、第五章 病毒的致病机理

这一部分主要介绍病毒的一般规律,如形态结构、复制特点、遗传变异、病毒的培养及对细胞的致病作用、致病机制等。

### 第六部分 病毒学各论,包含十章

第一章 双股DNA病毒、第二章 单股DNA病毒、第三章 具有反转录过程的病毒、第四章 双股RNA病毒、第五章 单负股病毒目、第六章 分节段的负股RNA病毒、第七章 套式病毒目、第八章 其他正股RNA病毒、第九章 朊病毒、第十章 噬菌体

## 4. 课程建设规划

### 4-1 课程建设目标及预期效果

#### 教学目标:

(1) 专业教育 主要针对动物医学、动物药学、水产养殖专业在校学生,作为线下教学的有效补充,起到替代或半替代线下课程教学的作用,为学生预习和复习该课程提供有效的平台,所设的习题和试题可以自我检验学习效果。

(2) 科普教育 主要面对社会大众,普及动物传染病和人畜共患病病原的知识,提高公众传染病预防意识和能力。

#### 受众定位:

(1) 高等院校兽医相关专业学生 该部分人群是本课程的主要听众,他们具有兽医学相关的理论基础和一定的实践能力。

(2) 普通社会大众 希望了解兽医微生物相关知识的群体,可通过专题讲座、诊断检索系统、图片资料等获得其所关心的知识。

#### 学习效果:

(1) 提高学习兴趣 该课程相比其他课程知识点分散,比较难学,本课程提供了大量图片、模式图、录像、动画、视频,使得学生对微生物病原的认识更加直观和生动。

(2) 提高学习效果 课程资源提供了各个章节的知识点、重点和难点,提高了学习效率。此外,课程资源中提供了大量的练习题和试题,能及时检验学生学习效果。

#### 预期成果:

(1) 建成学校在线精品课程。

(2) 培养青年教师 4-5 名。

### 4-2 课程建设实施步骤、方法

#### 绪言

1. 微生物与微生物学、2. 微生物学的发展历程、3. 兽医微生物学的研究任务

习题要点: 微生物的概念、种类及特点。

本章重点、难点: 微生物的概念、种类和特点。

教学要求: 了解: 微生物学的发展历程。理解: 兽医微生物学的研究任务及研究意义。掌握: 微生物的概念、种类和特点。

#### 第二章 细菌的形态及构造

##### 第一节 细菌的形态

细菌大小、细菌的基本形态和形态变化、细菌的群体形态。

习题要点: 细菌大小的衡量单位。什么是菌落? 了解菌落有何实际意义?

##### 第二节 细菌的基本结构

包括细胞壁、细胞膜、核体、细胞质的结构、化学组成及功能;革兰氏染色原理。习题要点: 绘出细菌的结构示意图。比较革兰氏阳性菌和阴性菌的细胞壁结构及化学组成的差异。

革兰氏染色的方法和原理。

### 第三节 细菌的特殊结构

包括荚膜、S层、鞭毛、菌毛和芽孢的结构、化学组成及功能

习题要点：荚膜的概念及其功能；S层、鞭毛、菌毛和芽孢的结构及功能？

本章重点、难点：细菌个体形态与群体形态；革兰氏阳性和阴性菌细胞壁结构；细菌特殊结构及功能。

教学要求：了解：细菌的特点和基本形态。理解：细菌的革兰氏染色原理及其与细胞壁结构的关系。掌握：菌落的概念；革兰氏阳性和阴性菌细胞壁结构和化学组成上的差别；细菌特殊结构的功能。

## 第三章 细菌的生长繁殖

### 第一节 细菌细胞的代谢过程

#### 1. 物质摄取

单纯扩散、促进扩散、主动运输和基团转位的特点。

#### 2. 生物合成

#### 3. 聚合作用、4. 组装

习题要点：形成细菌个体的代谢过程有何特点？

### 第二节 细菌的生长繁殖

#### 1. 细菌个体的生长繁殖、2. 细菌群体的生长繁殖

习题要点：何谓细菌的生长曲线？有何意义？试述细菌生长的各个期的特点。

### 第三节 细菌的人工培养

培养基的概念、种类及其不同的用途、影响因素等。

习题要点：培养基有哪些种类？如何正确选用合适的培养基？

本章重点、难点：细菌群体生长繁殖的规律；培养基的种类及其用途。

教学要求：了解：细菌细胞的代谢过程。理解：细菌生长繁殖的规律。掌握：细菌生长曲线的四个时期及特点；培养基的种类及其不同用途。

## 第四章 消毒与灭菌

消毒、灭菌、防腐、无菌操作、抑菌、杀菌等概念。

### 第一节 物理因素对微生物的影响

1. 温度 低温：菌种保存；高温：干热灭菌和湿热灭菌法。 2. 辐射 可见光、阳光、紫外线和电离辐射。 3. 干燥 4. 超声波 5. 微波 6. 滤过

习题要点：何谓灭菌、消毒、防腐？举例比较它们的异同。试述影响微生物的主要物理因素及其实用价值。试述各种热力灭菌法的方法原理及其主要用途。试述滤过除菌的概念及其应用。

### 第二节 化学因素对微生物的影响

消毒剂和化学治疗剂的种类及影响因素。

习题要点：比较消毒剂、防腐剂、化学治疗剂的杀菌机制。



### 第三节 生物因素对微生物的影响

#### 1. 抗生素、植物杀菌素、细菌素

#### 2. 噬菌体

习题要点：抗生素、植物杀菌素、细菌素和噬菌体等生物因素的抗菌、杀菌机制。

本章重(难)点：物理因素影响微生物生长繁殖的机制及如何选取合适的方法进行灭菌或抑菌。

教学要求：了解：常见的影响微生物生长的化学和生物因素；噬菌体的生物学特性。理解：各种物理因素的杀菌机理。掌握：消毒、灭菌、防腐的概念。物理因素对微生物的影响，特别是干热灭菌和湿热灭菌法的种类及适用范围。

### 第五章 细菌的感染与致病机理

#### 第一节 细菌的致病性和毒力

##### 1. 细菌致病性的确定 2. 细菌毒力的测定

习题要点：经典的和基因水平的柯赫法则的内容。半数致死量和半数感染量的概念及其测定。

#### 第二节 细菌的毒力因子及分泌系统

##### 1. 侵袭力 2. 毒素 3. III型分泌系统

习题要点：细菌定植、干扰宿主防御机制和在体内扩散的原理及过程。内毒素与外毒素的区别。

本章重点、难点：细菌致病性的确定及致病过程中涉及的毒力因素。

教学要求：了解：细菌的致病过程。理解：柯赫法则的内容及意义。掌握：半数致死量的概念；内毒素与外毒素的区别。

### 第六章 细菌的遗传变异

#### 第一节 细菌遗传的物质基础

##### 1. 基因组 2. 质粒 3. 转座因子 4. 毒力岛

习题要点：概述细菌遗传变异的物质基础。质粒有哪些主要特点及类型？试述毒力岛的概念及特点。

#### 第二节 基因突变

##### 1. 细菌变异的类型 2. 诱发细菌变异的方法

习题要点：常见的细菌变异有哪些类型？如何诱发细菌的变异？

#### 第三节 基因转移与重组

##### 1. 转化 2. 转导 3. 接合

习题要点：细菌的基因转移重组主要方式有哪几种？转化、转导、接合的概念。

#### 第四节 细菌遗传变异研究的实际意义

习题要点：研究细菌遗传变异在理论上有何重要意义及应用价值？

本章重点、难点：转化、转导和接合的概念及原理。

教学要求：了解：细菌常见的变异机制；质粒的种类与特点。理解：转化、转导和接合的原理及细菌变异研究的实际意义。掌握：转化、转导和接合的概念。

### 第七章 细菌的分类与命名

## 第一节 细菌的分类地位

习题要点：细菌的分类阶元。根据什么指标来确定？

## 第二节 细菌的命名

习题要点：举例说明细菌的拉丁文名的命名规则及中文译名特点。

## 第三节 细菌的鉴定

习题要点：目前用什么技术进行细菌分类鉴定？试述动物致病菌的鉴定程序。

本章重点、难点：细菌的分类地位及命名原则。

教学要求：了解：细菌的分类地位及分类体系。理解：细菌的鉴定方法。掌握：细菌的拉丁文双命名规则；世界公认的细菌分类体系。

## 第八章 革兰氏阳性球菌

### 第一节 葡萄球菌属

习题要点：试述金黄色葡萄球菌的形态染色特点。金黄色葡萄球菌常致动物哪些疾病？试述金黄色葡萄球菌可产生的毒素和酶及其致病作用。试述鉴定致病性金黄色葡萄球菌的主要试验。

### 第二节 链球菌属

习题要点：阐述链球菌区分血清群的依据及各型的主要致病特性。链球菌各型的溶血表现及在血清肉汤中的生长特征如何？试比较猪链球菌与马链球菌兽疫亚种的致病性及微生物学诊断中的鉴别要点。

本章重点、难点：葡萄球菌属和链球菌属细菌的主要生物学特性及致病因子。

教学要求：了解：葡萄球菌属和链球菌属细菌的主要特性。理解：金黄色葡萄球菌的致病性及致病机制；链球菌属的兰氏分群。掌握：代表菌种的形态染色特点、培养特性、致病因子及微生物学诊断。

## 第九章 肠杆菌科

### 第一节 埃希菌属

习题要点：概述动物致病性大肠杆菌的分类、诊断以及毒力因子基本特性和致病机理。

### 第二节 沙门菌属

习题要点：概述沙门菌目前的分类方案及其致病性。试述沙门菌的毒力因子的种类及其基本特点

本章重点、难点：大肠杆菌和沙门菌的主要生物学特性及鉴别诊断。

教学要求：了解：肠杆菌科的致病性及致病机制。理解：大肠杆菌和沙门菌的培养特性和主要生化特性。掌握：大肠杆菌和沙门菌的鉴别诊断要点。

## 第十章 弧菌科

### 第一节 弧菌属

习题要点：副溶血弧菌如何检测？它有何致病意义？试述鱼类弧菌病的病原及其主要特点。

### 第二节 气单胞菌属

习题要点：试述运动性气单胞的概念及其意义。嗜水气单胞菌有哪些重要的毒力因子？其特

性如何？

本章重点、难点：副溶血弧菌和嗜水气单胞菌的毒力因子及诊断要点。

教学要求：了解：副溶血弧菌和鳃弧菌的致病性。理解：嗜水气单胞菌的致病性及毒力因子。

掌握：嗜水气单胞菌的的微生物学诊断要点。

## 第十一章 巴氏杆菌科及相关属

### 第一节 巴氏杆菌属

习题要点：多杀性巴氏杆菌形态染色特点、培养特性。如何进行多杀性巴氏杆菌病的微生物学诊断？

### 第二节 里氏杆菌属

习题要点：简述鸭疫里氏杆菌的名称和分类的变化及微生物学诊断要点。

### 第三节 嗜血杆菌属

习题要点：试述猪胸膜肺炎放射杆菌的致病对象及毒力因子。什么是巧克力培养基？为什么分离培养嗜血杆菌常用它？引致猪格氏病及鸡传染性鼻炎的病原菌有何特点？

本章重点、难点：代表菌种的形态染色特点、培养特性、致病因子及微生物学诊断。

教学要求：了解：嗜血杆菌的致病性及致病机制。理解：嗜血杆菌的形态染色特点、培养特性。掌握：多杀性巴氏杆菌和鸭疫里氏杆菌的形态染色特点、培养特性、微生物学诊断要点。

## 第十二章 革兰氏阴性需氧菌

习题要点：布氏杆菌属有哪些成员？有何致病特点？试述布氏杆菌病的微生物学诊断要点及注意事项。

本章重点、难点：布氏杆菌的形态染色特点、培养特性、致病因子及微生物学诊断。

教学要求：了解：布氏杆菌属的分类。理解：布氏杆菌属致病性。掌握：布氏杆菌的主要培养特性和诊断方法。

## 第十三章 革兰氏阳性无芽胞杆菌

### 第一节 李氏杆菌属

习题要点：产单核细胞李氏杆菌的形态和染色特性是什么？简述单核细胞李氏杆菌的主要毒力因子及致病机理。

### 第二节 丹毒杆菌属

习题要点：试述猪丹毒杆菌的培养及致病特点。猪丹毒杆菌的微生物学诊断要点有哪些？阐明产单核细胞李氏杆菌与猪丹毒杆菌的区别。

本章重点、难点：代表菌种的形态染色特点、培养特性、致病因子及微生物学诊断。

教学要求：了解：产单核细胞李氏杆菌的致病特点。理解：猪丹毒杆菌的生物学特性及鉴定程序。掌握：李氏杆菌与猪丹毒杆菌的鉴别诊断。

## 第十四章 革兰氏阳性产芽胞杆菌

### 第一节 芽胞杆菌属

习题要点：试述炭疽芽胞杆菌的致病性及其毒素的作用机制。如何进行炭疽的微生物学诊断，采取检验材料应注意哪些事项？

## 第二节 梭菌属

习题要点：试述产气荚膜梭菌菌型的划分和各型菌所致疾病及微生物学诊断方法。产气荚膜梭菌的公共卫生意义何在？破伤风梭菌的主要特性和致病特点。

本章重点、难点：代表菌种的形态染色特点、培养特性、致病因子及微生物学诊断。

教学要求：了解：炭疽杆菌和产气荚膜梭菌的致病特点；破伤风梭菌的主要特性和致病特点。

理解：炭疽杆菌的抗原结构与致病因素。掌握：鉴别炭疽杆菌的重要生物学特性；产气荚膜梭菌的主要生物学特性。

## 第十五章 分支杆菌属及相似属

分支杆菌属：结核分支杆菌、牛分支杆菌、禽分支杆菌

习题要点：试述分枝杆菌的染色特性与细胞壁的结构的关系。结核分枝杆菌的致病作用有何特点。如何检测动物是否感染结核杆菌。

本章重点、难点：代表菌种的形态染色特点、培养特性、致病因子及微生物学诊断。

教学要求：了解：分支杆菌属特性及分类。理解：分支杆菌属细菌的抗酸染色及致病特点。

掌握：分支杆菌属细菌的形态染色、培养特性和诊断方法。

## 第十六章 病毒的结构

### 第一节 病毒的结构特征

习题要点：病毒颗粒的基本结构如何？画出模式图。病毒的核衣壳的对称型有哪些？各有什么特点？

### 第二节 病毒的化学组成

习题要点：阐述病毒核酸及蛋白的特点。如何确定病毒是否有囊膜？其依据何在？

### 第三节 病毒的分类

习题要点：简述病毒分类的机构和标准。脊椎动物的分类现状如何？

本章重点、难点：病毒基本结构、化学组成及特点。

教学要求：了解：病毒的分类命名；病毒的对称型。理解：病毒的化学组成及其特点。掌握：病毒基本结构及各部分结构的功能。

## 第十七章 病毒的复制

### 第一节 吸附、穿入与脱壳

习题要点：何谓病毒的 MOI 及一步生长曲线？解释病毒的复制周期及隐蔽期。举例说明病毒的特异性吸附与细胞的受体的关系。

### 第二节 生物合成

习题要点：病毒的生物合成有何特点？举例说明。

### 第三节 组装与释放

习题要点：什么是病毒的自我组装？有囊膜的病毒如何成熟与释放？

本章重点、难点：病毒增殖的一般规律及不同核酸类型病毒的复制过程。

教学要求：了解：病毒增殖的一般规律。理解：不同类型病毒核酸的复制特征。掌握：病毒复制的概念和双股 DNA、单正股 RNA、单负股 RNA 及反转录病毒的增殖过程。

## 第十八章 病毒的遗传与进化

### 第一节 突变

习题要点：病毒的基因组变异有哪些类型？举例说明病毒表型变异的特点及应用价值。什么是缺损型干扰突变？有何特点和意义？

### 第二节 诱变

习题要点：定点诱变如何进行？

### 第三节 基因重组

习题要点：举例说明分子内重组与重配的结果与意义。

本章重点、难点：病毒发生变异的机制。

教学要求：了解：常见的病毒变异现象。理解：病毒发生变异的机制。掌握：掌握 DI 突变株的概念和特点。

## 第十九章 病毒与细胞的相互作用

### 第一节 病毒的细胞培养

习题要点：细胞培养与动物或鸡胚相比，培养病毒各有什么优缺点？细胞有哪些类型？

### 第二节 病毒与细胞的相互作用

习题要点：什么是细胞病变？其表现形式及涉及的细胞结构如何？什么是空斑试验？有什么用途？阐述包涵体的类型、本质及诊断意义。介绍干扰素的性质、类型及作用。

本章重点、难点：细胞培养的优点、类型，病毒致细胞病变效应及干扰素抗病毒作用特点及机制等。

教学要求：了解：病毒动物接种、鸡胚接种和细胞培养的优点。理解：病毒培养的意义及病毒致细胞病变的机理。掌握：细胞培养的类型、常见的细胞病变效应以及干扰素抗病毒作用机制。

## 第二十章 双股 DNA 病毒

### 第一节 痘病毒科

习题要点：痘病毒的结构与形态有何特征？举例说明痘病毒感染的宿主谱的类型。对绵羊致病的有哪些痘病毒？如何鉴别？研究鸡痘病毒有何意义？

### 第二节 非洲猪瘟病毒科

习题要点：试述非洲猪瘟病毒形态、基因组结构及传播方式的特点。

### 第三节 疱疹病毒科

习题要点：阐述疱疹病毒科的分类及共同特点。如何解释伪狂犬病感染猪及其它动物的不同后果？鸡马立克病毒的致病特点如何？

### 第四节 腺病毒科

习题要点：试述腺病毒的结构特点。犬传染性肝炎病毒、减蛋综合征病毒的致病特点。

本章重点、难点：病毒科的特点及代表病毒的主要特性及微生物学诊断。

教学要求：了解：绵羊痘病毒、山羊痘病毒、鸡痘病毒、口疮病毒的主要特征、培养特性、致病性、诊断、防制。理解：非洲猪瘟病毒的致病特点；犬传染性肝炎病毒、减蛋综合征病

毒的致病机理、诊断与防制。掌握：伪狂犬病毒、禽传染性喉气管炎病毒、马立克病病毒的致病特点、诊断与防制。

## 第二十一章 单股 DNA 病毒

### 第一节 细小病毒科

习题要点：细小病毒的基因组及病毒颗粒有何结构特点？简述细小病毒对犬、猫、猪致病的共性及各自的特点。犬细小病毒病如何诊断与预防？试述鹅细小病毒致病特点。

### 第二节 圆环病毒科

习题要点：鸡贫血病毒和猪圆环病毒的致病机理、诊断与防制。

本章重点、难点：病毒科的特点及代表病毒的主要特性及微生物学诊断。

教学要求：了解：鸡贫血病毒的致病性及其意义。理解：猪圆环病毒的致病机理。掌握：犬细小病毒、猪细小病毒的致病特点、诊断与防制。

## 第二十二章 具有反转录过程的病毒

习题要点：反录病毒科的分类及主要特性；禽白血病的致病机理、诊断与防制。

本章重点、难点：病毒科的特点及代表病毒的主要特性及微生物学诊断。

教学要求：了解：牛白血病与马传染性贫血病毒的致病性及其意义。理解：禽白血病的致病机理及诊断与防制。掌握：反录病毒科的主要特性。

## 第二十三章 双股 RNA 病毒

### 第一节 呼肠孤病毒科

习题要点：呼肠孤病毒科有哪些重要的属？比较其异同。蓝舌病毒的病原及致病特点如何？蓝舌病毒需与哪些病毒作鉴别诊断？如何进行？分析轮状病毒的致病性、电泳型及抗原性。草鱼出血病病毒的致病特点如何？怎样预防？

### 第二节 双 RNA 病毒科

习题要点：阐述传染性囊病病毒的致病机理及主要致病特点。

本章重点、难点：病毒科的特点及代表病毒的主要特性及微生物学诊断。

教学要求：了解：正呼肠孤病毒属、环状病毒属、轮状病毒属、水生呼肠孤病毒属代表病毒的致病性及其意义。理解：传染性法氏囊病病毒的致病特点。掌握：传染性法氏囊病病毒的基本特征及诊断与防制。

## 第二十四章 单负股病毒目

### 第一节 副粘病毒科

分类与主要特性；新城疫病毒、犬瘟热病毒的致病机理、诊断与防制。

习题要点：副粘病毒科的主要特点。试述新城疫病毒的致病机理及检测手段和预防措施。阐述犬瘟热病毒的致病特点及检测。

### 第二节 弹状病毒科

分类与主要特性；狂犬病毒的致病机理、诊断与防制。

习题要点：试述狂犬病毒的致病机理及如何控制野生动物狂犬病毒的传播？

本章重点、难点：病毒科的特点及代表病毒的主要特性及微生物学诊断。

教学要求：了解：副粘病毒科和弹状病毒科的分类；牛瘟病毒的致病特点。理解：狂犬病毒的致病机理、诊断与防制。掌握：副粘病毒科的主要特性；新城疫病毒、犬瘟热病毒的致病机理、诊断与防制。

## 第二十五章 分节段的负股 RNA 病毒

习题要点：正粘病毒科的分类与主要特性。流感病毒如何命名？举例说明。禽流感病毒的致病机理、诊断与防制。什么是高致病性禽流感病毒？阐述其致病机理及生态学特点。

本章重点、难点：病毒科的特点及代表病毒的主要特性及微生物学诊断。

教学要求：了解：正粘病毒科的分类；猪流感病毒的一般特性、培养、致病性、诊断、免疫。理解：禽流感病毒的致病机理。掌握：禽流感病毒的主要特性、诊断与防制。

## 第二十六章 套式病毒目

### 第一节 冠状病毒科

习题要点：引致猪腹泻的冠状病毒的病原及致病特点有何差异？以禽传染性支气管炎病毒为例，试述冠状病毒变异的复杂性。

### 第二节 动脉炎病毒科

习题要点：阐述猪繁殖与呼吸综合征病毒的致病特点。

本章重点、难点：病毒科的特点及代表病毒的主要特性及微生物学诊断。教学要求：了解：冠状病毒科和动脉炎病毒科的分类与主要特性。理解：猪传染性胃肠炎病毒、禽传染性支气管炎病毒、猪呼吸与繁殖综合征病毒的致病机理。掌握：猪传染性胃肠炎病毒、禽传染性支气管炎病毒、猪呼吸与繁殖综合征病毒的主要特性及诊断与防制。

## 第二十七章 其他正股 RNA 病毒

### 第一节 微 RNA 病毒科

习题要点：试述微 RNA 病毒科的主要特点及分类。口蹄疫病毒有哪些血清型。阐述口蹄疫病毒的流行、致病特点及对策。如何鉴别口蹄疫病毒野毒感染与疫苗接种？比较猪水泡病毒与口蹄疫病毒的异同。

### 第二节 黄病毒科

习题要点：黄病毒科如何分类？各有何特点？瘟病毒属主要成员的关系如何？牛病毒性腹泻病毒有哪些生物型？其致病性及基因结构有何差异？试述猪瘟病毒的传播特点及检测手段。

本章重点、难点：病毒科的特点及代表病毒的主要特性及微生物学诊断。

教学要求：了解：微 RNA 病毒科和黄病毒科的分类与主要特性；猪水泡病病毒、牛病毒性腹泻病毒的致病机理、诊断与防制。理解：口蹄疫病毒、猪瘟病毒的致病特点及机理。掌握：口蹄疫病毒与猪瘟病毒的主要特性和诊断与防制。

## 第二十八章 朊病毒

习题要点：为什么说朊病毒不是传统意义上的病毒？朊病毒有哪些主要的生物学特性？比较并分析 PrPc 及 PrPsc 的主要异同。牛海绵状脑病的致病机理、诊断与防制。

本章重点、难点：朊病毒的本质及重要生物学特性。

教学要求：了解：朊病毒的研究历史；痒病的致病特点。理解：朊病毒的本质及复制特点。

掌握：朊病毒的重要生物学特性；牛海绵状脑病的致病机理、诊断与防制。

## 第二十九章 螺旋体、霉形体、立克次氏体及衣原体

习题要点：螺旋体有哪些主要生物学特性？伯氏疏螺旋体引致何病？如何诊断？支原体与其它微生物比较有何特点？立克次体有何基本特点？立克次体和衣原体的形态及培养特点是什么？

本章重点、难点：螺旋体、霉形体、立克次氏体及衣原体的重要生物学特性。

教学要求：了解：螺旋体、霉形体、立克次氏体及衣原体的分类。理解：螺旋体、霉形体、立克次氏体及衣原体的致病特点。掌握：螺旋体、霉形体、立克次氏体及衣原体的主要生物学特性。

## 第三十章 真菌学

### 第一节 概述

习题要点：什么叫真菌？其主要特性是什么？酵母菌的构造有哪些？有哪几种繁殖方式？霉菌有哪几种繁殖方式？产生哪些孢子？外界条件对真菌生长繁殖影响的因素有哪些？真菌对动物的致病作用表现在哪几个方面？

### 第二节 感染性病原真菌

习题要点：对动物的感染性真菌有哪些？怎样进行微生物学诊断？马属动物及禽类的感染性真菌主要有哪些？如何进行微生物学诊断？

### 第三节 产毒素病原真菌

习题要点：举例说明中毒性病原真菌产生主要的毒素及其作用。试述青霉属中产生毒素的成员及其作用。镰刀菌毒素有哪几类？对动物各有何致病性？烟曲霉菌致病有何特点？哪些霉菌产生黄曲霉毒素？其毒性作用如何？

本章重点、难点：真菌的繁殖和培养特性及常见病原真菌的致病机制。

教学要求：了解：真菌的概念及常见病原真菌的致病性。理解：真菌的繁殖特点及病原真菌的致病机制。掌握：真菌的培养特性及诊断要点。



#### 4-3 课程建设的创新点

##### 1. 现有平台的转型和升级，更有效地实现资源共享和知识传播

根据兽医微生物课程群中不同的具体课程，如本科生课程：兽医微生物学、水产微生物学和动物病原学等，以及研究生课程兽医细菌学及细菌学技术等，根据本学科的发展，追踪学科前沿，不断更新教学内容，使学生在掌握本课程基本理论体系的同时，了解学科研究进展，丰富知识体系。

##### 2. 启发学生主动学习相关知识，充分利用课堂时间与学生交流

不断强化实践教学环节，着力培养学生的课程感知与实践动手能力。在课程组织教学的过程中，指导学生预习相关教学内容，让学习带着相关问题去尝试解答相应问题。在正式上课时，与学生交流他们预习的成果，并指导他们解答不懂的部分。

##### 3. 课程论文和自学课程安排

在兽医课程学习的不同阶段，安排内容新颖，有知识点，学生感兴趣的小课程论文 2-3 篇，如某些理论的来历和背景；或以班为单位，或自由组合，或个人完成，激励主动学习的兴趣和能力，并鼓励他们用 PPT 的方式讲解出来，通过实践提升了学生对本课程的兴趣，提高了教学效果。

##### 4. 外文文献或国外原版教材引入教学

积极开展“双语教学”一直是高等教育改革的主要内容，也是培养国内人才具有“国际竞争力”的有效手段，本课程教学中，在动医强化班实行双语教学。普通班则尽可能增加用英语对专业词语及概念的解释，积极鼓励学生选读国外原版教材的个别章节或部分，培养了学生对文献理解和对教材直接信息理解的能力，提高学生外语水平，促进学生趋近学科前沿。

##### 5. 注重实验课的教学工作

兽医微生物学这门课的教学包括理论教学和实验技术两大部分，为了适应学科高速发展和多学科交叉的趋势，理论教学部分，教学内容的组织上注意不断补充学科发展前沿内容，先后两次对教学大纲进行了修订。增加了一些的病原、新的检测方法等内容，使教学内容具有鲜明的时代性和实用性。

学生对现在的微生物学实验教学反应良好，但因为现在的微生物学实验涉及先进的分子生物学诊断技术较少，针对这种状况，先后申请了两个校级“创新性实验实践教学项目”，强化分子生物学诊断技术在兽医微生物学中的应用，促进了学生对新技术的掌握，取得了良好的效果。

##### 6. 网络课程的更新和完善

根据国家级精品资源共享课程建设的要求，对原有的教学录像进行了更新，采用了高清画面录制，并上传到相关网站，实现了资源的共享。

## 5. 课程基础及教学资源

### 5-1 课程建设基础（含课程现状、课程评价及教学效果）

“兽医微生物学”是动物医学、动物药学、动物健康与动物生产强化班及水产养殖等专业的必修课，属专业基础课，为专业核心课程。兽医微生物学的教学内容包含动物传染性疫病的所有病原，其中涉及许多人畜共患病病原，且是国家执业兽医资格考试的必考内容。

扬州大学 刘秀梵教授：该教研室为全国规划教材主编单位，对教材内容以及教学方法有深刻的了解和规划，具有重视教学的优良传统，教学手段多样化，并充分利用多媒体等手段，授课过程中在强化学科发展的前沿知识的同时，注重与兽医临床实践相结合，实现了教学相长，培养学生独立思考和创新能力，堪称同类课程的典范。

浙江大学动物科学院 方维焕教授：该教研室对《兽医微生物学》的主编单位，对教材了解深刻，具有优良的教学传统，寓教于乐，教学互动，堪称典范。

中国农业大学动物医学院 杨汉春教授：南京农业大学动物医学院兽医微生物学教研室为全国规划教材《兽医微生物学》的主编单位，拥有全国农业院校中一流的从事兽医微生物的课程教学团队，具有重视兽医微生物学教学的优良传统，能充分把握教学内容，将教材内容很好的融入到教学的各个环节，并对教学方法有深刻的了解。教学手段和形式多样化，在教学工作中能充分利用现代教学手段。而且，在强调兽医微生物学发展的前沿理论和先进技术的同时，十分注重与兽医的临床结合，很好的实现了教学互动，有利于培养学生的创新思维能力和实践技术，其教学质量和教学效果堪称全国农业院校同类课程的典范。

《兽医微生物学》课程在教学中不断巩固寓教于乐的教学理念，探索高效的教学方法，不断丰富教学手段，历年来，在学生学期教学质量测评中均评为“优秀”。自1997级学生上课至今，学生对任课教师姚火春教授的教学组织和讲授方法普遍感到满意。

### 5-2 基本资源清单

授课指导用书：教材：《兽医微生物学》第五版，陆承平编著，中国农业出版社，2012，ISBN 978-7-109-17286-9。

参考书：《微生物学》第二版，沈萍，陈向东编著，高等教育出版社，2006，ISBN 7-04-019690-5。

《微生物学教程》第二版，周德庆编著，高等教育出版社，2002，ISBN 7-04-011116-0。

《医学微生物学》第五版，陆德源，人民卫生出版社，2002，ISBN 7-117-04041-6。

Clinical Veterinary Microbiology, Quinn P J et al, Wolfe Publishing, 1994, ISBN 0-7234-1711-3。

授课PPT及授课视频：江苏省精品课程体系

### 5-3 拓展资源建设及使用情况

- (1) 完成了该课程的“国家精品课程”和“国家精品课程资源共享课”网站建设。
- (2) 定期对课程网站进行更新和维护。回答在线咨询与提问。不定期的将微生物学学科前沿知识、研究动态和重要消息在课程网站发布，发布内容累计达7万字以上。
- (3) 适时修订教学大纲，对课程教案、教学日历、课件等教学资源不断充实、规范和更新。课程建设期间，修改教学大纲2次，课件更新3次，近期5位主讲教师每人用了3个多月时间对课件的内容和格式等方面进行了修改和完善，使课件更具知识性和观赏性。
- (4) 为提高学生综合、灵活运用理论知识的能力，结合“国家兽医执业资格”考试大纲，不断改革教学内容，改进教学方法，强化学生对疾病的诊断和防治能力。
- (5) 改变课程考核模式，建立试题库，做到考试题型多样化。目前练习题和试题的数量达400多题，试题60%以上与“国家兽医执业资格”考试题型一致。
- (6) 进行实践教学改革，在常规实验教学的基础上，选择综合性强的教学内容，使用“自助式”教学模式，培养学生自主学习能力、综合运用知识能力及创新能力。课程建设期间积极申报教学改革项目，其中创新性实验实践教学项目“细菌性病原临床分离株致病性判定法则的应用实践”和“如何建立动物细菌病原的分子生物学鉴定系统”均获得南京农业大学立项资助，通过本组教师的讨论实践，在传统的教学设计内容中添加了新的实验技术和方法，锻炼学生的创新意识和专业实验技术的掌握水平。
- (7) 注重教学资源的积累，不断更新教学课件，课程教学录像累计时长300多学时，覆盖全部教学内容。聘请专业人员对视频材料进行加工处理。

## 6. 自编教材

主编 基本 信息	姓 名	陆承平	性 别	男	出生年 月	1945.04	
	最终学历	博士	专业技 术职务	教授	电 话	025484395328	
	学 位	博士	职 务	全国兽医专业学 位教育指导委员 会副主任委员	传 真	02584395328	
	工作单位	南京农业大学		E-mail	lucp@njau.edu.cn		
	通信地址（邮编）		210000				
	研究方向		兽医微生物学				
教材 基本 信息	教材名称		兽医微生物学				
	出版社		中国农业出版社				
	书 号		ISBN 978-7-109-17286-9				
	版 次		5				
	印 数						
该教材是否为成人高等教育专门编写？ 是（ ） 否（ <input checked="" type="checkbox"/> ）							
教材 使用 情况	教材自 1979 年编撰以来，修订至第五版。相对于上一版，此版新增、删减和大量修改的章节很多，并通过这些更新，融入了最近几年微生物基因组学和蛋白组学跨越式发展的成果，介绍了新发现的一些病原微生物（包括 SARS 病毒），采用了国际上微生物最新分类标准，增加了 RNA 干扰(RNAi)、细菌毒力岛检测方法等新理论和新技术。第四版自从 2007 年出版，得到广泛使用，2008 年被教育部评为“普通高等教育精品教材”，本书第五版被列入“普通高等教育农业部“十二五”规划教材”。						

注：如果本课程使用自编教材，需要填写本栏目信息。

## 7. 学校政策支持

学校将对该课程后续建设提供足够的人力、财力、物力保障及政策支持，严格按照江苏省《关于开展成人高等教育重点专业(含精品资源共享课程)建设工作的通知》(苏教高[2016]21号)文件及校发《南京农业大学关于开展江苏省成人高等教育重点专业(含精品资源共享课程)立项申报工作的通知》(校继发[2016]499号)的要求进行后续建设，不断开展教学改革，丰富课程网络资源，及时更新相关内容，确保课程建设的高水平和高质量。

(学校立项建设文件见附件)

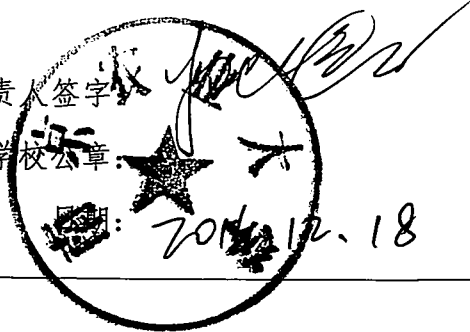
## 8. 承诺与责任

学校和课程负责人保证：

1. 课程资源内容不存在政治性、思想性、科学性和规范性问题；
2. 申报所使用的课程资源知识产权清晰，无侵权使用的情况；
3. 课程资源及申报材料不涉及国家安全和保密的相关规定，可以在网络上公开传播与使用；

课程负责人签字

学校公章



# 南京农业大学文件

校继发〔2016〕499号

---

## 南京农业大学关于开展江苏省成人高等教育重点专业(含精品资源共享课程)立项申报工作的通知

各相关学院及单位:

为贯彻落实《国家中长期教育改革和发展规划纲要(2010-2020年)》关于“加快发展继续教育”的要求和2015年全省高等学校学历继续教育改革发展推进会精神,根据江苏省教育厅《关于开展成人高等教育重点专业(含精品资源共享课程)建设工作的通知》(苏教高[2016]21号)文件要求,不断提高我校成人高等教育人才培养质量,更好地服务“强富美高”新江苏建设,学校决定开展江苏省成人高等教育重点专业(含精品资源共享课程,下同)立项申报工作。现就有关事项转发与通知如下。

## 一、指导思想

全面贯彻党的十八大和十八届三中、四中、五中全会精神，深入学习贯彻习近平总书记系列讲话特别是视察江苏重要讲话精神，坚持立德树人根本宗旨，以服务经济社会发展和人民群众学习需求为导向，创新成人高等教育人才培养模式，优化专业结构，强化内涵建设，深化教学内容、课程体系、教学方法改革，着力打造一批综合实力强、内涵积淀深、人才培养质量高、社会声誉好的成人高等教育重点专业与精品资源共享课程，切实提高在职从业人员理论知识、职业道德、实践能力和综合素质，更好地发挥成人高等教育在终身学习体系建设中的骨干引领作用。

## 二、建设目标

今年重点建设3个校级成人高等教育重点专业，每个重点专业至少建成2门主干课程作为精品资源共享课程。充分发挥重点专业及精品资源共享课程的品牌示范效应，促进我校成人高等教育专业建设水平和人才培养质量的整体提升。

## 三、建设原则

1. 服务发展，需求导向。依据经济社会发展需求和成人高等教育资源状况，集中力量，重点建设具有行业特色、区域优势和符合市场需求，支撑江苏支柱产业、优势产业、新兴产业发展的专业与课程，充分发挥其骨干示范和引领作用，进一步增强我校成人教育的社会服务能力。

2. 彰显特色，打造品牌。引导我校树立品牌意识，强化优势特色，切实加强成人高等教育专业的内涵建设，优化人才培养结构，创新人才培养模式，提升人才培养质量，努力培养经济社会发展急需的高素质、应用型、复合型人才。

3. 标准引领，好中选优。重点专业应以完备的课程体系和优质的资源共享课程为支撑，依据遴选条件和建设标准，同时参考各学院成人教育专业建设的整体水平、建设成效、社会声誉和市场需求，择优遴选。以标准为引领，切实加强我校成人高等教育专业建设。

#### 四、遴选立项

##### （一）遴选程序

成人高等教育重点专业建设点遴选，按照学院申报、专家评审、结果公示、文件认定的程序进行。学校依据遴选条件和建设标准(见附件1)择优申报。

##### （二）经费来源

我校成人高等教育专业建设工作纳入学校专业发展整体规划并予以相应的资金支持，对通过学校遴选的专业按不低于20万元/个的标准予以资助，其中精品资源共享课程按不低于平均5万元/门的标准予以资助。

#### 五、申报要求

##### （一）书面材料



申报材料确保内容真实、数据准确、文字精练、装订规范，按专业或课程装袋（详见附件 7、8）。申报书、汇总表均须加盖学校公章。申报材料不予退回，请自行备份。

1. 成人高等教育重点专业建设点申报材料。请各学院对照申报条件和遴选标准，推荐名额进行申报，并认真准备以下申报材料：

(1) 重点专业建设点申报书(3份，详见附件 3)；

(2) 重点专业建设点申报汇总表(1份，详见附件 5)，并将 Excel 格式的汇总表电子文档发送至 [lijuan@njau.edu.cn](mailto:lijuan@njau.edu.cn)；

(3) 相关证明材料（含教师学历、职称、论文、教学科研成果等）复印件一套。教材、论著，需提供封面及版权页复印件。

2. 成人高等教育精品资源共享课程申报材料。请各院校对照申报条件和遴选标准（详见附件 2），推荐名额进行申报，并认真准备以下申报材料：

(1) 精品资源共享课程申报书(3份，详见附件 4)；

(2) 精品资源共享课程申报汇总表(1份，详见附件 6)，并将电子文档发送至 [lijuan@njau.edu.cn](mailto:lijuan@njau.edu.cn)；

(3) 包含课程基本资源与拓展资源的 CD-ROM 光盘。存储路径：一级目录为“申报院校”，如“南京农业大学”等；二级目录为“申报课程”，如“不动产估价”等；三级目录为“基本资源”，如“课程介绍”、“网络课件或演示文稿”、“教学录像”等。

(4) 相关证明材料(含教师学历、职称、论文、教学科研成果等)复印件一套。教材、论著,请提供封面及版权页复印件。

3. 报送时间。各学院申报材料请集中于2016年11月28日前提交;联系人:李娟、周波、徐风国;联系电话:84395131、84396043, 13382021215、15850574769;电子邮箱:lijuan@njau.edu.cn。

## (二) 电子材料

1. 重点专业建设点申报书与相关证明材料(附件3,合并为一个PDF文件,文件命名规则为“学校名称+专业名称”);精品资源共享课程申报书与相关证明材料(附件4,合并为一个PDF文件,文件命名规则为“学校名称+专业名称+课程名称”)。

2. 重点专业建设点申报汇总表与精品资源共享课程申报汇总表(附件5与附件6,Excel格式)。

## (三) 网站材料

1. 在本校校园网站或继续教育网站上建设成人高等教育重点专业(精品资源共享课程)建设网页(专栏),采用文字、图片与视频相结合的方式介绍成人高等教育重点专业建设情况。网页(专栏)内容从项目申报、过程管理、阶段性成果展示、总结验收等方面系统考虑,参照《江苏省成人高等教育重点专业建设标准》一、二级指标设计,包括项目申报书和相关佐证材料,便于江苏省教育厅进行过程监控和校际间交流学习。专家通讯评议期间需保证网站畅通运行。

2. 网上精品资源共享课程展示应含课程基本资源与拓展资源,基本资源包括课程介绍、教学大纲、网络课件或演示文稿、作业、参考资料目录和课程教学录像(按照教学单元录制)等反映教学活动必需的资源;拓展资源指反映课程特点,应用于各教学与学习环节,支持课程教学和学习过程,较为成熟的多样性、交互性辅助资源,包括素材资源库、专题讲座库、试题库系统、作业系统、在线自测/考试系统,课程教学、学习和交流工具及综合应用多媒体技术建设的网络课程等。提交的所有课程资源须符合《国家级精品资源共享课建设技术要求》。凡申报江苏省成人高等教育精品资源共享课的全部资源必须具有清晰的知识产权,不存在侵犯其他公民、法人、组织知识产权的问题。

具体附件及相关要求可从继续教育学院网站(chjw.njau.edu.cn)的“资料下载”栏目内下载。



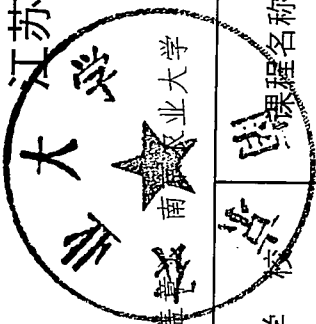
---

南京农业大学校长办公室

2016年11月22日印发

附件 6

江苏省成人高等教育精品资源共享课程申报汇总表



学校名称 (盖章) 南京农业大学

填表人: 姚火春

联系电话: 13951021883

电子邮箱: yaohch@njau.edu.cn

序号	学校	课程名称	所属学科专业	所属学科类代码	课程层次	办学形式	课程类型	课程负责人	总课时数	是否为省级成人高等教育精品课程
1	南京农业大学	兽医微生物学	动物医学类	090600	专升本	函授	专业基础课	姚火春	40	否

说明:

1. “所属学科专业”为《普通高等学校本科专业目录》中的学科门类下设的二级类名称、《普通高等学校高职高专教育指导性专业目录》中的专业类名称;
2. 课程层次为: 高起专, 高起本, 专升本;
3. 办学形式为: 函授, 业余, 脱产;
4. 课程类型为: 公共课, 基础课, 专业基础课, 专业课。

课程平台登录路径: <http://yc.njau.edu.cn:801/etcs/login/reLogin.jsp>

用户名: jpyzgxkc

密码: 123456

江苏省成人高等教育精品资源共享课程

# 《兽医微生物学》



(含教师学历、职称、论文、教学科研成果等)

南京农业大学

二〇一六年十二月

## 目录

主讲教师、教学 辅助人员 基本信息	姓名	性别	出生年月	单位	职称	学科专业	在课程建设中 承担的工作
	姚火春	男	1963.02	南京农业大学	教授	预防兽医学	主持
	刘永杰	女	1972.03	南京农业大学	教授	预防兽医学	参与
	潘子豪	男	1980.07	南京农业大学	讲师	预防兽医学	参与
	吴宗福	男	1981.08	南京农业大学	副教授	预防兽医学	参与
	张炜	男	1976.11	南京农业大学	教授	预防兽医学	参与
	刘广锦	女	1984.08	南京农业大学	讲师	预防兽医学	参与

# 博士研究生

## 毕业证书



研究生 陈辉 性别 男，一九六三年 月 日生，于

一九九零年 月 日至 二〇〇〇年 月 月在 预防兽医学

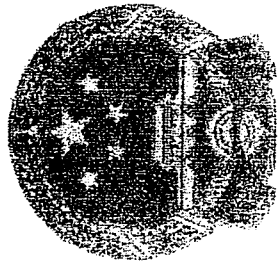
专业学习、学制 三年，修完博士研究生培养计划规定的全部课程，成绩合格，  
毕业论文答辩通过，准予毕业。

培养单位：南京农业大学

校(院、所)长：郑小波

证书编号：103071200901000291

二〇〇〇年 月 十八日



# 博士学位证书

姚火春，男，1963年2月3日生。在南京农业大学  
 预防兽医学 学科（专业）已通过博士学位的课程  
 考试和论文答辩，成绩合格。根据《中华人民共和国学位条例》的规  
 定，授予农学博士学位。



南京农业大学 校长 郑办斌  
 学位评定委员会主席

证书编号：1030722009000262

二〇〇九年十二月三十一日





姓名：姚火春

男

性别：

出生年月：1963.02

学科：预防兽医学

工作单位：南京农业大学

编号：G-1188

经济

技术资格

研究员级高级工程师

姚火春

同志已具备

任职资格。



学术委员会

2009年12月

# 博士研究生

# 毕业证书

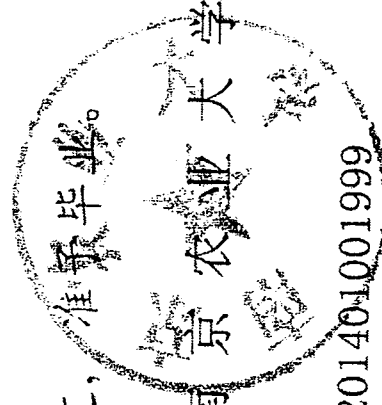


研究生潘子蒙

性别男，一九八〇年七月十日生，于

二〇一〇年九月至二〇一四年十二月在 预防兽医学

专业学习，学制三年，修完博士研究生培养计划规定的全部课程，成绩合格，  
 毕业论文答辩通过，

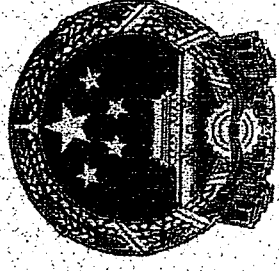


培养单位：南京农业大学

校(院、所)长：

证书编号：103071201401001999

二〇一四年十二月二日



# 博士学位证书

潘子豪，男，1980年7月10日生。在南京农业大学

预防兽医学 学科(专业)已通过博士学位的课程

考试和论文答辩，成绩合格。根据《中华人民共和国学位条例》的规

定，授予农学博士学位。

南京农业大学

校长

学位评定委员会主席



潘子豪  
2010207024

证书编号: 1030722014002082

二〇一四年十二月二十三日



持证人：潘子豪

性别：男

出生年月：1980年07月

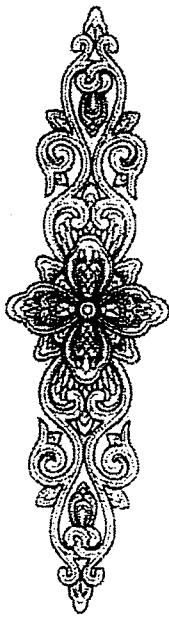
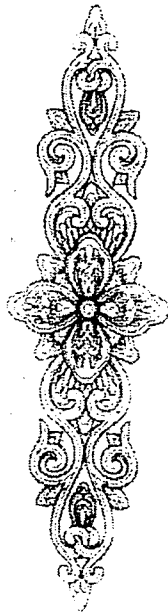
民族：汉

身份证号码：620502800710041

资格种类：高等学校教师资格

任教学科：

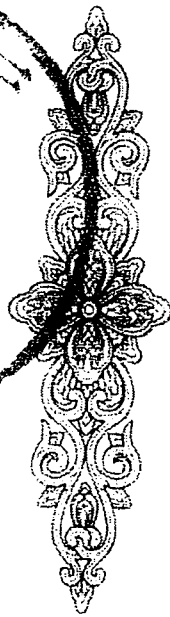
证书号码：2005320017J007132



根据《中华人民共和国  
教师法》及《教师资格条例》

的规定，认定  
潘子豪  
高等学校  
具备

教师资格。



刘永杰教授

# 南京农业大学文件

校人发〔2013〕124号

---

## 南京农业大学关于公布 2012 年 教师及其他专业技术岗位聘用结果的通知

各学院、各单位：

根据国家有关文件及《南京农业大学关于开展 2012 年教师及其他专业技术岗位晋级聘用工作的通知》（校人发〔2012〕465 号）精神，经个人申请，各单位岗位聘用工作小组、学校专家组评议，校岗位聘用工作小组和校岗位设置与聘用工作领导小组审核，并经 2013 年 4 月 8 日校长办公会议审定，同意聘用王源超等 618 位同志至相应的专业技术岗位等级（其他人员按学校有关规定原岗位

等级聘用), 聘期4年, 时间自2013年1月1日至2016年12月31日。

特此通知

附件: 教师及其他专业技术岗位聘用人员名单



附件

## 教师及其他专业技术岗位聘用人员名单

(按姓氏笔画排序)

### 一、正高二级岗位聘用人员名单

丁艳锋 王恬 王源超 朱晶 吴益东 邹建文 周明国  
徐国华

### 二、正高三级岗位聘用人员名单

王锋 王怀明 王秀娥 王鸣华 兰叶青 刘凤权 刘文斌  
刘永杰 刘志民 刘泽文 刘祖云 朱艳 朱月林 江玲  
邢邯 吴俊 吴群 李飞 李放 李艳 李友生  
李国清 沈文飏 陈超 陈东平 陈利根 周宝良 房经贵  
罗英姿 范红结 郑永华 胡浩 徐阳春 郭世伟 郭巧生  
陶小荣 顾振新 崔中利 盛下放 麻浩 黄水清 龚怡祖  
惠富平 智海剑 窦道龙 鲍恩东 熊正琴 熊爱生 蔡庆生

### 三、副教授一级岗位聘用人员名单

丁霞 于汉寿 王琦 王苏玲 冯祯银 叶锡君 刘桂玲  
吕波 吕慧能 孙长海 庄苏 吴清太 宋润霞 张鸣  
张友琴 李明 李玉泉 李志华 杨方美 杨宪民 苏建亚  
邹晓葵 陈青春 陈胜甫 周中建 周应堂 和文龙 居志建

屈卫群 范 晴 姜 迪 施桂珍 洪幼平 胡忠明 胡金良  
费荣梅 聂信天 袁静亚 郭春华 梁敬东 黄克明 曾玉珊  
曾伦武 缪培仁 张燕雯 马锦义 李鹏宇 张蜀宁

#### 四、副教授二级岗位聘用人员名单

丁绍刚 丁晓蕾 孔繁霞 王 群 王广东 王备新 王建军  
付光磊 史立新 史红专 史丽萍 叶永浩 甘立军 薛晓峰  
仲高艳 刘 康 刘世家 刘兆磊 刘庆友 刘雅坤 刘德营  
孙 敬 孙 锦 许家荣 许晓明 何琳燕 吴 未 张 禾  
张东宇 张克云 张春玲 张海峰 李春保 李娟玲 李新华  
杨 珉 杨志民 杨超光 肖红梅 陆 红 陆 巍 陈长青  
陈会广 陈光明 陈兵林 陈晓红 陈素梅 林光华 欧维新  
武 锐 郑永兰 姜 海 姜 梅 姜卫华 姜小三 娄群峰  
施晓琳 赵 力 赵立艳 唐圣菊 夏如兵 徐迎春 翁忙玲  
钱国良 钱春桃 顾向阳 高 英 高志红 崔 瑾 曹 慧  
章兆丰 黄 芬 黄 明 游 雄 游衣明 董彩霞 蒋建东  
韩兆玉 韩美贵 滕年军 杭苏琴 茆达干 刘 强 吴菊清

#### 五、讲师一级岗位聘用人员名单

丁兰英 王美蓉 王晓娟 王超群 邓益锋 冯祎高 古 华  
刘世英 孙玉华 成艳芬 朱红梅 朱昌华 许家平 吴 健  
吴 亮 张 萍 时跃华 李 明 杨春莉 陆应林 陆静霞  
陈桂云 陈辉东 姜 涛 徐 军 徐红芳 徐秀英 殷 玮  
曹兆霞 阎素兰 黄国庆 韩 英 谭 放 魏 瑜



## 六、讲师二级岗位聘用人员名单

马保亮	尹雪英	方星星	王卉	王暄	王鹏	王慧
王燕	王子玉	王凤英	王菊芳	王歆	冯军政	卢冬丽
卢礼萍	石碧	石磊	石志华	伍洁	刘君	刘璎璎
吕成绪	孙福成	安秋	朱云	朱国宗	纪燕玲	何朝晖
何静	吴芳	吴凤凰	吴威	张充	张敏	张群
张丽	张京卫	张树志	张浩	张莉莉	张捷	张新华
张澄宇	张震	李伟	李永博	李和	李林	李艳杰
李璎	杨钦	杨婷	杨飞	杨伟	杨建国	汪秀川
汪松陵	连新明	邹修国	陆明洲	陈玉仑	陈兆娟	陈彩蓉
陈朝霞	周蕾	周永清	孟为国	於海明	林科学	罗良
罗庆云	郑会明	郑良友	姚雪霞	段华平	胡新	胡滨
胡志强	赵月霞	赵志刚	赵青松	赵海燕	唐学玉	徐立新
徐峙晖	翁达来	贾雯	郭小清	钱燕	高强	高辉松
崔春红	曹林	梁玉泉	黄颖	焦凌佳	程明	葛继红
蒋楠	覃凤飞	韩喜秋	阚贵珍	潘增祥	戴丽	

## 七、助教一级岗位聘用人员名单

白茂强 白荻 吕后刚 孙国祥 朱从先 李征 胡冬临  
徐东波

## 八、其他专业技术副高一级岗位聘用人员名单

牛有生 冯蕾 刘智元 成何珍 杨井华 肖俊荣 陆芹英  
陈鸥 陈铭达 席庆奎 钱宝英 顾义军 高翔 黄宁昌

程正芳

### 九、其他专业技术副高二级岗位聘用人员名单

方 鹏 毛莉菊 牛文娟 王建新 王祥珍 冯金侠 石晓蓉  
任建鸾 孙小伍 庄 菊 宋华明 宋雪飞 张 彬 张 斌  
张 鲲 李 远 李献斌 周 孜 周 钢 周权锁 武晓维  
姜 岩 胡琼英 赵艳兵 夏爱红 钱存忠 顾 南 顾 珍  
黄明睿 缪建兰

### 十、其他专业技术中级一级岗位聘用人员名单

尤兰芳 王 平 王泗宁 王桂萍 王海红 王淮宪 邓国勇  
冯瑞芳 刘川宁 刘天行 吉东风 吕心泉 孙仁帅 朱芳蘅  
江惠云 汤亚芬 纪昌秀 吴彦宁 宋 珂 张 云 张仁萍  
张文浩 张国富 张春兰 张彩琴 李 慧 李井葵 李红旗  
李芳兰 杨 娟 杨 冰 苏晓红 辛厚建 邹 静 陆红缨  
陆建刚 陈月红 陈兆夏 陈学友 陈晓玲 单玉荣 孟凡美  
孟繁星 郁隐梅 姚 薇 姜建良 柳心安 胡 燕 (图书馆)  
胡必强 胡孙苏 赵桂龙 钟于群 徐安德 徐颖洁 班 宏  
秦福臻 莫国香 陶丁祥 陶金才 高莎丽 梁剑茹 阎 燕  
黄 云 黄在新 彭其军 韩红梅 鲁 英 褚建宇 解学芬  
缪 健

### 十、其他专业技术中级二级岗位聘用人员名单

丁爱珍 马月花 马洪雨 仇海涛 孔育红 王 霞 王 敏  
王兆焯 王志茹 冯秀珍 冯绪猛 卢 黎 田素妍 刘 丹

刘 军	刘 浩	刘为浒	刘玉涛	刘红梅	刘怡辰	刘琳莉
华玉明	孙环云	朱建春	朱琳琳	朱锁玲	许承保	闫修荣
何东方	余德贵	张 松	张红霞	张春华	张桂荣	李 询
李 珣	李占华	李阿特	李剑红	李晓晖	杨 明	杨 娜
杨建平	杨海莉	汪 瑾	邵苏宁	邵海英	陈 进	陈 俐
陈永忠	陈林海	陈雅莉	周 泳	周 勇	周广礼	周建国
周莉莉	周菊红	宗 芳	林江辉	林桂娟	林庶民	罗国富
范馨亚	郑 岚	贺平清	赵 阳	赵丹丹	赵艳艳	倪 浩
徐风国	郭 盈	郭丽娟	高天武	康若祎	章世秀	傅雷鸣
蒋毅蓉	韩 梅	廖永萍	滕秀梅	潘宏志	戴 芸	戴青华
戴逸芳	鞠卫平					

### 十一、其他专业技术初级一级岗位聘用人员名单

于小波	马德元	尹显凤	王乙明	王世伟	王明峰	王胜楠
王 雪	邓丽华	史秋峰	叶 敏	刘传俊	刘 荣	孙清玲
朱媛媛	权灵通	邢 鹏	闫相伟	何建明	吴妍妍	吴洪彬
吴熙妹	张义东	张正伟	张玉玲	张 丽	张 兵	张 祎
李业俊	李海燕	李 焯	杨绕宝	杨 悦	杨 梅	杨 博
汪素美	辛 闻	邹春富	陆忆维	陈 骅	陈海林	单晓红
周 丹	季 燕	郑广隶	郑立荣	郑爱莲	金慧瑾	姚明霞
姜 华	施玉萍	胡秀义	胡晓璐	贺子义	贺亚玲	赵玲玲
赵焯焯	赵 莲	赵 静	唐 玲	夏 磊	徐雪萍	钱正霖
顾晓彤	高素琴	崇小姣	黄文昕	彭 玲	童 菲	董 艳

蒋苏娅 蒋欣 蒋菠 蒋薇薇 鲁杨 张莉霞 赵道远  
巢玲 李学林

十二、专职辅导员讲师一级岗位聘用人员名单

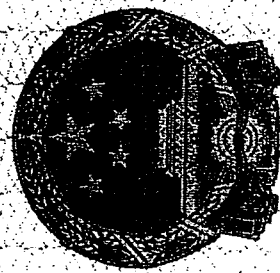
钱凤英

十三、专职辅导员讲师二级岗位聘用人员名单

刘照云 祖海珍

十四、专职辅导员助教一级岗位聘用人员名单

张权



# 博士学位证书

吴宗福，男，1981年8月30日生。在南京农业大学  
 预防兽医学 学科（专业）已通过博士学位的课程  
 考试和论文答辩，成绩合格。根据《中华人民共和国学位条例》的规  
 定，授予农学博士学位。

南京农业大学

校长

郑小波

学位评定委员会主席



吴宗福  
20062076

证书编号：10307220090000016

二〇〇九年六月二十六日

# 博士研究生 毕业证书



研究生 吴宗福 性别男，一九八一年八月三十日生，于

二〇〇六年九月至二〇〇九年六月在 预防兽医学

专业学习，学制三年，修完博士研究生培养计划规定的全部课程，成绩合格，  
毕业论文答辩通过，准予毕业。

培养单位：南京农业大学

校(院、所)长：郑小波

证书编号：103071200901000016

二〇〇九年六月十四日

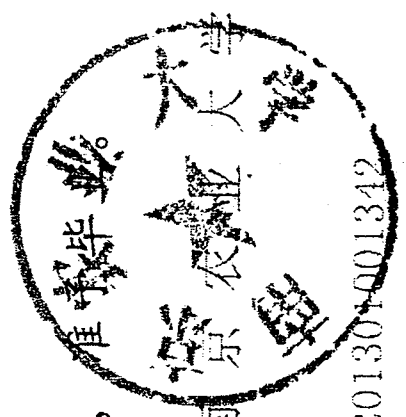
# 博士研究生 毕业证书



刘广锦  
2010207023

研究生 刘广锦 性别 女, 一九八四年八月三日 生, 于  
二〇一〇年九月至二〇一三年六月 在 预防兽医学

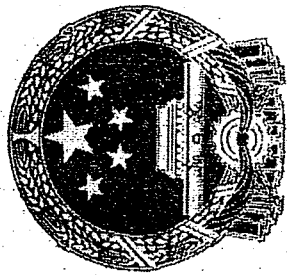
专业学习, 学制三年, 修完博士研究生培养计划规定的全部课程, 成绩合格,  
毕业论文答辩通过,



培养单位: 南京农业大学

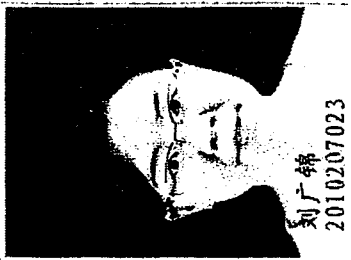
校(院、所)长: 刘先宏

证书编号: 103071201304001342 二〇一三年六月六日



# 博士学位证书

刘广锦，女，1984年8月3日生。在南京农业大学  
预防兽医学



学科(专业)已通过博士学位的课程  
考试和论文答辩，成绩合格。根据《中华人民共和国学位条例》的规

定，授予农学



校 长

刘先法

学

学位评定委员会主席

证书编号：10307220130001506

二〇一三年六月二十五日



# 南京农业大学文件

校人发(2015)43号

---

## 南京农业大学关于 徐文等 135 位同志专业技术职务聘任和周兆胜 等 13 位同志同级转聘的通知

各学院、各单位：

根据学校有关规定，经校职改办审核，同意聘任徐文等 135 位同志相应的专业技术职务，聘任时间自 2014 年 12 月 31 日起开始计算。同意周兆胜等 13 位同志同级转聘，现将名单公布如下：

### 一、讲师

徐文	徐东波	于景金	章永年	陆德荣
胡冬临	孙荣山	安红利	陈园园	国静

崔海燕	汪快兵	张 瑾	张 帆	殷志华
万永杰	陈兴祥	汤 芳	刘广锦	吴文达
罗 慧	王全祥	钱筱林	葛艳艳	魏 艾
张嫦娥	郑恩来	杨 松	芮 昕	杨润强
王绍琛	周 莉	叶可萍	顾家冰	吴智丹
熊 航	桑秀芝	李 莲	张 宁	张懿彬
杨 亮	杨海水	张小虎	李 刚	李国强
徐 良	安玉艳	王彦杰	朱旭君	张 楠
朱冰莹	张爱华	黎孔清	何海琳	邹山梅
孙明明	刘志鹏	顾 冕	唐 仲	刘秦华
原现军	陈 凯	韩正彪	庄 倩	沈立轲
刘 峰	张紫刚	戴 琛	师 亮	任 昂
崔为体	邹珅珅	叶文武	王兴亮	华修德
李延森	李平华	王 超	余凯凡	申军士
吴望军	田 亮	李向飞	肖 阳	

## 二、实验师

郑 颖 王晓莉

## 三、助理研究员

陈志亮 任 阳 邢 鹏 吴 玥 贾媛媛

吴熙娃 郝佩佩 于 春

## 四、馆员

胡文亮

## 五、主治医师

吴妍妍

## 六、助教

刘 方	于阳露	孙雅薇	赵 朦	王 彬
韩李美萱	窦 靛	史文韬	姜晓玥	李艳丹
王晓月	吕一雷	曹晓萱	陆佳俊	卢茂春
朱 朋				

## 七、助理实验师

张 羽	滕 爽	孙 月	周少霞	徐晓红
-----	-----	-----	-----	-----

## 八、助理实习员

冯 莉	章 凡	陈 雷	刘 燕	毛 竹
张 琳	雷 翊	雷 颖	苏 怡	于 璐
吴 蓉	章利华			

## 九、助理馆员

郑新梅	陈宏原	高 俊	杜丰烨
-----	-----	-----	-----

## 十、助理编辑

李 欢 尹 欢

## 十一、专业技术职务同级转聘

### (一) 副教授

周兆川	吴 敏	刘馨秋	何红中
-----	-----	-----	-----

### (二) 讲师

车建红

(三) 助理研究员

邱小华 戴青华 桑大志 鞠卫平 夏德峰

(四) 实验师

周 华

(五) 研究实习员

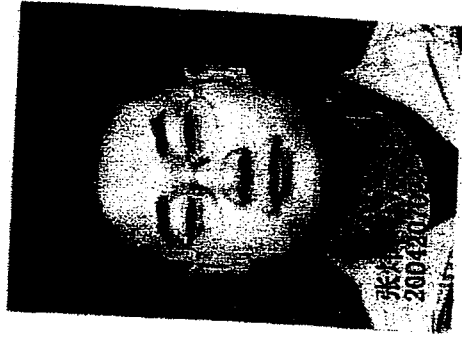
孙 华

(六) 注册会计师

崇小华



# 博士研究生 毕业证书



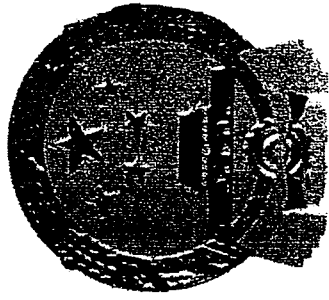
研究生 张炜 性别男 ，一九七六年十一月十七日生，于  
二〇〇四年九月至二〇〇七年九月在 预防兽医学

专业学习，学制三年，修完博士研究生培养计划规定的全部课程，成绩合格，  
毕业论文答辩通过，准予毕业。

培养单位：南京农业大学 校(院、所)长： 郑小波

证书编号：103071200701000196

二〇〇七年九月二日



# 博士学位证书

张炜 系安徽滁州

人，一九七六年十一月

十七日生。在我校

预防兽医学

学科(专业)已通过

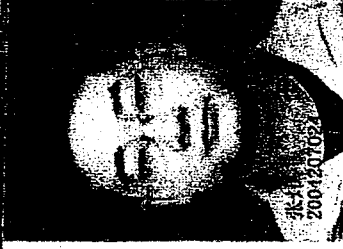
博士学位的课程考试和论文答辩，成绩合格。根据《中华人民共和国学位条例》的规定，授予 农学 博士学位。

南京农业大学 校长

学位评定委员会 主席

郑小波

二〇〇七年十二月三十一日





## Genetic diversity and features analysis of type VI secretion systems loci in avian pathogenic *Escherichia coli* by wide genomic scanning



Jiale Ma, Min Sun, Yinli Bao, ZiHao Pan, Wei Zhang, Chengping Lu, Huochun Yao\*

Key Lab of Animal Bacteriology, Ministry of Agriculture, Nanjing Agricultural University, Nanjing 210095, China

### ARTICLE INFO

#### Article history:

Received 6 August 2013

Received in revised form 24 September 2013

Accepted 30 September 2013

Available online 8 October 2013

#### Keywords:

Avian pathogenic *Escherichia coli*

Type VI secretion system

Prevalence

Diversity

Genomic

VgrG protein

### ABSTRACT

Avian pathogenic *Escherichia coli* (APEC) strains frequently cause extra-intestinal infections and significant economic losses. Recent studies revealed that the type VI secretion system (T6SS) is involved in APEC pathogenesis. Here we provide the first evidence of three distinguishable and conserved T6SS loci in APEC genomes. In addition, we present the prevalence and comparative genomic analysis of these three T6SS loci in 472 APEC isolates. The prevalence of T6SS1, T6SS2 and T6SS3 loci were 14.62% (69/472), 2.33% (11/472) and 0.85% (4/472) positive in the APEC collections, respectively, and revealed that >85% of the strains contained T6SS loci which consisted of the virulent phylogenetic groups D and B2. Comprehensive analysis showed prominent characteristics of T6SS1 locus, including widely prevalence, rich sequence diversity, versatile VgrG islands and excellent expression competence in various *E. coli* pathotypes. Whereas the T6SS2 locus infatuated with ECOR groups B2 and sequence conservation, of which are only expressed in meningitis *E. coli*. Regrettably, the T6SS3 locus was encoded in negligible APEC isolates and lacked several key genes. An in-depth analysis about VgrG proteins indicated that their COG4253 and gp27 domain were involved in the transport of putative effector islands and recognition of host cells respectively, which revealed that VgrG proteins played an important role in functions formation of T6SS.

© 2013 The Authors. Published by Elsevier B.V. Open access under CC BY license.

### 1. Introduction

Avian pathogenic *Escherichia coli* (APEC) is an important member of the extra-intestinal pathogenic *E. coli* (ExPEC), and systemic infections caused by APEC are economically devastating to poultry industries (Dho-Moulin and Fairbrother, 1999; Ewers et al., 2003). APEC enters and colonizes the avian respiratory tract, leads to localized infections, such as airsacculitis and pneumonia. In certain cases, it leads to acute septicemia, which commonly results in sudden death (Dho-Moulin and Fairbrother, 1999; Ewers et al., 2003; Rodriguez-Siek et al., 2005). APEC strains are closely related to human ExPEC strains. Therefore, some closely related clones could be involved in extra-intestinal infections in both humans and poultry, suggesting that these isolates are not host specific (Rodriguez-Siek et al., 2005; Moulin-Schouleur et al., 2006, 2007; Johnson et al., 2007; Mora et al., 2009).

Recent researches have described a new secretion system, called the type VI secretion system (T6SS), in several bacterial spe-

cies including APEC, representing a new paradigm in protein secretions (Filloux et al., 2008). de Pace et al. (2010) found that the mutants of T6SS core genes (ClpV and Hcp) of APEC strain SEPT362 displayed decreased adherence and actin rearrangement on epithelial cells. A similar result was observed from the Hcp mutant of the neonatal meningitis *E. coli* (NMEC) strain RS218 (Zhou et al., 2012). Therefore, the role that T6SS plays in contributing to the virulence of APEC warrants further investigations.

Some studies have revealed that T6SS gene clusters are assembled from at least 13 core proteins, called 'core components' (Parsons and Heffron, 2005; Bonemann et al., 2009), which comprise the minimal machinery necessary for the functionality of T6SS. However, most T6SS gene clusters actually encode additional proteins, the function of which remains unknown. VgrG protein, one of the core components performing diverse functions, has been demonstrated to be secreted by the T6SS. The N-terminal of VgrG may serve in assembly of the T6SS machinery, while the C-terminal portion functions as effector (Pukatzki et al., 2007; Ma et al., 2009). Former researches have reported the function of evolved C-terminal portion that carries unknown proteins encoded in the VgrG islands in different bacterial species (De Maayer et al., 2011; Sarris et al., 2011). The N-terminal of VgrG protein contains a gp27 domain and a gp5 domain, which leads to the VgrG trimeric structure organized in a similar way as the (gp27)<sub>3</sub>–(gp5)<sub>3</sub> complex does of bacteriophage T4 (Leiman et al., 2009). The lysozyme activity of

\* Corresponding author. Tel./fax: +86 25 84395328.

E-mail address: [yaohch@njau.edu.cn](mailto:yaohch@njau.edu.cn) (H. Yao).

bacteriophage gp5 protein is capable of penetrating the outer cell membrane and locally dissolving the periplasmic cell wall (Arisaka et al., 2003). The gp27 protein acts as tail fiber protein in bacteriophage which confers a high degree of host specificity by binding to the specific receptor of sensitive bacteria (Zhang et al., 2009; Xu et al., 2013).

In this study we present the results in silico analyses of putative T6SS-related genes found in the genome of APEC strain ED205. According to the result of prevalence analysis in 472 APEC isolates, all identified T6SS loci were sequenced. We aimed to perform an extensive comparative genomic analysis among abundant APEC isolates to further explore the properties characteristics of T6SS loci in APEC.

## 2. Materials and methods

### 2.1. Bacterial strains

A total of 472 APEC strains were isolated from the brains of ducks with septicaemic and neurological symptoms as previously described (Wang et al., 2011) (Table S3). The identity of each strain was confirmed as *E. coli* by using the VITEK 2 system (BioMérieux Vitek, Inc., Hazelwood, MO, USA). Some APEC isolates used as important representative strains in this study are marked in red in Fig. 3. The APEC ED205 strain was chosen for genome sequencing.

In addition, the *E. coli* reference strains (EHEC O157, ETEC PE114, EPEC PE059, UPEC 536, NMEC RS218 and APEC\_01) used in this study were purchased from the Control Institute of Veterinary Bioproducts and Pharmaceuticals of China, and identified to encode the T6SS1 and T6SS2 loci. All *E. coli* strains were grown in Luria–Bertani (LB) medium at 37 °C with aeration.

### 2.2. In silico identification of the T6SS loci in APEC

APEC ED205 strain genome sequencing was performed by using a Roche 454 genome sequencer FLX system. The draft genome sequence was uploaded to the bioinformatics analysis platform (<http://www.chinasscontrol.com/biosystem/index.php>) of Nanjing Agricultural University. Nucleotide sequences from enteroaggregative *E. coli* (EAEC) Sci-I and Sci-III 042 strain and NMEC T6SS locus RS218 strain were used for BLASTN and reverse BLAST against the ED205 draft genome in the bioinformatics analysis platform. Clusters containing at least five genes encoding proteins with similarity to known T6SS core proteins from NMEC or EAEC were considered as part of a putative T6SS locus in APEC ED205 genomes. These putative genomic regions were then extended by examining 10 kb up-stream and down-stream for putative conserved genes associated with T6SS by reverse blast analysis against the EAEC 042 genome.

### 2.3. Sequencing of T6SS loci

T6SS loci were detected by multiplex PCR using specific oligo-nucleotide primers for amplification of 3 conserved T6SS primary core gene: IcmF (membrane-bound protein), ClpV (ATP bind protein) and VgrG (spike protein). T6SS loci were defined by the presence of at least two of the three genes, and used primers were shown in Supplementary Table S1. All of the APEC T6SS loci detected in this study were amplified and sequenced, being performed by following the structure feature of gene clusters to reduce the workload. This process was carried out by Shanghai Sunny Biotechnology Co., Ltd., and each cluster was assembled as one containing the entire T6SS locus. Phylogenetic groups were determined for the 472 APEC isolates by using the triplex polymer-

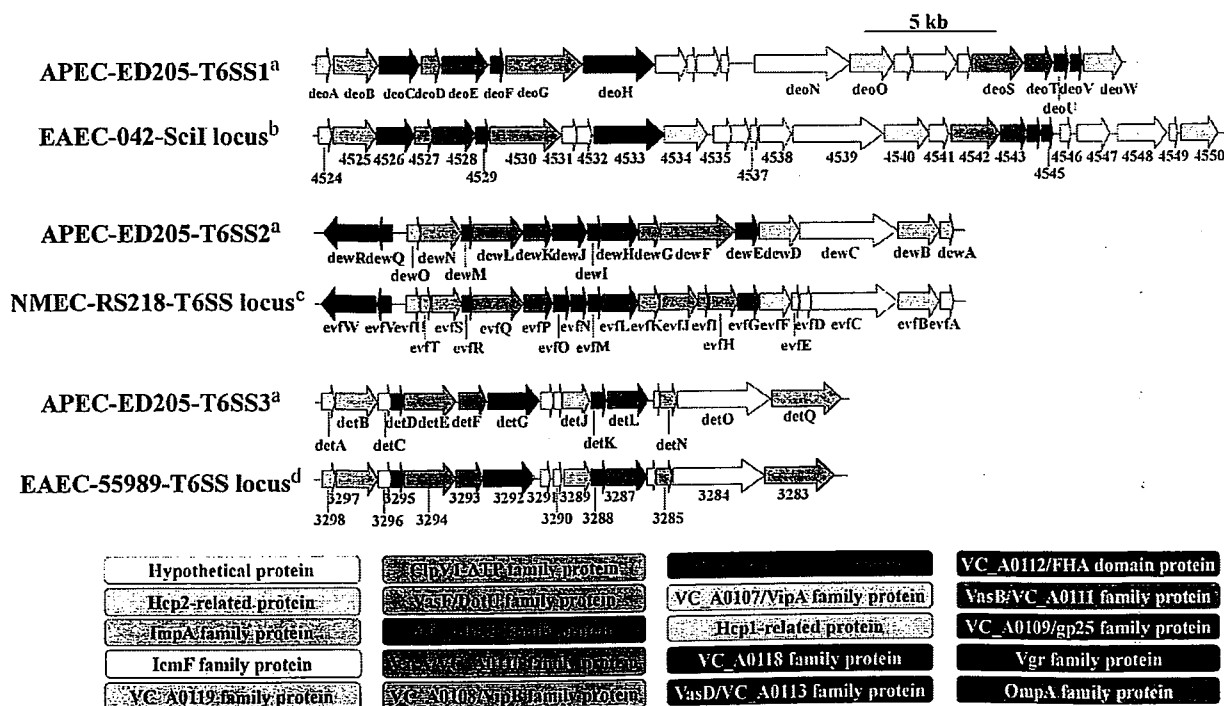


**Fig. 1.** Comparative genome alignments of APEC ED205 and reference strains. Genes encoding conserved domain proteins were represented by the same colors. White arrows indicate other genes encoded in the T6SS loci which were not identified as part of the conserved core described by Boyer et al. (2009). The direction of the arrows indicates the direction of transcription. The color keys for the functional classes of genes in the T6SS loci are shown at the bottom. (a) The ED205 draft genome sequenced by our lab. (b) The NCBI reference number of EAEC-042 genome is NC\_017626. (c) The NCBI reference number of NMEC-RS218 T6SS cluster is JN837480. (d) The NCBI reference number of EAEC-55989 genome is NC\_011748.



ase chain reaction (PCR) as previously described (Clermont et al., 2000).

#### 2.4. Phylogenetic analyses

Phylogenetic analyses were performed following the procedures outlined by Bingle et al. (2008). A ClustalW alignment with default parameters was used with the entire T6SS loci nucleic acid sequences and VgrG amino acid sequences. Then, the T6SS clusters phylogenetic tree was constructed with the MEGA (v.5.0.3) software package using the neighbor-joining method, with *P*-distance, complete gap deletion and bootstrapping (*N* = 1000) parameters. The similar approach was used to construct the phylogenetic tree of VgrG proteins, which only differs in using the Poisson correction instead of *P*-distance.

#### 2.5. Sequence annotation and GC content analysis

T6SS-related genes were named according to the T6SS genes of *Vibrio cholerae* (Pukatzki et al., 2006). Maps of the genomic islands were constructed manually in the VECTOR NTI program and Microsoft PowerPoint. Visual representation of the alignments using nucleotide similarities (tblastx) of the T6SS loci and VgrG genes were carried out with the Artemis Comparison Tool (ACT) (Carver et al., 2005). The nucleic acid or translated proteins were compared with those in GenBank database by the BLAST network service. The average GC content of the whole T6SS loci and the VgrG islands (see below) were determined using the Bioedit (v.7.0.5.3) package.

#### 2.6. Analyses of the VgrG islands

VgrG islands were defined according to procedures outlined by De Maayer et al. (2011). In this study, only the APEC-T6SS1 locus encoded visible VgrG islands. The amino acid sequences for the proteins encoded in the VgrG islands were analyzed for sequence identity by Blast *P* analysis against the NCBI protein database. The presence of conserved domains was identified by Blast analysis against the Conserved Domain Database (CDsearch). In addition, the GC contents of the VgrG genes were determined for the conserved N-terminal region, including the conserved Vgr and Gp5 domains, as well as the C-terminal extensions which were all considered to be nucleotides located at the 3' end of the Gp5 domain. All of the proteins containing conserved domains were used to analyze possible functions.

#### 2.7. Proteins structure prediction and modeling

The amino-terminal and central domains of VgrG proteins resemble the T4 bacteriophage gp27 protein and the C-terminal domain of gp5, respectively (Pukatzki et al., 2007). In this study, the structure comparison between gp27 domain of VgrG and gp27 protein of T4 bacteriophage (gp27-T4) was performed. All of the models were generated by employing the SWISS-MODEL server (<http://swissmodel.expasy.org>) (Arnold et al., 2006). The model of gp27-T4 protein was released by Kanamaru et al. (2002). The model of gp27-T6SS1 was drawn based on template 2p5z.X (VgrG protein from *E. coli* CFT073 c3393), sharing 89.84% sequence identity. The model of gp27-T6SS2 was drawn based on template 1wru.A (tail protein from bacteriophage Mu gp44) (Kondou et al., 2005), sharing 31.48% sequence identity and the modeled domain ranged from residues 8–358 aa. As no a highly similar template could be referenced, the gp27-T6SS3 could not be drawn a high-quality model. However, a referential model was still drawn based on 2p5z.X, sharing only 14.86% sequence identity, while the modeled domain ranged from residues start to end.

#### 2.8. Analysis of VgrGs expression

To analyze the expression competence of VgrG proteins in different *E. coli* pathotypes, an indirect ELISA assay was carried out using antibody against VgrG protein. Briefly, wells of an ELISA plate were coated using 100 µl bacterial ( $\approx 10^9$  cfu/ml) supersonic lysate at 4 °C for 12 h. Then, VgrG-ELISA was performed as reported previously (Dreyfus et al., 2004), and each sample was measured for three times. A sample A450 value/negative control A450 value (*S/N*) >2 was used as the positive standard. 15% mice macrophage lysate was added in Trypticase Soy Broth (Difco Laboratories, Detroit, MI) for bacterial strains culture, which could help to activate the T6SS vitality (Ma et al., 2009). Because the T6SS3 locus encoded an incomplete T6SS cluster and was not encoded in most of *E. coli* strains, only VgrG-T6SS1 and VgrG-T6SS2 were analyzed by ELISA assays. The VgrG-T6SS1 and VgrG-T6SS2 monoclonal antibodies used in this study were prepared by GenScript USA Inc. as the service SC1040 (Kohler and Milstein, 1975).

#### 2.9. Statistical analysis

The data were analyzed by using SPSS version 17.0 (SPSS Inc., Chicago, IL). The difference between mean values among groups was evaluated, first by one-way analysis of variance (ANOVA) and then by pairwise comparison of the mean values between the two groups, followed by Tukey's student rank test. Differences in a *P* value of <0.05 were considered significant, while a *P* value of <0.01 was considered greatly significant.

### 3. Results and discussion

#### 3.1. Identification of orthologous T6SS loci occur in APEC

By baiting with conserved proteins from the characterized T6SS loci in human pathogenic *E. coli*, three distinguishable T6SS loci were identified in the draft genome sequences of APEC ED205 strains (Fig. 1). The embedded orders of conserved T6SS core genes in T6SS1, T6SS2 and T6SS3 loci were fully consistent with the Scil locus of EAEC 042 strain, the T6SS locus of NMEC RS218 strain and the T6SS locus of EAEC 55989 (Fig. 1) respectively. The prevalence of T6SS1, T6SS2 and T6SS3 loci were 14.62% (69/472), 2.33% (11/472) and 0.85% (4/472) positive in the APEC collections, respectively, and revealed that >85% of the strains contained T6SS loci which consisted of the virulent phylogenetic groups D and B2 (Fig. 2). 11 APEC isolates contained within the T6SS2 locus also encoded the T6SS1 locus, and only ED205 strains contained all of three T6SSs. The phylogenetic tree of whole T6SS clusters displayed the sequence identity of three branches less than 15% (Fig. 3), which indicated that these clusters were three distinguishable genetic T6SS loci again (see Table 1).

The T6SS1 loci of APEC isolates were between 27.1 and 33.6 kb in size and encompass 18–25 protein coding sequences. Fifteen of these belonged to conserved T6SS proteins outlined by Boyer et al. (2009) (Figs. 1 and 3B). Almost all of the T6SS2 loci, consisted of only seventeen T6SS core genes, ranged a size of around 23 kb, of which the cluster from ED069 strain was the only exception (Fig. 3). The T6SS3 loci ranged a size of around 18.5 kb and encompassed 16 ORFs (Figs. 1 and 3B).

#### 3.2. VgrG islands analysis in T6SS loci

The concept of VgrG islands was first proposed by De Maayer et al. (2011) and has been applied to most of the T6SS loci from a variety of Gram negative bacteria. In this study, we also made a VgrG island analysis in APEC isolates, indicating that only T6SS1

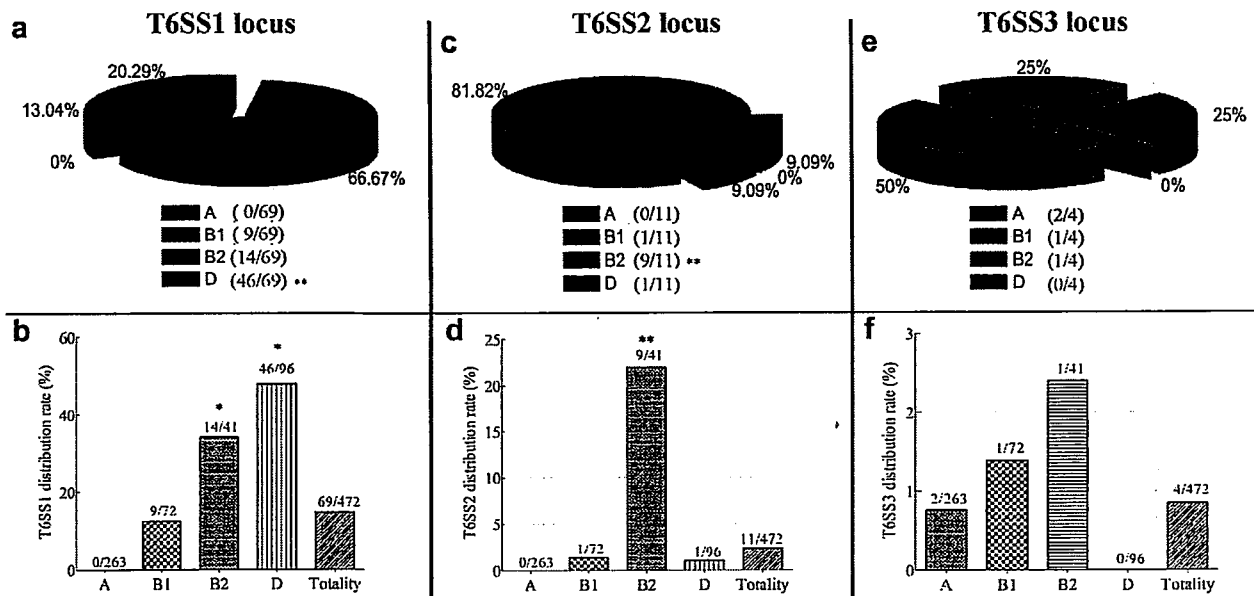


**Fig. 2.** The prevalence and phylogenetic groups analysis of T6SS loci among APEC isolates. (a), (c) and (e): The proportion of T6SS-positive isolates belongs to different phylogenetic groups. (b), (d) and (f): The distribution rate of three T6SS loci in different phylogenetic groups of APEC respectively. The T6SS1 is described by figures (a) and (b), the T6SS2 is described by figures (c) and (d), the T6SS3 is described by figures (e) and (f). Statistical significance was determined by a Student's *t* test based on comparisons with other groups (\*\* $P < 0.01$ ; \* $P < 0.05$ ).

loci contained both "COG4253" VgrGs and a visible island structure (Figs. 4 and 5). Although the T6SS1 locus shared conserved and syntenous cores in this study, considerable variability in the VgrG downstream regions was observed. Interestingly, the conserved core proteins of T6SS1 locus were arranged in two syntenous clusters (blocks I and III, see Fig. 5C), between which sandwiched a variable region (block II, see Fig. 5C), which was speculated to link with the VgrG gene encoded in the middle region of these clusters (De Maayer et al., 2011). The COG4235 is a part of the DUF 2345 superfamily, which contains VgrG-Rhs (rearrangement hot spot) proteins. The Rhs domain of the VgrGs was verified to potentially drive effector acquisition and diversity in a previous study (Wang et al., 1998).

The GC content analysis showed that the variable and unknown regions (43.97%) had a lower average value than the conserved core regions (56.9%) (Table S2). A phenomenon was noticed that the C-terminal extensions (putative effector-activity domain) of VgrGs had a similar value (48.24%) with the variable regions, while the N-terminal regions containing gp27 and gp5 domains (Cascades, 2008) (Fig. 5A) shared an approximate value (58.95%) with the conserved regions (Table S2). The presence of multiple non-homologous or highly divergent forms of unexploited genes and the C-terminal extensions of VgrGs, together with the lower GC content of these regions, supporting the view that these genes may have been imported into APEC (or their ancestors) on multiple occasions by an unknown mechanism of VgrGs.

To further prove this hypothesis, the proteins encoded in the variable VgrG islands were analyzed for its sequence similarity, structural homology and the presence of conserved domains to known proteins. The majority of proteins encoded on the islands showed homology to proteins of unknown function. However, a number of island proteins shared high sequence identity and contained conserved domains which suggested that they might represent T6SS effectors with putative functions in host–microbe and inter–bacterial interactions (Table 2). We found 12 proteins that contained conserved domains (named Pro1 to Pro12, Table 2, Fig. 5C). Each of them could be encoded in multiple APEC isolates.

### 3.3. The T6SS1 locus encode a multipurpose T6SS

The prevalence analysis displayed that the T6SS1 locus was more widely distributed in 472 APEC isolates (14.62%) compared with the T6SS2 and 3 (Fig. 2). Of 69 T6SS1 strains, 42 (66.67%) belonged to phylogenetic group D, while 14 (20.29%) belonged to group B2 and 9 (13.04%) belonged to group B1, but no strain belonged to group A (Fig. 2a). These data indicated that the T6SS1 locus had extensive adaptability in different background APEC strains, and also suggested the function diversity of T6SS1. Moreover, the distribution rate of T6SS1 locus was significantly higher in group D (47.92%) and B2 (34.15%), suggesting that T6SS1 was mainly encoded in virulent isolates of groups B2 and D (Johnson et al., 2006) and thus made contribution to APEC pathogenicity.

The T6SS1 locus of APEC isolates could be clearly divided into seven branches by the phylogenetic analysis (Fig. 3A), while the similar situation did not appear in the T6SS2 and 3 loci. Likewise, DNA sequence comparisons and linear interactive plots displayed that the T6SS1 locus presented great variability in both gene number and sequence polymorphism (Fig. 3B). This likely reflected the complex evolutionary mechanisms in APEC which facilitated the adaptation of T6SS1 to different hosts. A longer sequence and more unknown genes of T6SS1 locus provided the possibility to perform adjustable functions aiming different host cells.

The functional diversity can be observed more directly by analyzing of effectors encoded in VgrG islands. Based on the analysis of a substantial number of hypothetical effector proteins, we supposed that the VgrG islands of T6SS1 locus function in mediating virulence, competition proliferation and bacteria evolution. The importance of T6SS in pathogenesis is becoming increasingly obvious. In this study, a zinc-dependent metalloproteinase (Pro6), which is associated numerous times with pathogenicity in previous researches (Wassif et al., 1995; Woods et al., 2001), was found to be encoded in VgrG islands of APEC. Furthermore, the PGAP1-like protein (Pro1) found in this study contained a conserved domain of lipases, which had been shown to represent a major virulence factor in both animal and plant pathogens (Nardini et al., 2000; Ham et al., 2011). However, *E. coli* is an opportunistic path-

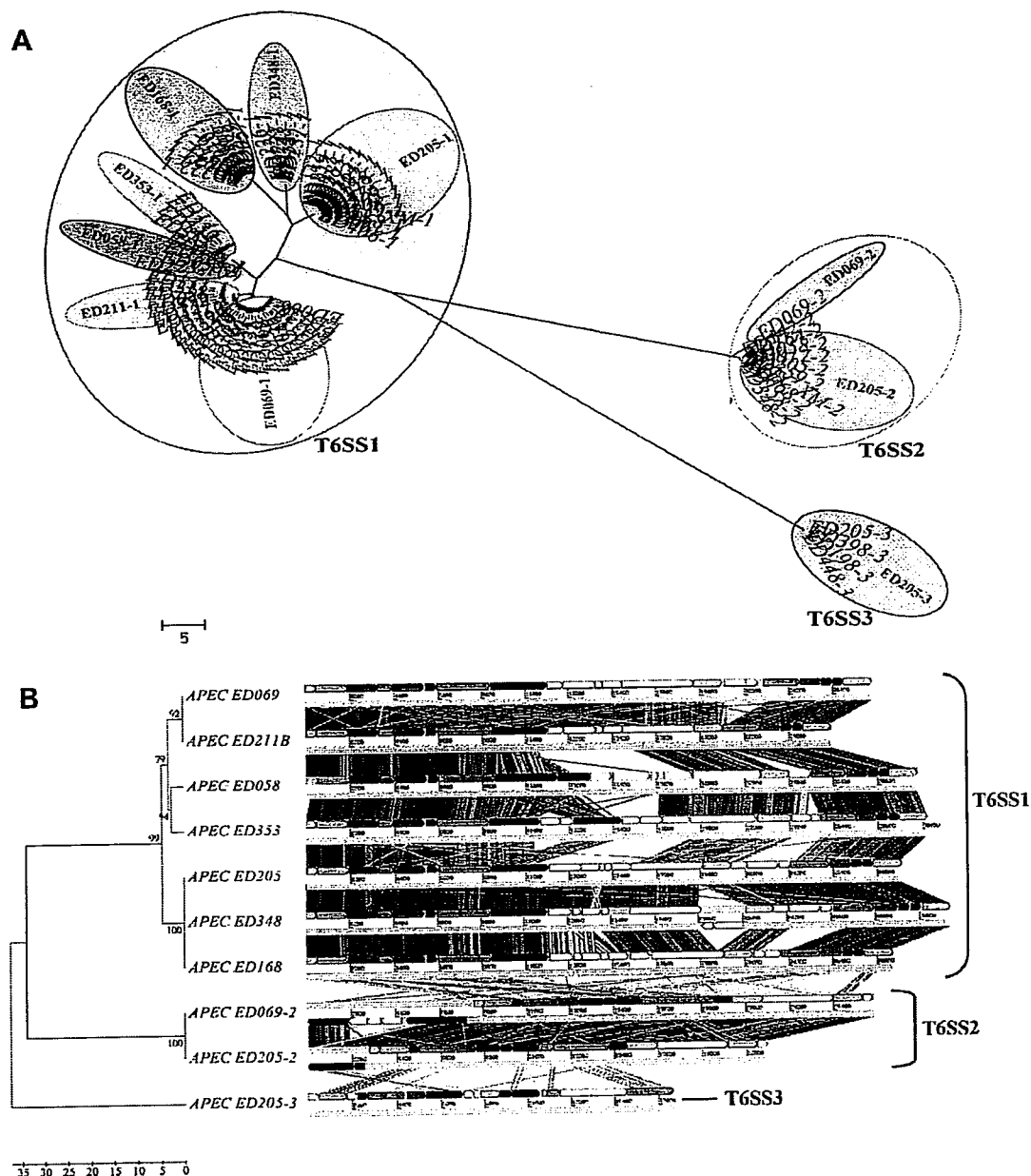


**Fig. 3.** The phylogenetic trees construction and comparative genomics analysis. (A) Sequence relationship of all T6SS clusters. The whole T6SS nucleotide sequences were aligned with ClustalW, and the MEGA software version 5.0 was used to perform a 2000 bootstrap phylogenetic analysis using the neighbor joining method. Large clades are indicated by colored and named by representative isolates. (B) Comparative genome alignments of 10 T6SS loci selected according to the result of Fig. 3A. The color key for the functional classes of genes and relevant information are the same as shown in Fig. 1. Phylogenetic relationships of the T6SS loci were obtained using a neighbor-joining tree (bootstrap  $N = 1000$ ) based on a ClustalW alignment of the complete T6SS nucleotide sequences. Visual representation of the alignments using nucleotide similarities (tblastx) of the T6SS loci and were carried out with the Artemis Comparison Tool (ACT) (Carver et al., 2005).

ogen, and many *E. coli* strains with genomes encoding T6SS locus are not known to be pathogenic or even symbionts. In this study, the analysis of hypothetical effectors encoded in VgrG islands revealed that many proteins were not associated with pathogenicity, which suggested T6SS may also function in nonpathogenic bacteria–host interactions. Based on our analysis of the VgrG islands proteins contained conserved domains, the nonpathogenic function of T6SS1 locus could be summarized as competition proliferation and bacteria evolution. The PAAR-repeat domain of Pro5, 11 and 12 in VgrG islands could sharpen and diversify the T6SS spike and were required for full functionality of the T6SS in *V. cholerae* and *Acinetobacter baylyi* (Shneider et al., 2013). The presence of

bacteriocin-like proteins (Pro11) in the T6SS1 locus of these APEC isolates supported the finding of a potential function for the T6SS in antibiosis and competition (Hood et al., 2010; Russell et al., 2011). The bacteriocins could take part in killing closely related bacterial species (Lesic et al., 2009). Furthermore, the VgrG trimer showed structural resemblance with the  $(gp27)_3$ – $(gp5)_3$  spike complex of T4 bacteriophage, which was used as the cell-puncturing apparatus to deliver viral DNA into bacterial target cells (Cascales, 2008). Coincidentally, many VgrG island proteins of APEC in this study contained integrase (Pro10) and helicase (Pro8) core domains and performed a transposase function, and these transposase are considered to be correlated with bacteriophage. These

**Table 1**  
The large clades of phylogenetic tree of T6SS nucleotide sequences and their representative isolate.

T6SS locus	Group	Number of orthologous locus	Representative isolates			Length of the T6SS locus <sup>a</sup> (bp)	Number of orfs <sup>b</sup>	GenBank accession No.
			Name	Serogroups	Phylogenetic groups			
T6SS1	I	3	ED058	O7	B1	30,000–31,000	22	KF678356
	II	21	ED069	O6	D	28,000–29,000	20–22	KF678354
	III	11	ED168	Unknown	B2	29,000–30,000	20–22	KF678357
	IV	17	ED205	O2	B2	29,000–30,000	22–24	KF678351
	V	7	ED211B	O75	D	26,000–27,000	17–19	KF678358
	VI	6	ED348	O1	B2	32,000–33,000	23–25	KF678359
	VII	4	ED353	Unknown	B2	30,500–31,500	24	KF678360
		Total 69						
T6SS2	VIII	10	ED205	O2	B2	22,000–24,000	17	KF678352
	XI	1	ED069	O6	D	28,461	21	KF678355
		Total 11						
T6SS3	X	4	ED205	O2	B2	18,000–19,000	16	KF678353
		Total 4						

<sup>a</sup> From the first to last conserved core gene of T6SS.

<sup>b</sup> Ignoring flanking genes.

observations suggested that T6SS1 locus might play an important role in the evolutionary mechanism of APEC, which relies on the bacteriophage to evolve.

A phylogeny based on the VgrG–T6SS1 proteins showed that all of them were from different *E. coli* pathotypes, but mixed together. It was difficult to pinpoint which one was from ExPEC or which one was from intestinal pathogenic *E. coli* (Fig. 4). Interestingly, the expression competence of each VgrG proteins was very close in levels, thus no significant difference was observed among seven pathotypes (Fig. 5B). It seemed that the T6SS1 locus could function in every *E. coli* pathotype and would played versatile roles in a variety of survival environments.

The original study of T6SS was in the context of pathogenic bacterial–host interactions, though it should not be limited in such narrow space. Several papers had highlighted the diverse potentials of T6SS functions (Jani and Cotter, 2010). The versatile T6SS may also function to promote commensal or mutualistic relationships between bacteria and eukaryotes (Hood et al., 2010), or to mediate both cooperative and competitive interactions between bacteria (Robinson et al., 2009). These latest progresses seemed to explain why the APEC T6SS1 locus had the sequence and effectors diversity, wide distribution and expression. In conclusion, we speculated that the APEC T6SS1 locus was not just for pathogenesis anymore.

### 3.4. The T6SS2 loci encode a single-minded T6SS

The prevalence of T6SS2 locus was very single-minded, and had an addition to encode in phylogenetic group B2. Of 472 APEC isolates, 11 strains (2.33%) were confirmed to encode the T6SS2 locus. Among them, 9 (81.82%) belonged to group B2, and the remaining two belonged to group B1 and D respectively (Fig. 2c). Group B2 (21.95%) was the most prevalent phylogenetic group within the T6SS2 locus (Fig. 2d). These results indicated that the function of T6SS2 locus seemed to focus on an unknown aspect. In the previous study, the group B2 was proved to have a higher chance to produce virulent strains, which seemed to suggest that the T6SS2 locus make contribution to APEC virulence.

Although 11 T6SS2 loci of APEC isolates could be divided into two branches by the phylogenetic analysis (Fig. 3A), the small branch contained only one strain (ED069). T6SS2 loci of the ten APEC isolates from the big branch shared a sequence of more than 95% identity, and retained a conserved and compact gene cluster structure by observing the representative T6SS2 cluster from ED205 (Fig. 3). There were not any variable and unknown regions inserted into sequences of most T6SS2 locus. The above description

suggested that the T6SS2 might have particular function aiming specific target cells, and was critical in some special mechanisms.

The phylogenetic tree of VgrG–T6SS2 proteins showed that they branched into two distinct clades (Fig. 4), which suggested distinct evolutionary backgrounds of these paralogous proteins. All of the VgrGs from APEC T6SS2 locus were assigned to ExPEC branch, which indicated that the same function was performed in extra-intestinal survival proliferation or pathogenic mechanism. Surprisingly, their expression competence of VgrG–T6SS2 also had huge difference between ExPEC and intestinal pathogenic *E. coli*. Only the NMEC and APEC had a high expression level, while the UPEC barely reached a normal level (Fig. 5B). The same result was shown by the research of de Pace et al. (2010). According to him, the APEC strain expressed T6SS genes at significantly higher levels than EHEC strain did through a transcriptomics analysis. Coincidentally, the T6SS2 locus of NMEC had been reported to play an important role in the invasion of human brain microvascular endothelial cells (Zhou et al., 2012). These results suggested that the T6SS2 might also perform an important function in avian *E. coli* causing meningitis.

The prevalence which only appeared in group B2, conserved and compact cluster structure, “ExPEC branch” VgrG proteins and expression only in meningitis *E. coli*, all of these evidences suggested that the APEC T6SS2 locus might perform a role in the meningitis mechanisms.

### 3.5. The T6SS3 loci encode a unserviceable T6SS

A prevalence analysis was performed to discover the phylogenetic distribution of the T6SS3 in 472 APEC isolates. However, unlike previous surveys of T6SS1 and 2, only 4 strains (0.85%) were revealed to encode the T6SS3 locus, and they belonged to three different phylogenetic groups (A, B1, and B2) (Fig. 2). These results were neither statistically significant, nor inspirational. The amount of APEC isolates encoded T6SS3 locus was negligible, apparently suggesting that it did not contribute to the pathogenicity of APEC or perform other special missions.

The phylogeny based on the whole T6SS loci showed a greater evolutionary distance between the T6SS3 and the other two T6SS loci (Fig. 3A), indicating that it might have been acquired through horizontal gene transfer. This could also be correlated with greater diversity in GC and gene content between the T6SS3 and other two T6SS loci (Fig. 3B). The GC content of conserved core regions was significantly lower in the T6SS3 loci (38.12%) than in the T6SS1 and 2 loci (56.93%), supporting the view that the T6SS3 locus might have been imported into APEC (or their ancestors) from distant

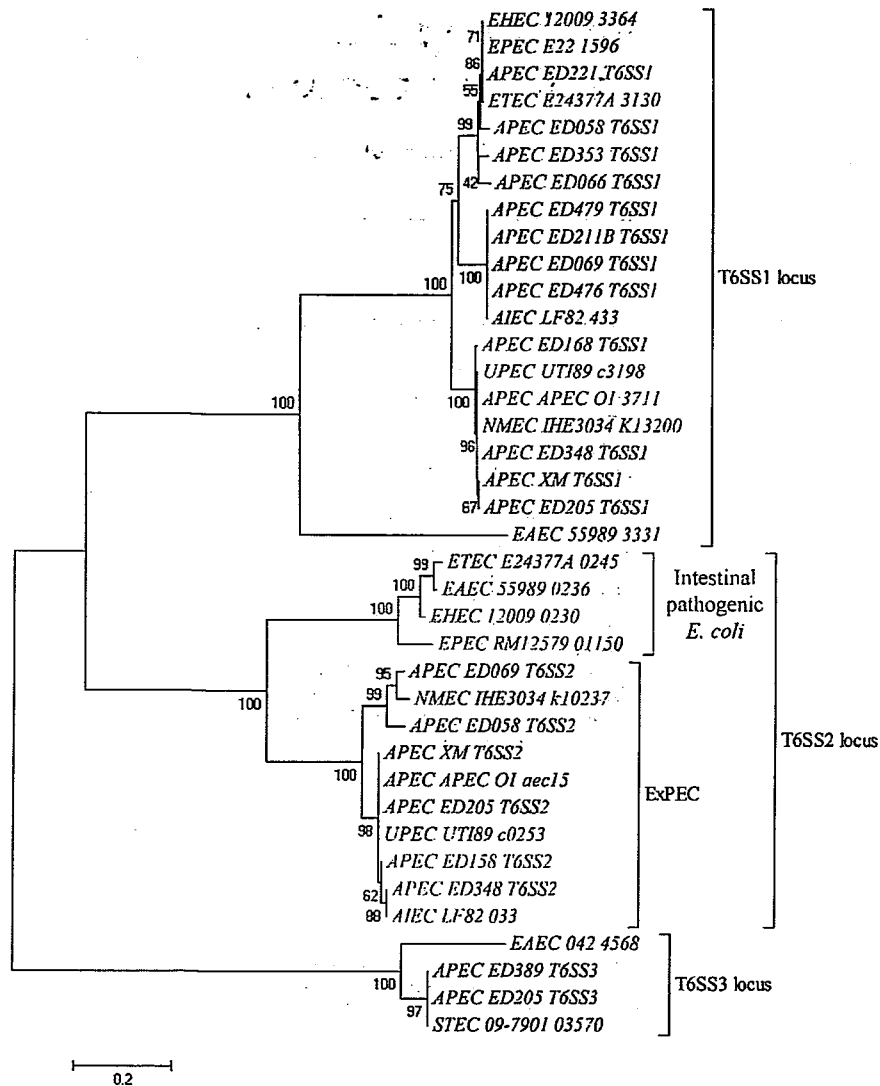


Fig. 4. Evolutionary relationships of VgrG proteins. A neighbor-joining tree (bootstrap  $n = 1000$ ; Poisson correction) was constructed based on a ClustalW alignment of the VgrG amino acid sequences from the APEC T6SS loci and orthologous loci in other *E. coli* pathotypes.

species without correct transcription and translation guaranteed. In addition, only twelve of the T6SS conserved core proteins identified by Boyer et al. (2009) were encoded within the T6SS3 locus. Genes encoding orthologs of the Hcp-related, VC\_A0112/FHA, VC\_A0113, VC\_A0119 and VC\_A0118 family proteins are absent (Figs. 1 and 3B). Hcp-related protein is an essential component of the T6SS injection machine, and the Hcp hexamer assemble is likely the shaft of a "bolt gun" that is loaded with effectors before being fired into a target cell (Silverman et al., 2013). The phosphorylation of FHA protein can promote the clustering of ClpV, and the latter provided the force required for the assembly of the secretion machine as well as for the translocation of exported proteins (Mougous et al., 2006). The absence of the two key proteins above indicated that the T6SS3 locus could not be assembled as a fully functional T6SS complex.

### 3.6. The properties difference of three T6SS loci may be supervised by the VgrG proteins

As previously described De Maayer et al. (2011) all VgrG orthologues could be divided into three different groups ("COG4253"

VgrG (Blondel et al., 2009), evolved VgrG and ordinary VgrG; Figs. 4 and 5Ab). The transportation capability of effectors genes presented a huge difference in the three VgrGs groups, which determined the high or low sequence identity of T6SS. In this study, the "COG4253" group contained all of the T6SS1 VgrG proteins, which encoded a conserved domain of unknown function (COG4253) which was absent in the T6SS2 and 3 loci VgrG proteins (Fig. 4). Interestingly, all T6SS1 clusters that encoded a "COG4253" VgrG carried more variable and unknown genes than other T6SS loci, suggesting that the VgrG island structure might be associated with the COG4253 domain. Therefore, the COG4253 conserved domain might be involved in the anchorage of the VgrG transporter to the effector proteins. These suggestions also implied that COG4253-positive and COG4253-negative T6SS VgrG proteins had different targets and functions (Blondel et al., 2009). Furthermore, some of the proteins encoded in the hypothetical VgrG islands showed sequence homology and contained conserved domains found in the C-terminal extensions of VgrG proteins. For example, the Pro-4 of some APEC isolates shared 83% amino acid identity with the C-terminal region of their VgrG-T6SS1 and encoded a COG4253 domain (Table 2). Moreover, the ED058\_Vn

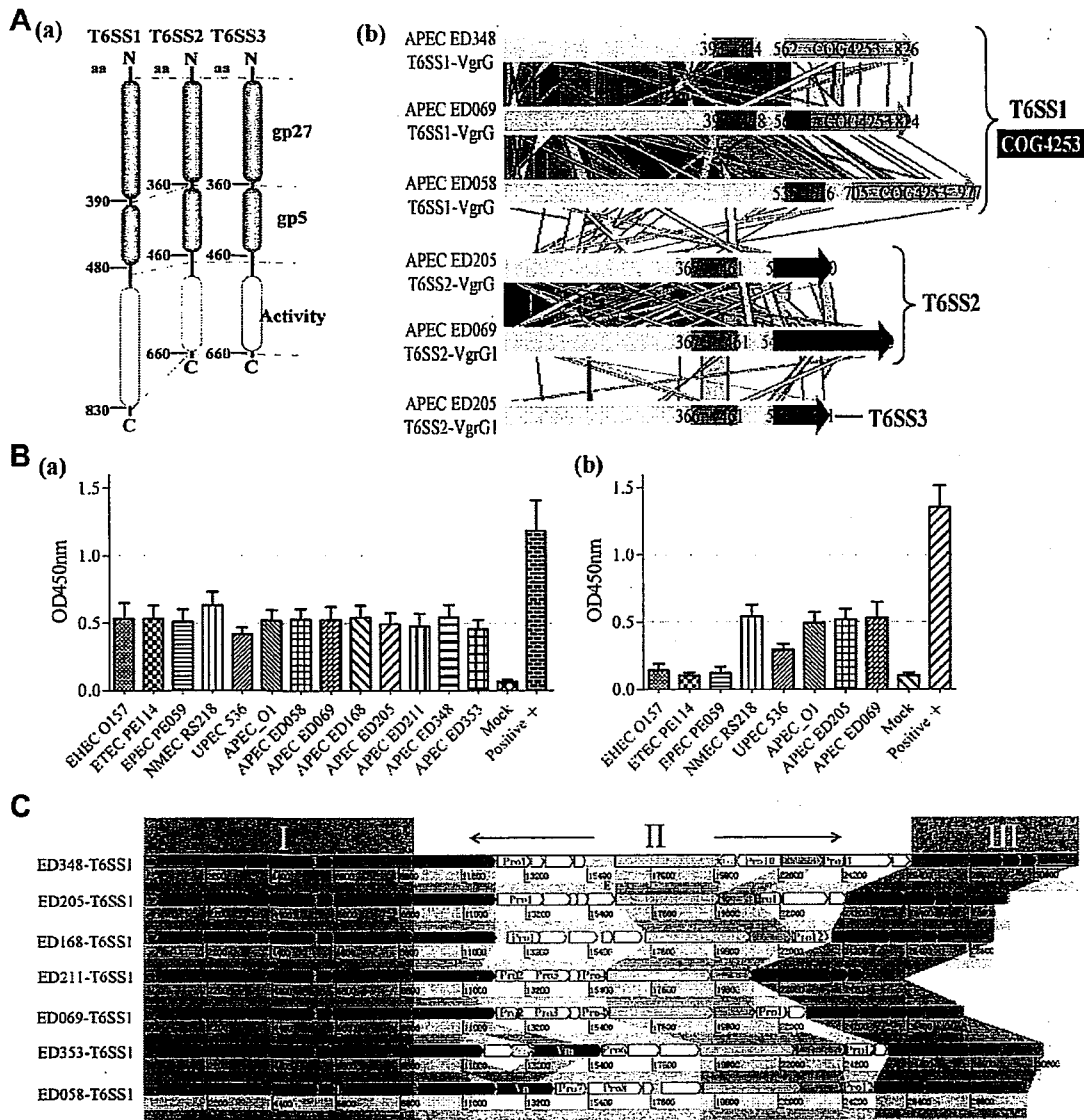


**Fig. 5.** The conserved domains and expression competence analysis of VgrG proteins and the hidden VgrG islands. (A) Domain organization of VgrG. (a): The conserved domains analysis of ED205 VgrG proteins, according to the domains and structures bank of NCBI. (b): Comparisons of 6 different VgrG proteins selected according to the result of Fig. 4. The conserved VgrG domains are shown in blue, Gp5 domains are shown in gray, the non-conserved C-terminal extensions are shown in red, COG4253 domains in purple. (B) ELISA analysis of the VgrGs expression. A sample A450 value/negative control A450 value (S/N) >2 was used as the positive standard. (a): The expression competence of VgrG-T6SS1 proteins in different *E. coli* pathotypes. (b): The expression competence of VgrG-T6SS2 proteins in different *E. coli* pathotypes. (C) Hypothetical VgrG islands hidden in block II of T6SS1 locus of the APEC strains. The conserved regions are shaded in grey, while non-conserved regions are not shaded. The blocks I and III sequences only encode conserved core genes and have a high identity, while the block II sequences contained several variable and unknown genes. Several color-coded genes were analyzed as the putative effectors and described in detail at the Table 2. (For interpretation of the references to color in this figure legend, the reader is referred to the web version of this article.)

and ED353\_Vm amino acid sequences shared 68% and 92% amino acid identity with the C-terminal region of their T6SS1 VgrG (Table 2). These above cases have been reported to present in other bacterial species, indicating that "COG4253"VgrG proteins had a stronger capability and played an important role in the formation of specific function of T6SS1. The VgrG-T6SS2 protein of APEC ED069 represented the "evolved" group, which encoded a longer variable C-terminal extensions (Fig. 5Ab) that might led to the insertion of three unknown genes and the second VgrG protein (see Fig. 3B). Almost all of the T6SS2 and T6SS3 VgrG proteins were considered to be ordinary, and kept a stable length (660 aa; Figs. 4 and 5Ab). The size of their C-terminal regions was less than 150 aa, thus was not enough to be capable of the transporting effectors genes. Therefore, both T6SS2 locus and T6SS3 locus kept high se-

quence identity and compact structure. In summary, the VgrG proteins partly determined the sequence diversity of T6SS loci and had a significant impact to the functional characteristics of T6SS among APEC isolates.

Each VgrG protein contained three parts, a gp27 domain, a gp5 domain and the variable activity domain (Cascales, 2008) (Fig. 5Aa). The similarity between gp27 domain and tail fiber protein of bacteriophage has been proved many times (Leiman et al., 2009). A recent research showed that tail fiber protein of *V. cholerae* phage VP3 could function as a receptor-binding protein and responsible for host cells recognition (Zhang et al., 2009). Therefore, we speculated that host specificity, which shared a similar mechanism with bacteriophage, was also presented in different T6SSs. In this study, the comparative analysis of gp27 domains of

**Table 2**  
Properties of proteins in the hypothesized VgrG islands.

Number of proteins <sup>a</sup>	Conserved domains	Homologous function proteins (amino acid identity)	Function
Pro1	PGAP1[pfam07819]	PMI17_02526 of <i>Pantoea</i> sp. GM01 (41%)	PGAP1-like protein
Pro2	PRK01096[PRK01096]	FF52_01210 of <i>Flavobacterium</i> sp. F52 (48%)	Glycoside hydrolase
Pro3	Abhydrolase_1[pfam00561]	A225_2636 of <i>Klebsiella oxytoca</i> E718 (46%)	Transmembrane protein
Pro4	COG4253/ DUF2345[pfam10106]	VgrG C-terminal extensions sequence of every isolate, respectively (>80%)	Unknown
Pro5	COG5433/ PAAR_motif[pfam05488] <sup>b</sup>	ECSTEC94C_0675 of <i>Escherichia coli</i> STEC_94C (93%)	PAAR-repeat protein, transposase, IS4 family.
Pro6	M35_like_1[cd11007]	ECUMN_1706 of <i>E. coli</i> UMN026 (30%)	Putative zinc-dependent metalloproteinase
Pro7	DUF4123[pfam13503]	–	Domain of unknown function
Pro8	UvrD_C_2[pfam13538]	EC55989_3316 in <i>E. coli</i> 55989 (99%)	UvrD/REP helicase
Pro9	IstB_IS21[pfam01695]	ECDEC10F_1826 of <i>E. coli</i> DEC10F (99%)	IstB-like ATP binding protein
Pro10	Sigma70_r4/RVE[pfam00665]	TnpA of <i>E. coli</i> CB9615 (99%)	Transposase for ISEc12
Pro11	PAAR_motif[pfam05448] <sup>b</sup>	EC30301_3278 of <i>E. coli</i> 3030-1 (85%)	PAAR/S-type pyocin domain
Pro12	PAAR_motif[pfam05448] <sup>b</sup>	SSJG_02256 of <i>Shigella</i> sp. D9 (67%)	PAAR/S-type pyocin domain
Vm	VgrG[COG3501]/COG4253	Evolved VgrG proteins of ED353 (92%)	The second VgrG protein in T6SS1 locus of APEC ED353
Vn	VgrG[COG3501]/COG4253	VgrG C-terminal extensions sequence of ED058 (68%)	Shortened VgrG protein in T6SS1 locus of APEC ED058

<sup>a</sup> The number of unknown proteins in the VgrG islands is the same as that shown in Fig. 5C.

<sup>b</sup> The PAAR motif has been verified for the full functionality of T6SS is a must in a recent study (Shneider et al., 2013).

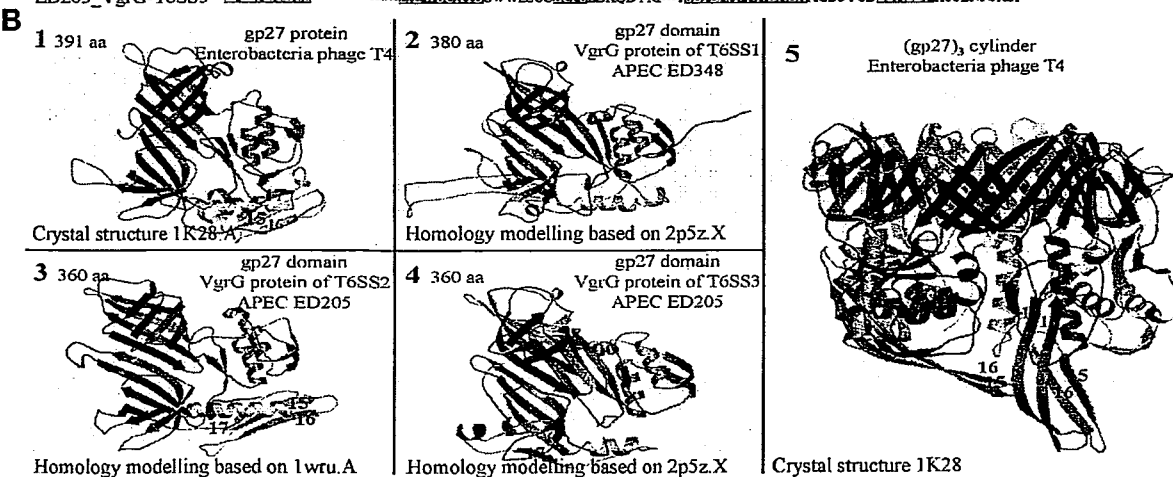
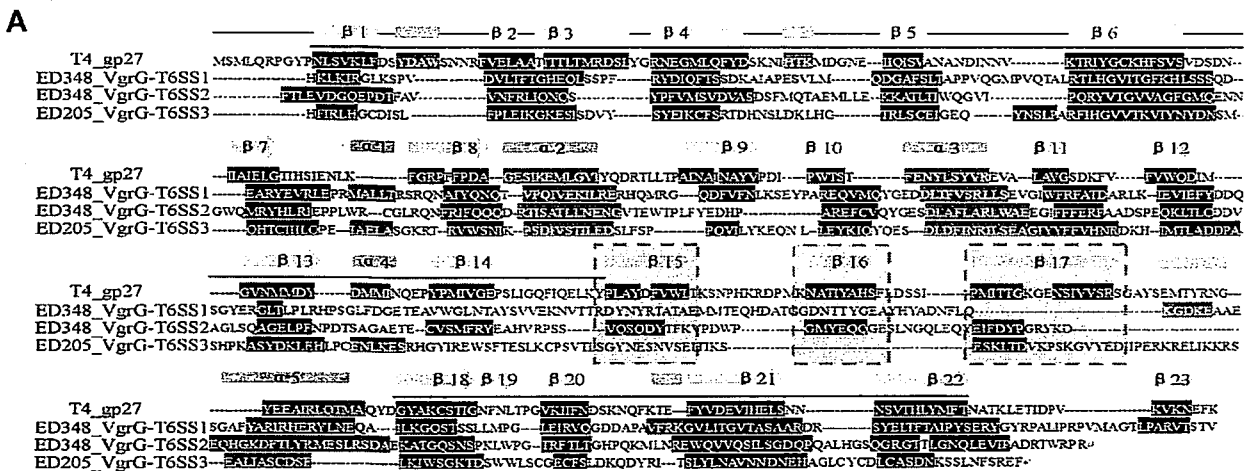


**Fig. 6.** The structure prediction and modeling of VgrGs proteins. (A) Sequence alignment and secondary structure of VgrGs proteins. The red line at the top of amino acid sequences indicates the first domain. The secondary structural elements are shown in the sequences as dark green blanket ( $\alpha$ -helices) and dark red blanket ( $\beta$ -sheets). The  $\alpha$ -helices and  $\beta$ -sheets of phage gp27 proteins are indicated as purple cylinders and blue arrows above the sequences again, respectively. The secondary structures of VgrG proteins are assigned using define secondary structure of proteins (DSSP) criteria of SWISS-MODEL (Arnold et al., 2006). (B) Homology modeling of gp27 homologues based on the crystal structure of c3393 of *E. coli* CFT073 (PDB code: 2p5z.X) or tail protein of bacteriophage Mu (PDB code: 1wru.A). Stereoview of gp27 domains in ribbon representation and rainbow coloring, from blue (N-term) to red (C-term). These models were generated by employing the SWISS-MODEL server (<http://swissmodel.expasy.org>) (Arnold et al., 2006). Model 1 is the ribbon representation of the gp27 protein crystal structure (PDB code: 1K28.A) from phage T4. Model 5 is the gp27 trimer of phage T4 (PDB code: 1K28). The different parts of gp27 s domain are labeled 15 $\beta$ , 16 $\beta$  and 17 $\beta$  sheets among the four proteins according to the result of Fig. 6A. (For interpretation of the references to color in this figure legend, the reader is referred to the web version of this article.)



three T6SS loci and gp27 protein of bacteriophage T4 was performed to provide a reference to predict the target cells diversity of T6SS.

The analysis showed that each monomer of gp27 domains contained at least 3  $\alpha$ -helices and 18  $\beta$ -sheets (Fig. 6). The gp27 domains were divided into two smaller domains (Kondou et al., 2005). The first domain (approximately, residues 10–90, residues 160–185, and residues 275–340) located on the left side of the models and consisted primarily of  $\beta$ -sheets. And the second domain (approximately, residues 90–160, residues 185–275, and 340–370) folded into a  $\alpha\beta$ -structure. APEC VgrG gp27 domains had the same folding topology as T4 phage gp27 (Fig. 6B). Despite the high degree of structural similarity, these four gp27 domains/proteins only shared 4% amino acid identity over the relevant 250 residue sequence (Fig. 6A). In particular, the first domain was more closely matched with the four proteins mentioned previously than the second domain (Fig. 6B). The DALI algorithm assigned 101 equivalent amino acid residues (59.41%) between the first domains of the four proteins, whereas the corresponding value for the second domain was only 64 equivalent positions (27.83%). Previous research has proved that the first domain mediated associations with other baseplate proteins in bacteriophage (Kanamaru et al., 2002; Kondou et al., 2005), while the second domain carried out frequent interaction with cell surface components. These results suggested that the second domain of gp27 might be a key unit of selecting host cells. The further analysis showed that the  $\beta$ 15, 16 and 17 sheets were absent or shortened in the second domain of T6SS1 and 3 gp27s (Fig. 6B). By observing the gp27 trimer, these three  $\beta$ -sheets were found to have more opportunities to perform extensive and in-depth exchanges interacting with cell surface (Fig. 6B). It seemed to suggest that had great potential to function as a receptor-binding protein. A previous research indicated that the shortening of these three  $\beta$ -sheets in gp44 (a tail fiber protein of Bacteriophage Mu) caused a more positive electrostatic potential (Kondou et al., 2005). Mu phage relies upon the electrostatic interactions of gp44 with the host cell membrane to initiate infection. This infection method would confer a low degree of host specificity and allow Mu phage to infect multiple different unrelated bacteria. This phenomenon seemed to tell us that the T6SS1 and 3 of APEC may have a wide host cells spectrum. The multipurpose T6SS1 clarified by previous description also proved this view. In addition, the second domain of T6SS2 gp27 kept a high similarity with one of phage gp27 protein, even longer  $\beta$ 15-sheet,  $\beta$ 16-sheet and  $\alpha$ 5-helice were observed in T6SS2 gp27 domain (Fig. 6). These indicated that the T6SS2 and phage T4 might share a high degree of host specificity and explained why only APEC and NMEC had high expression level of VgrG-T6SS2 protein. The above description also suggested that there was an indistinct correlation between single-minded T6SS2 and its high gp27-like VgrG protein.

In summary, the VgrG proteins were not only related to the cluster characteristics (sequence identity, effectors coding and cluster structure) of T6SS loci, but also played a key role in specific functions formation of T6SS among APEC isolates by participating in recognition of host cells. Therefore, we developed a divergent thought that the functional characteristics of T6SS loci may be supervised by the VgrG proteins.

#### 4. Conclusions

This study provides a basis for further focused investigations on this newly discovered and poorly understood secretion system in APEC. The three T6SS loci comparative genomics showed extensive diversity in prevalence analysis, number of core genes and sequence identity, which suggested that they might play respective roles in different mechanisms. The COG4253 and gp27 domains

of VgrGs were found to be associated with the transport of putative effector islands and conferring target cells specificity respectively, which clearly indicate the properties difference of T6SS might be supervised by the VgrG proteins.

#### Acknowledgments

This research was supported by the Special Fund for Advantage Discipline Construction of Colleges and Universities in Jiangsu, and National Nature Science Foundation (31372455), and Fundamental Research Funds for the Central Universities (KYZ201274).

We thank Jianjun Dai (Nanjing Agricultural University) and Yueming Wang (Shantung Academy of Agriculture) for kindly providing part of avian pathogenic *E. coli* isolates for this study.

#### Appendix A. Supplementary data

Supplementary data associated with this article can be found, in the online version, at <http://dx.doi.org/10.1016/j.meegid.2013.09.031>.

#### References

- Arisaka, F., Kanamaru, S., Leiman, P., Rossmann, M.G., 2003. The tail lysozyme complex of bacteriophage T4. *Int. J. Biochem. Cell Biol.* 35, 16–21.
- Arnold, K., Bordoli, L., Kopp, J., Schwede, T., 2006. The SWISS-MODEL workspace. A web-based environment for protein structure homology modelling. *Bioinformatics* 22, 195–201.
- Bingle, L.E., Bailey, C.M., Pallen, M.J., 2008. Type VI secretion: a beginner's guide. *Curr. Opin. Microbiol.* 11, 3–8.
- Blondel, C.J., Jimenez, J.C., Contreras, I., Santiviago, C.A., 2009. Comparative genomic analysis uncovers 3 novel loci encoding type six secretion systems differentially distributed in *Salmonella* serotypes. *BMC Genomics* 10, 354.
- Bonemann, G., Pietrosiuk, A., Diemand, A., Zentgraf, H., Mogk, A., 2009. Remodelling of VipA/VipB tubules by ClpV-mediated threading is crucial for type VI protein secretion. *EMBO J.* 28, 315–325.
- Boyer, F., Fichant, G., Berthod, J., Vandenbrouck, Y., Attree, I., 2009. Dissecting the bacterial type VI secretion system by a genome wide in silico analysis: what can be learned from available microbial genomic resources? *BMC Genomics* 10, 104.
- Carver, T.J., Rutherford, K.M., Berriman, M., Rajandream, M.A., Barrell, B.G., Parkhill, J., 2005. ACT: the Artemis Comparison Tool. *Bioinformatics* 21, 3422–3423.
- Cascales, E., 2008. The type VI secretion toolkit. *EMBO Rep.* 9, 735–741.
- Clermont, O., Bonacorsi, S., Bingen, E., 2000. Rapid and simple determination of the *Escherichia coli* phylogenetic group. *Appl. Environ. Microbiol.* 66, 4555–4558.
- De Maayer, P., Venter, S.N., Kamber, T., Duffy, B., Coutinho, T.A., Smits, T.H., 2011. Comparative genomics of the Type VI secretion systems of *Pantoea* and *Erwinia* species reveals the presence of putative effector islands that may be translocated by the VgrG and Hcp proteins. *BMC Genomics* 12, 576.
- de Pace, F., Nakazato, G., Pacheco, A., de Paiva, J.B., Sperandio, V., Da S.W., 2010. The type VI secretion system plays a role in type I fimbriae expression and pathogenesis of an avian pathogenic *Escherichia coli* strain. *Infect. Immun.* 78, 4990–4998.
- Dho-Moulin, M., Fairbrother, J.M., 1999. Avian pathogenic *Escherichia coli* (APEC). *Vet. Res.* 30, 299–316.
- Dreyfus, A., Schaller, A., Nivollet, S., Segers, R.P., Kobisch, M., Mieli, L., Soerensen, V., Hussy, D., Miserez, R., Zimmermann, W., Inderbitzin, F., Frey, J., 2004. Use of recombinant ApxIV in serodiagnosis of *Actinobacillus pleuropneumoniae* infections, development and prevalidation of the ApxIV ELISA. *Vet. Microbiol.* 99, 227–238.
- Ewers, C., Janssen, T., Wieler, L.H., 2003. Avian pathogenic *Escherichia coli* (APEC). *Berl. Munch. Tierarztl. Wochenschr.* 116, 381–395.
- Filloux, A., Hachani, A., Bleves, S., 2008. The bacterial type VI secretion machine: yet another player for protein transport across membranes. *Microbiology* 154, 1570–1583.
- Ham, J.H., Melanson, R.A., Rush, M.C., 2011. *Burkholderia glumae*: next major pathogen of rice? *Mol. Plant Pathol.* 12, 329–339.
- Hood, R.D., Singh, P., Hsu, F., Guvener, T., Carl, M.A., Trinidad, R.R., Silverman, J.M., Ohlson, B.B., Hicks, K.G., Plemel, R.L., Li, M., Schwarz, S., Wang, W.Y., Merz, A.J., Goodlett, D.R., Mougous, J.D., 2010. A type VI secretion system of *Pseudomonas aeruginosa* targets a toxin to bacteria. *Cell Host Microbe* 7, 25–37.
- Jani, A.J., Cotter, P.A., 2010. Type VI secretion: not just for pathogenesis anymore. *Cell Host Microbe* 8, 2–6.
- Johnson, J.R., Owens, K.L., Clabots, C.R., Weissman, S.J., Cannon, S.B., 2006. Phylogenetic relationships among clonal groups of extraintestinal pathogenic *Escherichia coli* as assessed by multi-locus sequence analysis. *Microbes Infect.* 8, 1702–1713.
- Johnson, T.J., Kariyawasam, S., Wannemuehler, Y., Mangiamale, P., Johnson, S.J., Doethkott, C., Skyberg, J.A., Lynne, A.M., Johnson, J.R., Nolan, L.K., 2007. The genome sequence of avian pathogenic *Escherichia coli* strain O1:K1:H7 shares



- strong similarities with human extraintestinal pathogenic *E. coli* genomes. *J. Bacteriol.* 189, 3228–3236.
- Kanamaru, S., Leiman, P.C., Kostyuchenko, V.A., Chipman, P.R., Mesyanzhinov, V.V., Arisaka, F., Rossmann, M.G., 2002. Structure of the cell-puncturing device of bacteriophage T4. *Nature* 415, 553–557.
- Kohler, G., Milstein, C., 1975. Continuous cultures of fused cells secreting antibody of predefined specificity. *J. Immunol.* 174 (2005), 2453–2455.
- Kondou, Y., Kitazawa, D., Takeda, S., Tsuchiya, Y., Yamashita, E., Mizuguchi, M., Kawano, K., Tsukihara, T., 2005. Structure of the central hub of bacteriophage Mu baseplate determined by X-ray crystallography of gp44. *J. Mol. Biol.* 352, 976–985.
- Leiman, P.G., Basler, M., Ramagopal, U.A., Bonanno, J.B., Sauder, J.M., Pukatzki, S., Burley, S.K., Almo, S.C., Mekalanos, J.J., 2009. Type VI secretion apparatus and phage tail-associated protein complexes share a common evolutionary origin. *Proc. Natl. Acad. Sci. USA* 106, 4154–4159.
- Lestic, B., Starkey, M., He, J., Hazan, R., Rahme, L.G., 2009. Quorum sensing differentially regulates *Pseudomonas aeruginosa* type VI secretion locus I and homologous loci II and III, which are required for pathogenesis. *Microbiology* 155, 2845–2855.
- Ma, A.T., McAuley, S., Pukatzki, S., Mekalanos, J.J., 2009. Translocation of a *Vibrio cholerae* type VI secretion effector requires bacterial endocytosis by host cells. *Cell Host Microbe* 5, 234–243.
- Mora, A., Lopez, C., Dabhi, G., Blanco, M., Blanco, J.E., Alonso, M.P., Herrera, A., Mamani, R., Bonacorisi, S., Moulin-Schouleur, M., Blanco, J., 2009. Extraintestinal pathogenic *Escherichia coli* O1:K1:H7;NM from human and avian origin: detection of clonal groups B2 ST95 and D ST59 with different host distribution. *BMC Microbiol.* 9, 132.
- Mougous, J.D., Cuff, M.E., Raunser, S., Shen, A., Zhou, M., Gifford, C.A., Goodman, A.L., Joachimiak, G., Ordóñez, C.L., Lory, S., Walz, T., Joachimiak, A., Mekalanos, J.J., 2006. A virulence locus of *Pseudomonas aeruginosa* encodes a protein secretion apparatus. *Science* 312, 1526–1530.
- Moulin-Schouleur, M., Reperant, M., Laurent, S., Bree, A., Mignon-Grasteau, S., Germon, P., Rasschaert, D., Schouler, C., 2007. Extraintestinal pathogenic *Escherichia coli* strains of avian and human origin: link between phylogenetic relationships and common virulence patterns. *J. Clin. Microbiol.* 45, 3366–3376.
- Moulin-Schouleur, M., Schouler, C., Tailliez, P., Kao, M.R., Bree, A., Germon, P., Oswald, E., Mainil, J., Blanco, M., Blanco, J., 2006. Common virulence factors and genetic relationships between O18:K1:H7 *Escherichia coli* isolates of human and avian origin. *J. Clin. Microbiol.* 44, 3484–3492.
- Nardini, M., Lang, D.A., Liebeton, K., Jaeger, K.E., Dijkstra, B.W., 2000. Crystal structure of *Pseudomonas aeruginosa* lipase in the open conformation. The prototype for family I.1 of bacterial lipases. *J. Biol. Chem.* 275, 31219–31225.
- Parsons, D.A., Heffron, F., 2005. *SciS*, an *icmF* homolog in *Salmonella enterica* serovar Typhimurium, limits intracellular replication and decreases virulence. *Infect. Immun.* 73, 4338–4345.
- Pukatzki, S., Ma, A.T., Revel, A.T., Sturtevant, D., Mekalanos, J.J., 2007. Type VI secretion system translocates a phage tail spike-like protein into target cells where it cross-links actin. *Proc. Natl. Acad. Sci. USA* 104, 15508–15513.
- Pukatzki, S., Ma, A.T., Sturtevant, D., Krastins, B., Sarracino, D., Nelson, W.C., Heidelberg, J.F., Mekalanos, J.J., 2006. Identification of a conserved bacterial protein secretion system in *Vibrio cholerae* using the Dictyostelium host model system. *Proc. Natl. Acad. Sci. USA* 103, 1528–1533.
- Robinson, J.B., Telepnev, M.V., Zudina, I.V., Bouyer, D., Monteneri, J.A., Bearden, S.W., Gage, K.L., Agar, S.L., Foltz, S.M., Chauhan, S., Chopra, A.K., Motin, V.L., 2009. Evaluation of a *Yersinia pestis* mutant impaired in a thermoregulated type VI-like secretion system in flea, macrophage and murine models. *Microb. Pathog.* 47, 243–251.
- Rodríguez-Siek, K.E., Giddings, C.W., Doetkott, C., Johnson, T.J., Nolan, L.K., 2005a. Characterizing the APEC pathotype. *Vet. Res.* 36, 241–256.
- Rodríguez-Siek, K.E., Giddings, C.W., Doetkott, C., Johnson, T.J., Fakhr, M.K., Nolan, L.K., 2005b. Comparison of *Escherichia coli* isolates implicated in human urinary tract infection and avian colibacillosis. *Microbiology* 151, 2097–2110.
- Russell, A.B., Hood, R.D., Bui, N.K., LeRoux, M., Vollmer, W., Mougous, J.D., 2011. Type VI secretion delivers bacteriolytic effectors to target cells. *Nature* 475, 343–347.
- Sarris, P.F., Zoumadakis, C., Panopoulos, N.J., Scoulica, E.V., 2011. Distribution of the putative type VI secretion system core genes in *Klebsiella* spp. *Infect. Genet. Evol.* 11, 157–166.
- Shneider, M.M., Buth, S.A., Hø, B.T., Basler, M., Mekalanos, J.J., Leiman, P.G., 2013. PAA-repeat proteins sharpen and diversify the type VI secretion system spike. *Nature* 500, 350–353.
- Silverman, J.M., Agnello, D.M., Zheng, H., Andrews, B.T., Li, M., Catalano, C.E., Gonen, T., Mougous, J.D., 2013. Haemolysin coregulated protein is an exported receptor and chaperone of type VI secretion substrates. *Mol. Cell.* 51, 584–593.
- Wang, S., Niu, C., Shi, Z., Xia, Y., Yaqoob, M., Dai, J., Lu, C., 2011. Effects of *ibeA* deletion on virulence and biofilm formation of avian pathogenic *Escherichia coli*. *Infect. Immun.* 79, 279–287.
- Wang, Y.D., Zhao, S., Hill, C.W., 1998. Rhs elements comprise three subfamilies which diverged prior to acquisition by *Escherichia coli*. *J. Bacteriol.* 180, 4102–4110.
- Wassif, C., Cheek, D., Belas, R., 1995. Molecular analysis of a metalloprotease from *Proteus mirabilis*. *J. Bacteriol.* 177, 5790–5796.
- Woods, R.G., Burger, M., Beven, C.A., Beacham, I.R., 2001. The *aprX-lipA* operon of *Pseudomonas fluorescens* B52: a molecular analysis of metalloprotease and lipase production. *Microbiology* 147, 345–354.
- Xu, J., Zhang, J., Lu, X., Liang, W., Zhang, L., Kan, B., 2013. O antigen is the receptor of *Vibrio cholerae* serogroup O1 El Tor typing phage VP4. *J. Bacteriol.* 195, 798–806.
- Zhang, J., Li, W., Zhang, Q., Wang, H., Xu, X., Diao, B., Zhang, L., Kan, B., 2009. The core oligosaccharide and thioredoxin of *Vibrio cholerae* are necessary for binding and propagation of its typing phage VP3. *J. Bacteriol.* 191, 2622–2629.
- Zhou, Y., Tao, J., Yu, H., Ni, J., Zeng, L., Teng, Q., Kim, K.S., Zhao, G.P., Guo, X., Yao, Y., 2012. Hcp family proteins secreted via the type VI secretion system coordinately regulate *Escherichia coli* K1 interaction with human brain microvascular endothelial cells. *Infect. Immun.* 80, 1243–1251.

# Identification of Candidate Susceptibility and Resistance Genes of Mice Infected with *Streptococcus suis* Type 2

Jie Rong, Wei Zhang, Xiaohui Wang, Hongjie Fan, Chengping Lu, Huochun Yao\*

Key Lab of Animal Bacteriology, Ministry of Agriculture, Nanjing Agricultural University, Nanjing, China

## Abstract

*Streptococcus suis* type 2 (SS2) is an important swine pathogen and zoonosis agent. A/J mice are significantly more susceptible than C57BL/6 (B6) mice to SS2 infection, but the genetic basis is largely unknown. Here, alterations in gene expression in SS2 (strain HA9801)-infected mice were identified using Illumina mouse BeadChips. Microarray analysis revealed 3,692 genes differentially expressed in peritoneal macrophages between A/J and B6 mice due to SS2 infection. Between SS2-infected A/J and control A/J mice, 2646 genes were differentially expressed (1469 upregulated; 1177 downregulated). Between SS2-infected B6 and control B6 mice, 1449 genes were differentially expressed (778 upregulated; 671 downregulated). These genes were analyzed for significant Gene Ontology (GO) categories and signaling pathways using the Kyoto Encyclopedia of Genes and Genomes (KEGG) database to generate a signaling network. Upregulated genes in A/J and B6 mice were related to response to bacteria, immune response, positive regulation of B cell receptor signaling pathway, type I interferon biosynthesis, defense and inflammatory responses. Additionally, upregulated genes in SS2-infected B6 mice were involved in antigen processing and presentation of exogenous peptides, peptide antigen stabilization, lymphocyte differentiation regulation, positive regulation of monocyte differentiation, antigen receptor-mediated signaling pathway and positive regulation of phagocytosis. Downregulated genes in SS2-infected B6 mice played roles in glycolysis, carbohydrate metabolic process, amino acid metabolism, behavior and muscle regulation. Microarray results were verified by quantitative real-time PCR (qRT-PCR) of 14 representative deregulated genes. Four genes differentially expressed between SS2-infected A/J and B6 mice, toll-like receptor 2 (*Tlr2*), tumor necrosis factor (*Tnf*), matrix metalloproteinase 9 (*Mmp9*) and pentraxin 3 (*Ptx3*), were previously implicated in the response to *S. suis* infection. This study identified candidate genes that may influence susceptibility or resistance to SS2 infection in A/J and B6 mice, providing further validation of these models and contributing to understanding of *S. suis* pathogenic mechanisms.

**Citation:** Rong J, Zhang W, Wang X, Fan H, Lu C, et al. (2012) Identification of Candidate Susceptibility and Resistance Genes of Mice Infected with *Streptococcus suis* Type 2. PLoS ONE 7(2): e32150. doi:10.1371/journal.pone.0032150

**Editor:** Eliane Namie Miyaji, Instituto Butantan, Brazil

**Received:** July 25, 2011; **Accepted:** January 23, 2012; **Published:** February 27, 2012

**Copyright:** © 2012 Rong et al. This is an open-access article distributed under the terms of the Creative Commons Attribution License, which permits unrestricted use, distribution, and reproduction in any medium, provided the original author and source are credited.

**Funding:** This work was supported by Cloning and Identification of the Resistance Genes of Swine Against Major Pathogenic Microorganism (2009ZX08009-1546), The Foundation of National Natural Science Foundation of China (No. 30671558), and The Priority Academic Program Development of Jiangsu Higher Education Institutions. The funders had no role in study design, data collection and analysis, decision to publish, or preparation of the manuscript.

**Competing Interests:** The authors have declared that no competing interests exist.

\* E-mail: yaohch@njau.edu.cn

## Introduction

*Streptococcus suis*, a Gram-positive encapsulated coccus, is considered to be an important swine pathogen, which not only causes septicemia but also affects the central nervous system (CNS) and other tissues, leading to meningitis, endocarditis, pneumonia and arthritis [1,2]. Although 33 serotypes have been recognized on the basis of capsular antigens, serotype 2 is still the most frequently isolated from diseased animals [3]. *S. suis* does not only cause disease in pigs but also affects humans. Human infection with *S. suis* mainly occur in people with occupational exposure to infected pigs or raw pork products and have been reported in different Asian and European countries, as well as in New Zealand, Australia, Argentina and Canada [4,5,6,7].

The pathogenesis of both systemic and CNS infections caused by *S. suis* is poorly understood. To induce clinical disease in swine, it is believed that *S. suis* enter through the respiratory route and remain localized in the tonsils. In humans, however, the route of infection is mainly through skin injuries when bacteria may gain access to the bloodstream, where they disseminate freely or as cell-bound bacteria attached to phagocytes [2] until reaching the CNS.

Septicemia and meningitis may be related to an exacerbated or uncontrolled inflammatory response that is also, in the case of meningitis, accompanied by an increase in the permeability or breakdown of the blood-brain barrier [2]. For example, *S. suis* can upregulate expression of adhesion molecules on monocytes, thereby increasing leukocyte recruitment to infection sites and boosting the inflammatory response [8]. It was reported that human and murine monocytes/macrophages recognize the intact *S. suis* or its purified cell wall components through a toll-like receptor 2 (Tlr2)-dependent pathway, with the possible participation of CD14, and release of cytokines and chemokines [9,10,11].

Animal models are essential to obtaining a better understanding of pathogenesis of *S. suis*, and mice have been used as an experimental model for evaluation of *S. suis* virulence [12,13,14]. Research by Williams *et al.* showed that the behavior of *S. suis* type 2 (SS2) in infected mice resembles that in pigs [12]. Previous research indicated that BALB/c and SS strains of mice are useful as experimental models of SS2 infections in pigs. The type strain and isolates of this *S. suis* type from diseased pigs produce septicemia and meningitis in BALB/c and SS mice inoculated with  $10^8$  colony forming units (CFU) of the bacteria and 60 to

100% of these infected mice die. In BALB/c mice that die or develop nervous signs due to SS2 infection, purulent meningoen- cephalitis, myocarditis, ophthalmitis, labyrinthitis and otitis media were observed [14]. Recently, a hematogenous model of *S. suis* infection in adult CD1 outbred mice was developed by Dominguez-Punaro and colleagues, and this experimental model may be useful for studying the mechanisms underlying sepsis and meningitis during bacterial infection [15]. Their further research demonstrated that A/J mice are significantly more susceptible to *S. suis* infection than C57BL/6 (B6) mice, especially during the acute septic phase of infection [16]. Assessment of susceptibility to *S. suis* using animal models has long been limited to monitoring mortality rates and histopathological studies, but the genetic basis of susceptibility to *S. suis* infection is largely unknown. Therefore, we used Illumina mouse BeadChips in this study to identify alterations in gene expression of mice injected with SS2 strain HA9801. Such whole transcriptome analyses would contribute to future studies of transmission, virulence and pathogenesis of *S. suis*.

## Materials and Methods

### Ethics statement

All animals used in this study, and animal experiments, were approved by Department of Science and Technology of Jiangsu Province. The license number was SYXK(SU) 2010-0005.

### Bacterial strains and culture conditions

SS2 HA9801, originally isolated by our laboratory, is considered a virulent strain [17,18,19,20]. Bacteria were grown overnight on sheep blood agar plates at 37°C, and isolated colonies were inoculated into 5 mL cultures of Todd-Hewitt broth (THB) (Oxoid), which were incubated for 12 h at 37°C with agitation. Working cultures were prepared by transferring 300  $\mu$ L of the 12 h cultures into 30 mL of THB, which were further incubated for 3–4 h at 37°C with agitation. Late log phase bacteria were washed twice in phosphate-buffered saline (PBS) (pH 7.4). The pelleted bacteria were then resuspended and adjusted to a concentration of  $5 \times 10^8$  CFU/mL. The inoculum for experimental infection was diluted in THB to obtain a final concentration of  $1 \times 10^8$  CFU/mL. This final suspension was plated onto blood agar to accurately determine the CFU/mL.

### Mice and experimental infection

Specific pathogen-free mice of the B6 and A/J strains were purchased from the Model Animal Research Center of Nanjing University. Female mice of 8–14 weeks of age were acclimated to standard laboratory conditions of a 12-h light/12-h dark cycle with free access to rodent chow and water. A preliminary study was performed to verify the 50% lethal dose (LD50) of the HA9801 strain and to determine the optimal bacterial dose and time points. For the microarray experiment, experimental and mock infections of mice were performed by intraperitoneal inoculations according to the following groups: Five A/J and five B6 mice were each injected with a 200  $\mu$ L volume of the SS2 HA9801 bacterial suspension ( $1 \times 10^8$  CFU/mL); Five A/J and five B6 control mice were each injected with a 200  $\mu$ L volume of the vehicle solution (sterile THB).

### Extraction of peritoneal macrophages

Control and SS2-infected A/J and B6 mice (three in each group) were sacrificed at 9 h post-infection. The peritoneal macrophages were harvested according to a procedure reported elsewhere [21]. Resident peritoneal macrophages were collected from A/J and B6 mice by flushing of the peritoneal cavity with 5 mL ice-cold Hank's balanced salt solution containing 10 U/mL of heparin. Peritoneal

cells were plated at a density of  $1 \times 10^6$  cells/cm<sup>2</sup> in RPMI medium supplemented with 10% FBS, and macrophages were left to adhere for 2 h in a humidified atmosphere at 37°C with 5% CO<sub>2</sub>. Non-adherent cells were washed off the plate, and the adherent cells were considered macrophages.

### RNA preparation

The peritoneal macrophages of each mouse were lysed, and total RNA was extracted using Trizol reagent (Invitrogen). The partial RNA from the peritoneal macrophages of each of three mice from each group were pooled to minimize biological variation in gene expression within a group [22]. The left RNA samples were remained for qRT-PCR. One sample of pooled RNA for each group was further purified using an RNeasy Mini kit (Qiagen) according to the manufacturer's instructions and submitted for microarray hybridization. The integrity of the isolated RNA was assessed both before and after pooling by formaldehyde denaturation gel electrophoresis. RNA concentration and purity were determined by spectrophotometry. Only those samples that had an OD260/OD280 ratio of approximately 2.0 and showed no degradation (ratio approaching 2:1 for the 28S and 18S bands) were used to generate labeled targets.

### Illumina BeadChip gene expression and data analysis

The RNA samples were sent to Biostar Genechip Inc. (Shanghai, China) for microarray hybridization. The pooled RNA sample from each group was hybridized to one Illumina mouse Genome Beadchip Array (catalog number 5022612022, Mouse WG-6\_V2, Illumina). Therefore, four BeadChips were used in total, one for each of the A/J and B6 infected and control mice groups. Biotin-labeled cRNA preparation and hybridization were performed as described previously [23]. The arrays were scanned on an Illumina BeadStation 500 System and the hybridization data analyzed using Illumina BeadStudio software. The following filtering criteria were used for selection of differentially expressed genes: positive gene in either test or control, and test DiffScore  $\geq +20$  or  $\leq -20$ . The differentially expressed genes were selected by comparing the following groups: SS2-infected A/J vs. SS2-infected B6; control A/J vs. control B6; SS2-infected A/J vs. control A/J; SS2-infected B6 vs. control B6. All data were MIAME compliant, and the raw data has been deposited in ArrayExpress database along with normalized data. The accession assigned is E-MTAB-745.

### Gene ontology (GO) category and pathway analysis

The differentially expressed genes between SS2-infected A/J and control A/J mice were intersected with those between SS2-infected A/J and SS2-infected B6. The same process was carried out with the differentially expressed genes between SS2-infected B6 and control B6. The differentially expressed genes between control A/J and control B6 mice were eliminated, as they were considered the genes that were inherently different between A/J and B6 mice. The remaining set of differentially expressed genes were analyzed for inclusion in GO categories and pathways. The concrete treatment for four groups of data is presented in Figure 1. Categorization in significant biological processes was performed using tools of the Gene Ontology project (<http://www.geneontology.org>) [24]. The test of statistical significance considers the number of differentially expressed genes found in each category compared with the total number of genes in the category represented on the chip. The pathway analysis was carried out using the Kyoto Encyclopedia of Genes and Genomes (KEGG) database [25]. Two-sided Fisher's exact test and  $\chi^2$  test were used to classify the GO category and pathway, and the false discovery rate (FDR) was calculated to correct the *P* value. *P* value < 0.05

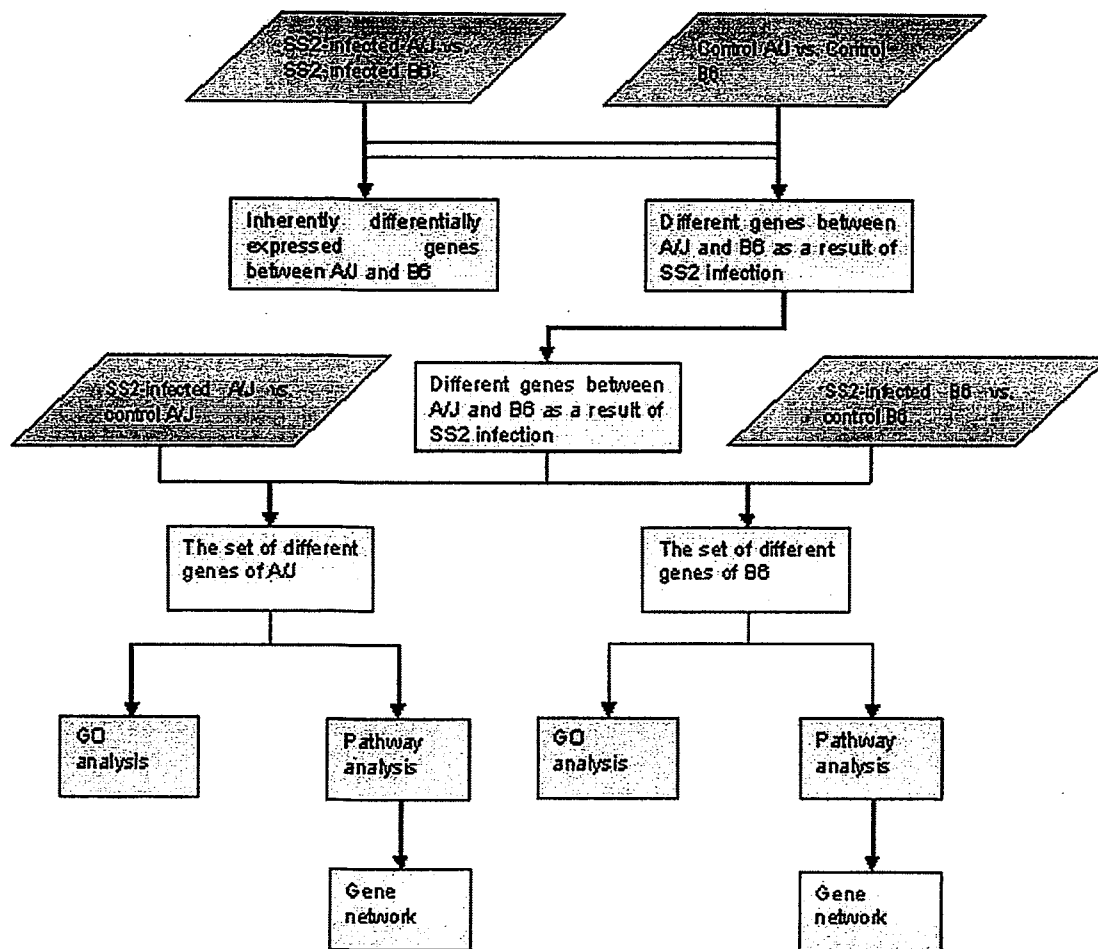


**Figure 1. The process of treatment of four groups of data for GO, pathway and gene network analysis.** (a) The differentially expressed genes between control AJ and control B6 mice were eliminated from those between SS2-infected AJ and SS2-infected B6 mice. (b) The remain of differential genes between SS2-infected AJ and SS2-infected B6 were intersected with differentially expressed genes between SS2-infected AJ and control AJ mice. (c) The remaining set of differentially expressed genes were analyzed for inclusion in GO categories and pathways. The same process was carried out with the differentially expressed genes between SS2-infected B6 and control B6 mice. doi:10.1371/journal.pone.0032150.g001

and  $FDR < 0.05$  were used as a threshold to select significant GO categories and KEGG pathways.

#### Gene network analysis

The gene network analysis of the differentially expressed genes involved in significant pathways was carried out using the KEGG database. Interactions of genes in the database were analyzed, and gene networks were established. The degree of connectivity was used to evaluate the role of genes in the network.

#### Confirmation of BeadChip results by quantitative real-time PCR (qRT-PCR)

Total RNA from each of three mice of each group was treated as same as the pooled RNA for BeadChips and the integrity was assessed. One microgram of total RNA from each of three mice of each group was used in a reverse transcription reaction of 20  $\mu$ L total volume to synthesize first strand cDNA using Transcriptor First Strand cDNA Synthesis Kit (Roche) according to the manufacturer's instructions. According to the relative researches

and network analysis results, the specific genes were selected for verification. Primers were designed to amplify sequences of 75–250 base pairs (bp) (Table 1). For real-time PCR, the 7300 Real-Time PCR System (ABI) and FastStart Universal SYBR Green Master (Roche) were used. Each reaction contained 1  $\mu$ L cDNA template and 9  $\mu$ L SYBR Green Master. Amplification conditions were 95°C for 10 min, followed by 40 cycles of 95°C for 15 s and 60°C for 60 s. Each sample and no template controls were run in duplicate. Glyceraldehyde-3-phosphate dehydrogenase (*CAPDH*) was also amplified under the same conditions as the internal control to normalize reactions. After completion of the PCR amplification, the relative fold change after infection was calculated based on the  $2^{-\Delta\Delta CT}$  method [26].

#### Results

##### Determination of LD50 of strain HA9801 and experimental infection for microarray analysis

The LD50 of strain HA9801 was determined by injecting mice with various doses, and mortality was monitored until 7 days post-

**Table 1.** Primers for selected genes analyzed using qRT-PCR.

Acronym	Gene name	Primer sequences (5'-3')	GenBank number	Product size (bp)
<i>Itgb2</i>	integrin beta 2	GGCTGGATGCCATAATGCAAG AAGCCATCGTCTGTGGCAAAC	NM_008404.4	94
<i>Itgal</i>	integrin alpha L	GGAATGACGCTGGCAACAGA AGGTAGCAGAGGCCACTGAGGTAA	NM_008400.2	107
<i>Pdpk1</i>	3-phosphoinositide dependent protein kinase-1	GCAGGACTCCACCATTGAGA GCCTAAACGCTTTGTGGCATC	NM_001080773.1	150
<i>Icam2</i>	intercellular adhesion molecule 2	CATCTCGGAGTACCAGATCCTTGAA GCAGTATTGACACCACCAGATG	NM_010494.1	86
<i>Irf9</i>	interferon regulatory factor-9	TGCTGCCAGCAATAAGTGTG CCAGAAATGTAGGGTTCCTGGA	NM_008394.3	119
<i>Stat1</i>	signal transducer and activator of transcription 1	GGCTGCCGAGAACATACCAGA CCAGTTCGCTTAGGGTCTGCA	NM_009283.2	138
<i>Stat2</i>	signal transducer and activator of transcription 2	TGCAGCGAGAGCACTGGAA CATTGGCAGGATGCTCTGTGA	NM_019963.1	137
<i>Socs2</i>	suppressor of cytokine signaling 2	CTGCGGAGCTCAGTCAAAC TAGTCGGTCCAGCTGACGCTTAAAC	NM_007706.3	163
<i>Tlr2</i>	toll-like receptor 2	GGAGCATCCGAATTGCATCAC TTATGGCCACCAAGATCCAGAAG	NM_001905.3	116
<i>Tnf</i>	tumor necrosis factor	GTTCTATGGCCAGACCCTCAC GGCACCAGTGTGGTGTCTTTG	NM_013693.2	175
<i>Mmp9</i>	matrix metalloproteinase 9	GCCCTGGAACCTCACAGACA TTGAAACTCACAGCCAGAAG	NM_013599.2	85
<i>Ptx3</i>	pentraxin related gene	ATGACTACGAGCTCATGTATGTGAA TGAACAGCTTGCCCACTCC	NM_008987.3	120
<i>Itga5</i>	integrin alpha 5	GTTTCAGGCTGGCTGTGAG CTGGTAGGGCATCTCAGAGCTTC	NM_010577.3	161
<i>Il10</i>	interleukin 10	GACCAGCTGGACAACATACTGCTAA GATAAGGCTTGGCAACCAAGTAA	NM_010548.1	77
<i>GAPDH</i>	glyceraldehyde-3-phosphate dehydrogenase	ATGCTGCTTCAACCTCTCT ATGTGCCGTCGTGGATCTGA	NM_008084.2	81

doi:10.1371/journal.pone.0032150.t001

infection. The mortality for A/J mice injected with a dose of  $10^7$  CFU between 12 h and 96 h was 50% (Table 2). The clinical signs of disease of A/J mice were depression-like behavior, rough appearance of hair coat and swollen eyes [15]. Mice exhibiting extreme lethargy were considered moribund and were humanely euthanized. All of B6 mice injected with a dose of  $10^8$  CFU survived, although they all died when injected with a high dose of  $10^9$  CFU (data not shown). Control mice showed no death or clinical signs of disease during the 7 days of observation. As B6 are known to be more resistant to *S. suis* infection than A/J mice, the results were in complete accordance with previous research [16]. On the basis of these results, experimental mice were injected with

$2 \times 10^7$  CFU for the microarray experiment. At 9 h post-infection, six infected mice (three A/J mice and three B6 mice) and six control mice (three A/J mice and three B6 mice) were selected for analysis.

#### Microarray analysis

We hypothesized that gene expression would vary in response to SS2 infection in the peritoneal macrophages of B6 and A/J after intraperitoneal inoculation. To identify such genes, studies were performed using Illumina BeadChip microarrays, which revealed 3,692 differentially expressed genes in peritoneal macrophages between A/J and B6 mice as a result of SS2 infection. (The

**Table 2.** LD50 of strain HA9801 on A/J mouse.

Strain	Infection dose(CFU)	Amount of mouse (No)	Mortality/total	LD50(CFU)
HA9801	$10^8$	6	4/6	$1.61 \times 10^7$
	$10^7$	6	3/6	
	$10^6$	6	1/6	
	$10^5$	6	1/6	
Control		3	0/3	

doi:10.1371/journal.pone.0032150.t002

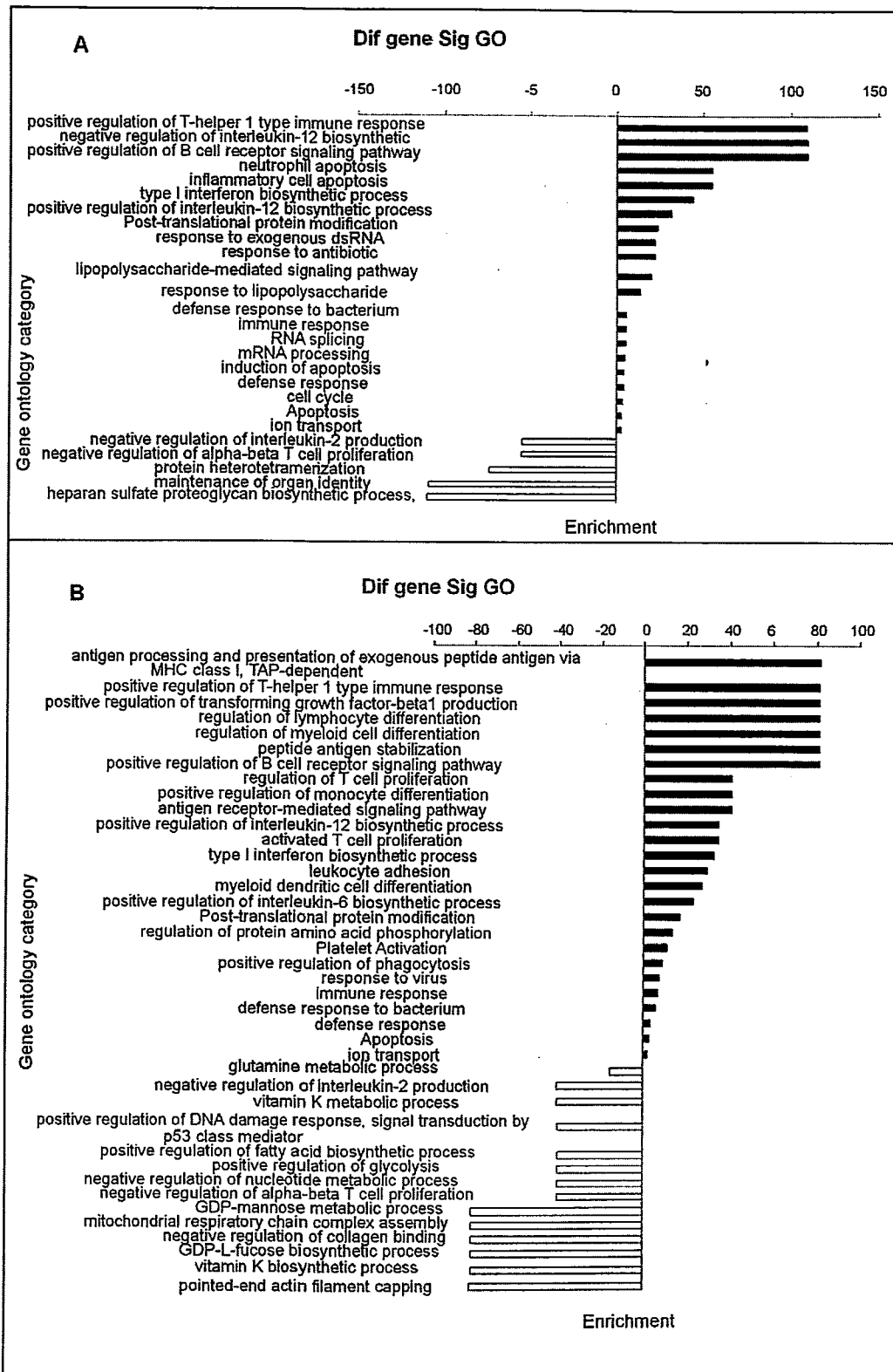


**Figure 2. GO categories of biological processes for significantly differentially expressed genes.** (A) between SS2-infected A/J and control A/J mice and (B) between SS2-infected B6 and control B6 mice.  $P$  value  $< 0.05$  and FDR  $< 0.05$  were used as thresholds to select significant GO categories.

doi:10.1371/journal.pone.0032150.g002

differentially expressed genes between control A/J and control B6 mice were used to exclude those genes which were thought to be inherently different between A/J and B6 mice.) Between the SS2-infected A/J and control A/J mice, 2646 genes were identified to be differentially expressed, of which 1469 genes were upregulated and 1177 genes downregulated. Between the SS2-infected B6 and control B6 mice, 1449 genes were differentially expressed, of which 778 genes were upregulated and 671 genes downregulated. The differentially expressed genes of the four groups and the group of 3,692 differentially expressed genes are summarized in Table S1.

### GO categorization

The differentially expressed genes of A/J and B6 mice after infection with strain HA9801 were classified into different functional categories according to the Gene Ontology project for biological processes. The main GO categories for significantly upregulated genes between SS2-infected A/J and control A/J mice were positive regulation of T-helper 1 type immune response, regulation of interleukin-12 biosynthetic process, positive regulation of B cell receptor signaling pathway, type I interferon biosynthetic process, defense response to bacteria, immune response, ion transport and inflammatory cell apoptosis. The main GO categories for significantly downregulated genes between SS2-infected A/J and control A/J mice included negative regulation of interleukin-2 production, negative regulation of  $\alpha\beta$ -T cell proliferation, protein heterotetramerization and heparan sulfate proteoglycan biosynthetic process (Fig. 2A).

The primary GO categories for significantly upregulated genes between SS2-infected B6 and control B6 mice were antigen processing and presentation of exogenous peptide antigen, positive regulation of T-helper 1 type immune response, peptide antigen stabilization, positive regulation of B cell receptor signaling pathway, regulation of lymphocyte differentiation, positive regulation of monocyte differentiation, antigen receptor-mediated signaling pathway, positive regulation of interleukin-12 biosynthetic process, type I interferon biosynthetic process, platelet activation, positive regulation of phagocytosis, immune response, defense response to bacterium and apoptosis. The primary GO categories for significantly downregulated genes between SS2-infected B6 and control B6 mice were pointed-end actin filament capping (The specific gene involved in this GO was *tmad3*, which was related to movement.), vitamin K biosynthetic process, GDP-L-fucose biosynthetic process, negative regulation of collagen binding, GDP-mannose metabolic process, negative regulation of nucleotide metabolic process, positive regulation of glycolysis, positive regulation of fatty acid biosynthetic process, negative regulation of alpha-beta T cell proliferation and glutamine metabolic process (Fig. 2B). The differentially expressed genes from this study classified into significant GO categories are summarized in Table S2.

### Pathway analysis

The pathway analysis based on the KEGG database was performed on the genes selected as described above. Significantly upregulated genes between SS2-infected A/J and control A/J mice were mainly involved in the toll-like receptor signaling pathway, cytokine-cytokine receptor interaction, T cell receptor signaling pathway, B cell receptor signaling pathway, natural killer cell

mediated cytotoxicity, antigen processing and presentation, leukocyte transendothelial migration. Significantly downregulated genes between SS2-infected A/J and control A/J mice were involved in only one pathway, olfactory transduction (Fig. 3A). The KEGG pathway analysis for significantly upregulated genes between SS2-infected B6 and control B6 mice showed that the genes were related to toll-like receptor signaling pathway, leukocyte transendothelial migration, cytokine-cytokine receptor interaction, B cell receptor signaling pathway, natural killer cell mediated cytotoxicity and antigen processing and presentation. The KEGG pathway analysis for significantly downregulated genes between SS2-infected B6 and control B6 mice showed that the genes were related to tryptophan and tyrosine metabolism, phenylalanine, tyrosine and tryptophan biosynthesis, fructose and mannose metabolism, fatty acid metabolism, aminoacyl-tRNA biosynthesis and renin-angiotensin system (Fig. 3B). The differentially expressed genes involved in significant pathways are summarized in Table S3.

### Gene network analysis

The differentially expressed genes involved in significant pathways were analyzed for their interaction, and the networks of genes involved in signal transduction during SS2 infection were established utilizing the KEGG database. In the gene network comprised of the differentially expressed genes involved in significant pathways of A/J mice infected with SS2, genes with a high degree of connectivity, such as *Sox2*, *Stat1*, *Stat2*, were in the core axis of the network. Genes were regulated by their upstream genes when their outdegrees were zero (e.g., *Ctad2*), or they regulated expression of downstream genes when their indegrees were zero (e.g., *Cish*). The key genes regulated by SS2 infection in the A/J mice were mainly involved in the Jak-STAT signaling pathway and related to cell apoptosis (Fig. 4A, Table 3).

In the gene network composed of the differentially expressed genes involved in significant pathways of B6 mice infected with SS2, some of the genes with a high degree of connectivity in the core axis were *Icam2*, *Igal*, *Ilgb2*. *Ptk2b* with an outdegree of zero is an example of a gene regulated by upstream genes, while *Rra* with an indegree of zero represents a gene which regulated expression of other downstream genes.

On the whole, the gene network could be divided into five parts, three of which were related to cell apoptosis in the left top, left bottom and middle bottom of the gene network (Fig. 4B, Table 4). Four genes (*H2-T10*, *H2-Q6*, *Tapbp*, *Tap1*) constituted a small signal transduction network associated with immune responses (center), and three genes (*Plxnb2*, *Sema4a*, *Sema4d*) composed a small nervous system net (bottom right) (Fig. 4B, Table 4).

### Confirmation of BeadChips results by qRT-PCR

In order to verify the data obtained by microarray analysis, qRT-PCR was performed. We tested 9 genes differentially expressed between SS2-infected A/J and control A/J mice, and 10 genes differentially expressed between SS2-infected B6 and control B6 mice. As shown in Table 5, the qRT-PCR results largely confirmed the data from the microarray. Notably, the diffscore is the filtering criteria of Illumina for selection of differentially expressed genes. There is no direct relationship with fold change by qRT-PCR. But they have the similar tendency.

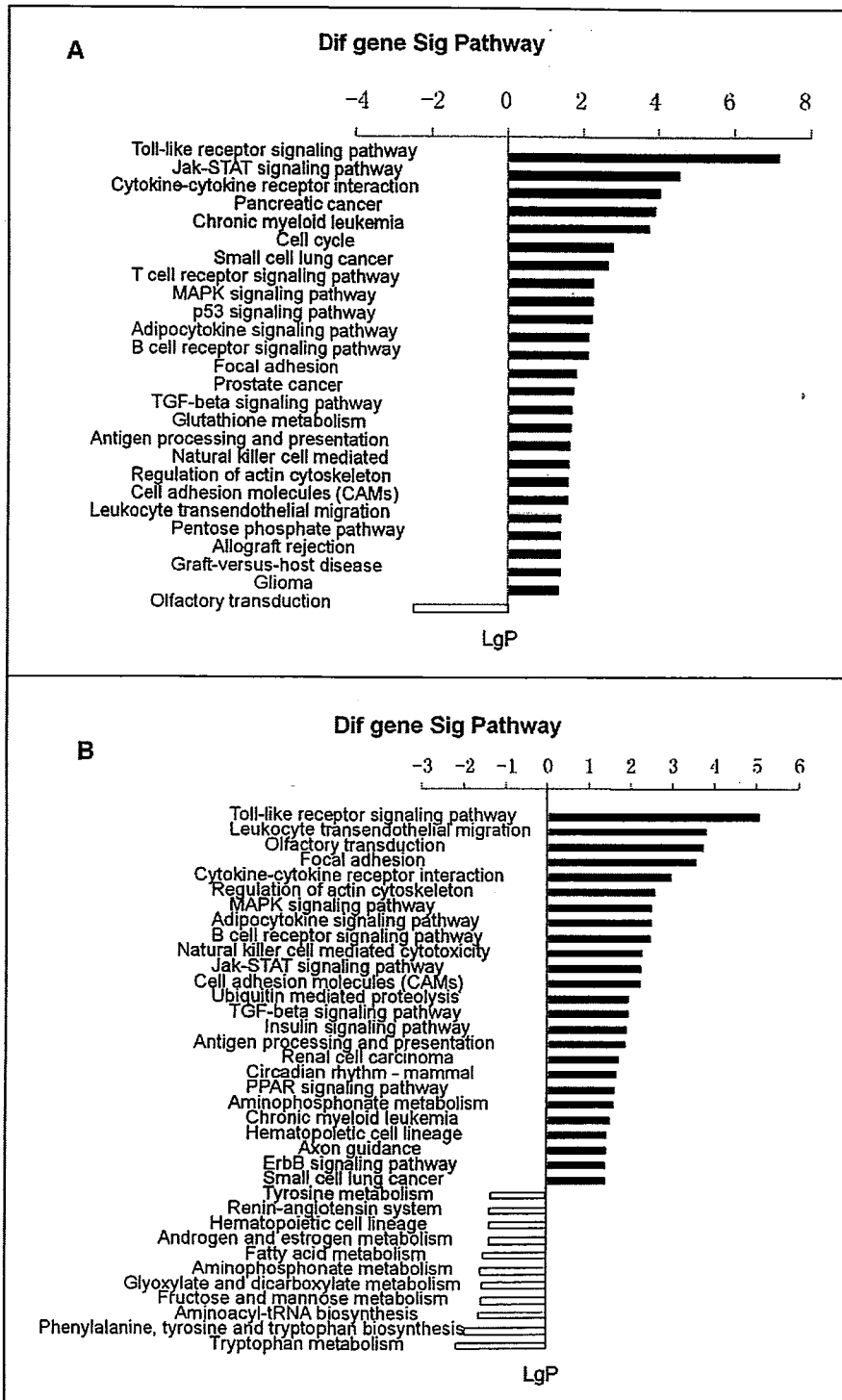


**Figure 3. KEGG pathway analysis for significantly differentially expressed genes (A) between SS2-infected A/J and control A/J mice and (B) between SS2-infected B6 and control B6 mice.  $P$  value < 0.05 and FDR < 0.05 were used as thresholds to select significant KEGG pathways. LgP is the base 10 logarithm of the  $P$  value.**  
 doi:10.1371/journal.pone.0032150.g003



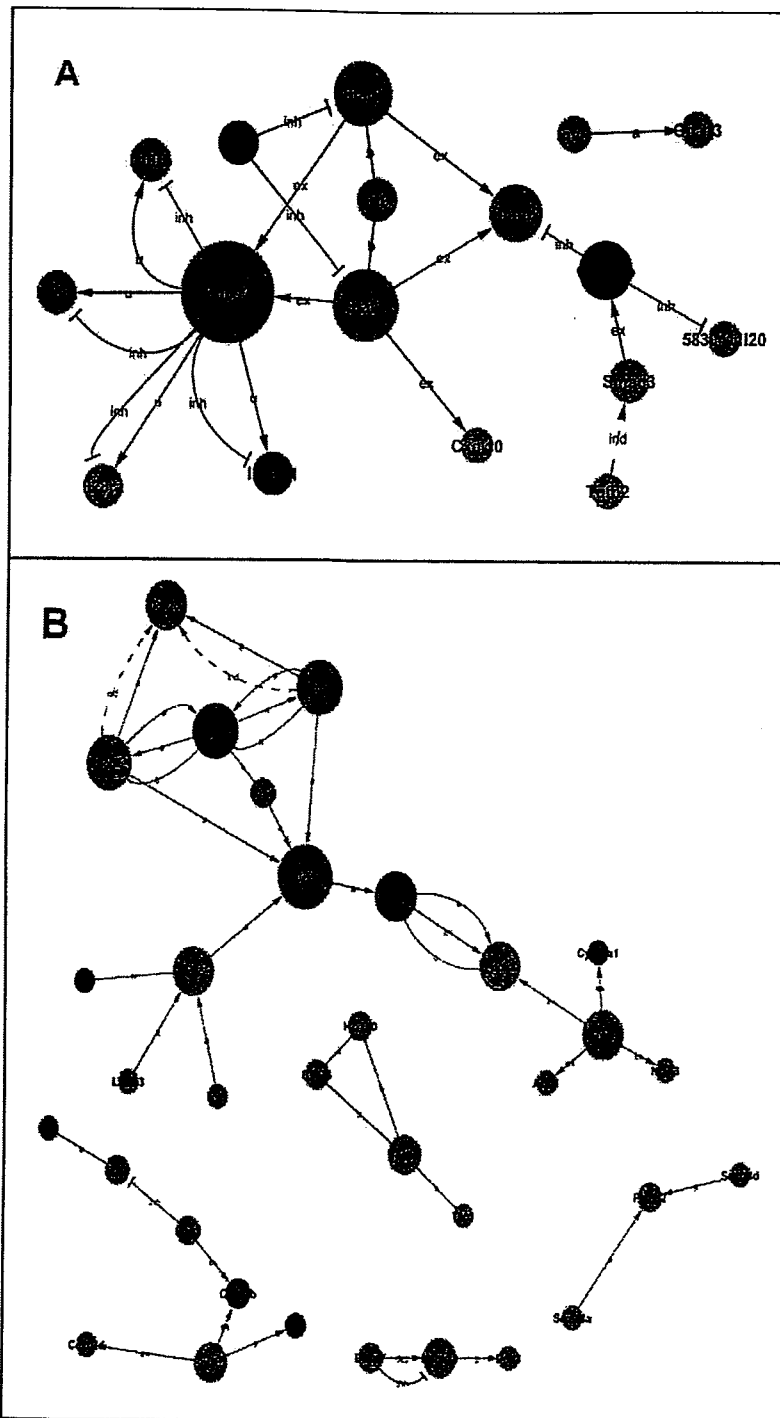


**Figure 4. Gene networks of differentially expressed genes involved in significant pathways.** The gene networks comprised of the differentially expressed genes involved in significant pathways of (A) A/J mice infected with SS2 and (B) B6 mice infected with SS2 are shown. Legend: each circle represents a gene; red, upregulation; blue, downregulation; line segment, interaction of genes; arrow, activation (a), flat-headed arrow, inhibition (inh); straight, binding (b); dashed line, indirect effect (ind); P, phosphorylation; dp, dephosphorylation; ex, expression; u, ubiquitination. doi:10.1371/journal.pone.0032150.g004

#### Comparison of gene expression

The expression level of toll-like receptor 2 (*Tlr2*) and tumor necrosis factor (*Tnf*) of A/J mice after infection with SS2 were

obviously upregulated. There were no changes in *Tlr2* of B6 mice, and the upregulated expression of *Tnf* of B6 mice was significant lower than that of A/J mice after infection with SS2. The

**Table 3.** Degree of key genes in gene network of SS2-infected A/J mice.

Vertex	degree	indegree	outdegree	description
<i>Socs2</i>	10	2	8	suppressor of cytokine signaling 2
<i>Stat1</i>	6	2	4	signal transducer and activator of transcription 1
<i>Stat2</i>	5	2	3	signal transducer and activator of transcription 2
<i>Irf9</i>	4	2	2	interferon regulatory factor 9
<i>Cdkn2b</i>	3	1	2	cyclin-dependent kinase inhibitor 2B (p15, inhibits CDK4)
<i>Smad3</i>	2	1	1	MAD homolog 3 ( <i>Drosophila</i> )
<i>Cish</i>	2	0	2	Cytokine-inducible SH2-containing protein
<i>Igf1r</i>	1	0	1	insulin-like growth factor I receptor
<i>Tgfb2</i>	1	0	1	transforming growth factor, beta 2
<i>Ccnd2</i>	3	3	0	cyclin D2
<i>Il28ra</i>	2	2	0	interleukin 28 receptor, alpha
<i>Il15ra</i>	2	2	0	interleukin 15 receptor, alpha chain
<i>Il11ra1</i>	2	2	0	interleukin 11 receptor, alpha chain 1
<i>Il10rb</i>	2	2	0	interleukin 10 receptor, beta
<i>Cxcl10</i>	1	1	0	chemokine (C-X-C motif) ligand 10
<i>Gna13</i>	1	1	0	guanine nucleotide binding protein, alpha 13
5830411120	1	1	0	Data not found

doi:10.1371/journal.pone.0032150.t003

pentraxin 3 (*Ptx3*) genes of both A/J mice and B6 mice were upregulated, but its expression level in B6 mice was obviously higher than that of A/J mice. The expression of matrix metalloproteinase 9 (*Mmp9*) in macrophages of B6 mice was lower than that in A/J mice post-infection (Fig. 5).

## Discussion

Gene expression profile analysis was used in this study to identify the candidate genes of susceptibility or resistance to SS2 infection in mice models. While several studies have been performed to evaluate host responses to SS2 infection, this was the first time that the genetic basis of susceptibility to SS2 infection has been studied at the whole transcriptome level.

To confirm host genetic differences in susceptibility to HA9801 infection, A/J and B6 mice were used to determine mortality and clinical signs after infection. We determined that the LD50 of HA9801 in A/J mice was  $1 \times 10^7$  CFU between 12 h and 96 h (Table 2), and chose to use just twice the LD50 ( $2 \times 10^7$  CFU) for subsequent microarray analysis. The inoculated mice showed expected clinical signs of disease such as depression-like behavior, rough appearance of hair coat and swollen eyes [15]. B6 mice injected with a dose of  $10^8$  CFU survived and were still active, while a high dose of  $10^9$  CFU was required for 100% mortality. The results confirmed that A/J mice were more susceptible to HA9801 infection than B6 mice, consistent with previous research [16].

Several studies have used human or mouse macrophages, porcine choroid plexus epithelial cells (PCPEC), or porcine brain micro-

**Table 4.** Degree of key genes in gene network of SS2-infected B6 mice.

vertex	degree	indegree	outdegree	description
<i>Icam2</i>	10	5	5	intercellular adhesion molecule 2
<i>Itgal</i>	7	2	5	integrin alpha L
<i>Itgb2</i>	7	2	5	integrin beta 2
<i>Tapbp</i>	6	3	3	TAP binding protein
<i>Crkl</i>	5	4	1	v-crk sarcoma virus CT10 oncogene homolog (avian)-like
<i>Itga5</i>	5	3	2	integrin alpha 5 (fibronectin receptor alpha)
<i>Pdpk1</i>	5	4	1	3-phosphoinositide dependent protein kinase-1
<i>Pik3cg</i>	5	2	3	phosphoinositide-3-kinase, catalytic, gamma polypeptide
<i>Ptk2b</i>	4	4	0	PTK2, protein tyrosine kinase 2 beta
<i>Plexn2</i>	2	2	0	plexin B2
<i>Cdkn2b</i>	2	2	0	cyclin-dependent kinase inhibitor 2B (p15, inhibits CDK4)
<i>Rxra</i>	4	0	4	retinoid X receptor alpha
<i>Smad3</i>	3	0	3	MAD homolog 3 ( <i>Drosophila</i> )

doi:10.1371/journal.pone.0032150.t004

**Table 5.** Confirmation of BeadChips results by qRT-PCR.

Gene	Fold change by qRT-PCR	Diffscore by BeadChip
<b>SS2-infected A/J vs. control A/J</b>		
<i>Irf9</i>	9.3	21.65
<i>Stat1</i>	5.46	24.06
<i>Stat2</i>	11.22	33.51
<i>Socs2</i>	3.18	21.42
<i>Il10</i>	6.3	50.89
<i>Tlr2</i>	2.71	31.12
<i>Tnf</i>	12.21	248.90
<i>Mmp9</i>	7.04	90.06
<i>Ptx3</i>	34.94	65.08
<b>SS2-infected B6 vs. control B6</b>		
<i>Icam2</i>	0.48	-30.68
<i>Itgal</i>	2.68	34.79
<i>Itgb2</i>	2.44	25.06
<i>Itga5</i>	3.51	27.16
<i>Pdpk1</i>	2.1	28.93
<i>Stat2</i>	5.97	39.24
<i>Tlr2</i>	1.06	1.86
<i>Tnf</i>	2.28	24.82
<i>Mmp9</i>	1.99	25.78
<i>Ptx3</i>	119	23.02

doi:10.1371/journal.pone.0032150.t005

vascular endothelial cells to determine the host response to *S. suis* infection [27,28,29]. We observed several similarities between those reports from *S. suis*-infected cells and our expression profile of SS2-infected mice. For example, we detected the induction of *Mmp9* in peritoneal macrophages in SS2-infected mice, which was also observed in a study using human macrophage cells [27]. Jobin *et al.* showed that whole *S. suis* cells are able to upregulate the production of *Mmp9* by human macrophage cells, which may play a critical role in blood brain barrier (BBB) disruption and tissue destruction [27]. *Mmp9* is a metalloproteinase that actively counteracts matrix proteins and is secreted by various cell types. Pathophysiological processes characteristic of bacterial meningitis, such as neutrophil extravasation, subarachnoid space inflammation, BBB disruption and brain edema, have all been ascribed to the action of *Mmps* [30,31]. Treatment with an *Mmp* inhibitor has been shown to reduce *Mmp9* levels in CSF and significantly attenuate brain damage [31]. Additionally, *Mmps* have broader functions in the regulation of inflammation and immunity, affecting the activity of cytokines, chemokines and other proteins [32]. In our study, the expression of the gene encoding *Mmp9* in SS2-infected A/J mice was increased by 7.04 fold compared with that of control A/J mice, while the fold change was only 1.99 in SS2-infected B6 mice. Therefore, *Mmp9* should be considered a candidate susceptibility gene of A/J mice to SS2 infection. Another example of the similarity between the reports from *S. suis*-infected cells and our transcription profile of SS2 infected mice was the induction of *Tlr2* and *Tnf* in peritoneal macrophages, which were also observed in a study of mouse macrophages [11]. Graveline *et al.* demonstrated that whole encapsulated *S. suis* could influence the relative expression of *Tlr2* and further trigger release of *Tnf* in mouse macrophages [11]. Dominguez-Punaro *et al.* provided evidence that the greater

susceptibility of A/J mice was associated with an exaggerated inflammatory response, as indicated by their higher production of *Tnf* [16]. Here, we observed that fold changes of *Tlr2* and *Tnf* expressions in peritoneal macrophages of SS2-infected A/J mice were 2.73 and 12.2, respectively, while *Tnf* was only upregulated by 2.28-fold, and no change was found in *Tlr2* of SS2 infected B6 mice. Accordingly, *Tlr2* and *Tnf* are candidate susceptibility genes of A/J mice to SS2 infection. Long pentraxin 3 (*Ptx3*) is a fluid-phase pattern recognition receptor, which plays a non-redundant role in resistance against selected pathogens. With antibody-like functions, *Ptx3* is induced by pathogen recognition. It recognizes microbial moieties, activates and regulates complement, and facilitates cellular recognition by phagocytosis [33,34,35,36,37,38,39,40,41]. A previous study provided evidence that *Ptx3* plays a role in opsonin for internalization of zymosan by mouse peritoneal macrophages [35]. Other lines of evidence have also shown that *Ptx3* can regulate inflammatory reactions [42,43,44,45]. For example, Deban *et al.* reported that *Ptx3* binds P-selectin and attenuates neutrophil recruitment at sites of inflammation [45]. In our study, *Ptx3* was induced up to 119-fold in peritoneal macrophages of B6 mice after SS2 infection, while the fold change of *Ptx3* was 34.9 in SS2-infected A/J mice. There was no significant difference in expression of *Ptx3* by peritoneal macrophages between control A/J and control B6 mice in BeadChip, while the diffscore between SS2-infected A/J and SS2-infected B6 mice was -36.67 (Table S1). Therefore, *Ptx3* is a candidate resistance gene of B6 mice against SS2 infection. Together, the studies mentioned above corroborate our findings and provide further validation of our results.

Induction of genes associated with immune responses, inflammatory responses and complement activation is an essential defense mechanism for the host organism, which may help to clear pathogens. Inflammation, a marker of *S. suis* infection, is thought to be responsible for most clinical signs of meningitis, septicemia and sudden death [46]. Dominguez-Punaro *et al.* provided evidence that the greater susceptibility of A/J mice is associated with an exaggerated inflammatory response [16]. Chabot-Roy *et al.* showed that in the presence of specific antibodies and/or complement, *S. suis* may be phagocytosed through different receptors, and that this may result in a faster rate of clearance [47]. In our study, some of the differentially expressed genes (e.g., *Ptx3*, *Fcgr1*) in macrophages between B6 SS2-infected and control mice were involved in positive regulation of phagocytosis. In the gene network composed of differentially expressed genes of B6 mice involved in significant pathways, some genes (*plxnb2*, *sema4a*, *sena4d*) were associated with the nervous system. Expression of these genes may be attributed to clinical signs of meningitis. Apoptosis has been shown to be induced by a wide range of gram-positive and gram-negative bacteria in epithelial and endothelial cells and leukocytes [28,48]. Therefore, it is plausible that some genes involved in cell apoptosis were upregulated in A/J and B6 SS2-infected mice.

Finally, we observed that muscle-specific gene (*Tmod3*, tropomodulin 3) related to movement, which was involved in pointed-end actin filament capping, was downregulated in SS2-infected B6 mice, potentially reflecting a mechanism in the animal to conserve energy while it combats the bacterial infection. Similar results were obtained in a study by Wu and colleagues that demonstrated muscle-specific genes of zebrafish are downregulated after SS2 infection [49].

The murine macrophage response to SS2 infection showed clear conservation with host responses detected in porcine cells, human cells and other mouse cell or mammalian models. The study produced a set of candidate genes that may influence susceptibility or resistance to SS2 infection in the A/J and B6

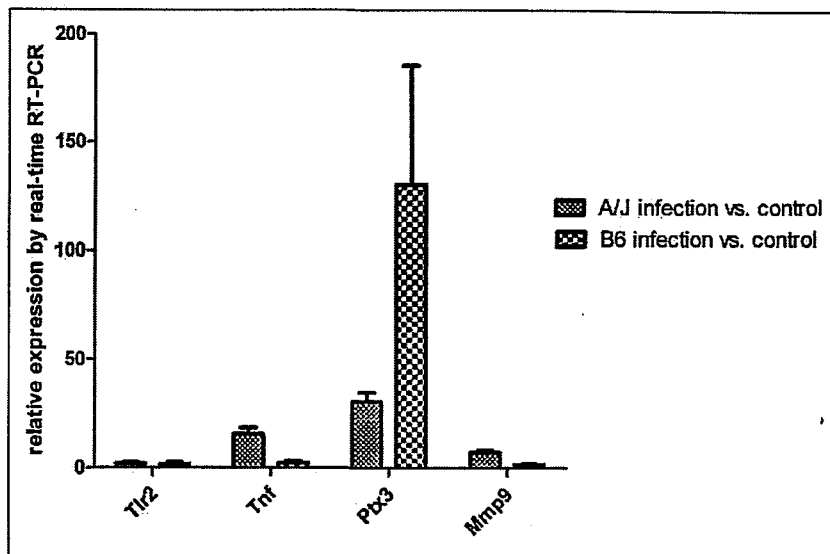


**Figure 5. Comparative analysis of gene expression in peritoneal macrophages.** Expression levels of *Tlr2*, *Tnf*, *Ptx3* and *Mmp9* in A/J and B6 mice were measured by qRT-PCR and normalized to the housekeeping gene *GAPDH*. Differences between A/J and B6 mice were statistically significant with a *P* value of <0.05 as determined by one-way ANOVA, except with the *Tlr2* gene. doi:10.1371/journal.pone.0032150.g005

mouse models. Among these, *Mmp9*, *Tlr2* and *Tnf* were identified as candidate susceptibility genes of A/J mice and *Ptx3* as a candidate resistance gene of B6 mice against SS2 infection. In future work, we will continue searching for infection markers using these models in order to provide leads for further investigation of *S. suis* pathogenesis.

## Supporting Information

**Table S1**  
(XLS)

**Table S2**  
(XLS)

## References

- Staats JJ, Feder I, Okwunabua O, Chengappa MM (1997) *Streptococcus suis*: past and present. *Vet Res Commun* 21: 381–407.
- Gottschalk M, Segura M (2000) The pathogenesis of the meningitis caused by *Streptococcus suis*: the unresolved questions. *Vet Microbiol* 76: 259–272.
- Hill JE, Gottschalk M, Brousseau R, Harel J, Hemmingsen SM, et al. (2005) Biochemical analysis, *cpn60* and 16S rDNA sequence data indicate that *Streptococcus suis* serotypes 32 and 34, isolated from pigs, are *Streptococcus orisratti*. *Vet Microbiol* 107: 63–69.
- Lun ZR, Wang QP, Chen XG, Li AX, Zhu XQ (2007) *Streptococcus suis*: an emerging zoonotic pathogen. *Lancet Infect Dis* 7: 201–209.
- Fittipaldi N, Gottschalk M, Vanier C, Daigle F, Harel J (2007) Use of selective capture of transcribed sequences to identify genes preferentially expressed by *Streptococcus suis* upon interaction with porcine brain microvascular endothelial cells. *Appl Environ Microbiol* 73: 4359–4364.
- Mai NT, Hoa NT, Nga TV, Linh le D, Chau TT, et al. (2008) *Streptococcus suis* meningitis in adults in Vietnam. *Clin Infect Dis* 46: 659–667.
- Yu H, Jing H, Chen Z, Zheng H, Zhu X, et al. (2006) Human *Streptococcus suis* outbreak, Sichuan, China. *Emerg Infect Dis* 12: 914–920.
- Al-Numani D, Segura M, Dore M, Gottschalk M (2003) Up-regulation of ICAM-1, CD11a/CD18 and CD11c/CD18 on human THP-1 monocytes stimulated by *Streptococcus suis* serotype 2. *Clin Exp Immunol* 133: 67–77.
- Segura M, Stankova J, Gottschalk M (1999) Heat-killed *Streptococcus suis* capsular type 2 strains stimulate tumor necrosis factor alpha and interleukin-6 production by murine macrophages. *Infect Immun* 67: 4646–4654.
- Segura M, Vadeboncoeur N, Gottschalk M (2002) CD14-dependent and -independent cytokine and chemokine production by human THP-1 monocytes stimulated by *Streptococcus suis* capsular type 2. *Clin Exp Immunol* 127: 243–254.
- Graveline R, Segura M, Radziach D, Gottschalk M (2007) TLR2-dependent recognition of *Streptococcus suis* is modulated by the presence of capsular polysaccharide which modifies macrophage responsiveness. *Int Immunol* 19: 375–389.
- Williams AE, Blakemore WF, Alexander TJ (1988) A murine model of *Streptococcus suis* type 2 meningitis in the pig. *Res Vet Sci* 45: 394–399.
- Beaudoin M, Higgins R, Harel J, Gottschalk M (1992) Studies on a murine model for evaluation of virulence of *Streptococcus suis* capsular type 2 isolates. *FEMS Microbiol Lett* 78: 111–116.
- Kataoka Y, Haritani M, Mori M, Kishina M, Sugimoto C, et al. (1991) Experimental infections of mice and pigs with *Streptococcus suis* type 2. *J Vet Med Sci* 53: 1043–1049.
- Dominguez-Punaro MC, Segura M, Plante MM, Lacouture S, Rivest S, et al. (2007) *Streptococcus suis* serotype 2, an important swine and human pathogen, induces strong systemic and cerebral inflammatory responses in a mouse model of infection. *J Immunol* 179: 1842–1854.
- Dominguez-Punaro Mde L, Segura M, Radziach D, Rivest S, Gottschalk M (2008) Comparison of the susceptibilities of C57BL/6 and A/J mouse strains to *Streptococcus suis* serotype 2 infection. *Infect Immun* 76: 3901–3910.
- Wu Z, Zhang W, Lu C (2008) Comparative proteome analysis of secreted proteins of *Streptococcus suis* serotype 9 isolates from diseased and healthy pigs. *Microb Pathog* 45: 159–166.
- Wang K, Lu C (2007) Adhesion activity of glyceraldehyde-3-phosphate dehydrogenase in a Chinese *Streptococcus suis* type 2 strain. *Berl Munch Tierarztl Wochenschr* 120: 207–209.
- Zhang W, Lu CP (2007) Immunoproteomics of extracellular proteins of Chinese virulent strains of *Streptococcus suis* type 2. *Proteomics* 7: 4468–4476.

**Table S3**  
(XLS)

## Acknowledgments

We thank HaoDan Zhu for useful suggestions and ShuJian Zhang, Di Gao and WenChao Song for assistance.

## Author Contributions

Conceived and designed the experiments: HY HF WZ JR. Performed the experiments: JR XW. Analyzed the data: JR HY WZ. Contributed reagents/materials/analysis tools: HY CL HF. Wrote the paper: JR.

20. Zhang W, Lu CP (2007) Immunoproteomic assay of membrane-associated proteins of *Streptococcus suis* type 2 China vaccine strain HA9801. *Zoonoses Public Health* 54: 253–259.
21. de Jonge WJ, van der Zanden EP, The FO, Bijlsma MF, van Westerloo DJ, et al. (2005) Stimulation of the vagus nerve attenuates macrophage activation by activating the Jak2-STAT3 signaling pathway. *Nat Immunol* 6: 844–851.
22. Lemay AM, Haston CK (2005) Bleomycin-induced pulmonary fibrosis susceptibility genes in AcB/BcA recombinant congenic mice. *Physiol Genomics* 23: 54–61.
23. Chemnitz JM, Driesen J, Classen S, Riley JL, Debey S, et al. (2006) Prostaglandin E2 impairs CD4+ T cell activation by inhibition of Ick: implications in Hodgkin's lymphoma. *Cancer Res* 66: 1114–1122.
24. Ashburner M, Ball CA, Blake JA, Bolstein D, Butler H, et al. (2000) Gene ontology: tool for the unification of biology. *The Gene Ontology Consortium*. *Nat Genet* 25: 25–29.
25. Ogata H, Goto S, Sato K, Fujibuchi W, Bono H, et al. (1999) KEGG: Kyoto Encyclopedia of Genes and Genomes. *Nucleic Acids Res* 27: 29–34.
26. Livak KJ, Tsai TQ (2001) Analysis of relative gene expression data using real-time quantitative PCR and the 2(-Delta Delta C(T)) method. *Methods* 25: 402–408.
27. Jobin MC, Gottschalk M, Grenier D (2006) Upregulation of prostaglandin E2 and matrix metalloproteinase 9 production by human macrophage-like cells: synergistic effect of capsular material and cell wall from *Streptococcus suis*. *Microb Pathog* 40: 29–34.
28. Tenenbaum T, Essmann F, Adam R, Seibt A, Janicke RU, et al. (2006) Cell death, caspase activation, and HMGB1 release of porcine choroid plexus epithelial cells during *Streptococcus suis* infection in vitro. *Brain Res* 1100: 1–12.
29. Vanier G, Fittipaldi N, Slater JD, de la Cruz Dominguez-Punaro M, Rycroft AN, et al. (2009) New putative virulence factors of *Streptococcus suis* involved in invasion of porcine brain microvascular endothelial cells. *Microb Pathog* 46: 13–20.
30. Kolb SA, Lahrtz F, Paul R, Leppert D, Nadal D, et al. (1998) Matrix metalloproteinases and tissue inhibitors of metalloproteinases in viral meningitis: upregulation of MMP-9 and TIMP-1 in cerebrospinal fluid. *J Neuroimmunol* 84: 143–150.
31. Leib SL, Leppert D, Clements J, Tauber MG (2000) Matrix metalloproteinases contribute to brain damage in experimental pneumococcal meningitis. *Infect Immun* 68: 615–620.
32. Parks WC, Lopez-Boado YS (2004) Matrix metalloproteinases as modulators of inflammation and innate immunity. *Nat Rev Immunol* 4: 617–629.
33. Garlanda C, Bottazzi B, Bastone A, Mantovani A (2005) Pentraxins at the crossroads between innate immunity, inflammation, matrix deposition, and female fertility. *Annu Rev Immunol* 23: 337–366.
34. Jeannin P, Bottazzi B, Sironi M, Doni A, Rusnati M, et al. (2005) Complexity and complementarity of outer membrane protein A recognition by cellular and humoral innate immunity receptors. *Immunity* 22: 551–560.
35. Diniz SN, et al. (2004) PTX3 function as an opsonin for the dectin-1-dependent internalization of zymosan by macrophages. *J Leukoc Biol* 75: 649–656.
36. Garlanda C, Hirsch E, Bozza S, Salustri A, De Acetis M, et al. (2002) Non-redundant role of the long pentraxin PTX3 in anti-fungal innate immune response. *Nature* 420: 182–186.
37. Soares AC, Souza DG, Pinho V, Vieira AT, Nicoli JR, et al. (2006) Dual function of the long pentraxin PTX3 in resistance against pulmonary infection with *Klebsiella pneumoniae* in transgenic mice. *Microbes Infect* 8: 1321–1329.
38. Deban L, Jarva H, Lehtinen MJ, Bottazzi B, Bastone A, et al. (2008) Binding of the long pentraxin PTX3 to factor H: interacting domains and function in the regulation of complement activation. *J Immunol* 181: 8433–8440.
39. Nauta AJ, et al. (2003) Biochemical and functional characterization of the interaction between pentraxin 3 and C1q. *Eur J Immunol* 33: 465–473.
40. Cotena A, Maina V, Sironi M, Bottazzi B, Jeannin P, et al. (2007) Complement dependent amplification of the innate response to a cognate microbial ligand by the long pentraxin PTX3. *J Immunol* 179: 6311–6317.
41. Garlanda C, Bastone A, Mantovani A (2005) Pentraxins at the crossroads between innate immunity, inflammation, matrix deposition, and female fertility. *Annu Rev Immunol* 23: 337–366.
42. Salio M, Chimentì S, De Angelis N, Molla F, Maina V, et al. (2008) Cardioprotective function of the long pentraxin PTX3 in acute myocardial infarction. *Circulation* 117: 1055–1064.
43. Ravizza T, Moneta D, Bottazzi B, Peri G, Garlanda C, et al. (2001) Dynamic induction of the long pentraxin PTX3 in the CNS after limbic seizures: evidence for a protective role in seizure-induced neurodegeneration. *Neuroscience* 105: 43–53.
44. Dias AA, et al. (2001) TSG-14 transgenic mice have improved survival to endotoxemia and to CLP-induced sepsis. *J Leukoc Biol* 69: 928–936.
45. Deban L, Russo RC, Sironi M, Moalli F, Scanziani M, et al. (2010) Regulation of leukocyte recruitment by the long pentraxin PTX3. *Nat Immunol* 11: 328–334.
46. Segura M, Vanier G, Al-Numani D, Lacouture S, Olivier M, et al. (2006) Proinflammatory cytokine and chemokine modulation by *Streptococcus suis* in a whole-blood culture system. *FEMS Immunol Med Microbiol* 47: 92–106.
47. Chahot-Roy G, Willson P, Segura M, Lacouture S, Gottschalk M (2006) Phagocytosis and killing of *Streptococcus suis* by porcine neutrophils. *Microb Pathog* 41: 21–32.
48. Fink SL, Cookson BT (2005) Apoptosis, pyroptosis, and necrosis: mechanistic description of dead and dying eukaryotic cells. *Infect Immun* 73: 1907–1916.
49. Wu Z, Zhang W, Lu Y, Lu C (2010) Transcriptome profiling of zebrafish infected with *Streptococcus suis*. *Microb Pathog* 48: 178–187.

# Construction and Characterization of a *Streptococcus suis* Serotype 2 Recombinant Expressing Enhanced Green Fluorescent Protein

Tao Chen, Qin Huang, Zhaolong Li, Wei Zhang, Chengping Lu, Huochun Yao\*

Key Lab of Animal Bacteriology, Ministry of Agriculture, Nanjing Agricultural University, Nanjing, China

## Abstract

*Streptococcus suis* serotype 2 (*S. suis* 2) is an important pathogen, responsible for diverse diseases in swine and humans. To obtain a *S. suis* 2 strain that can be tracked *in vitro* and *in vivo*, we constructed the Egfp-HA9801 recombinant *S. suis* 2 strain with *egfp* and *spc* genes inserted via homologous recombination. To assess the effects of the *egfp* and *spc* genes in HA9801, the biochemical characteristics, growth features and virulence in Balb/C mice were compared between the recombinant and the parent HA9801 strain. We detected the EGFP expression from Egfp-HA9801 by epifluorescence microscopy. The results showed that the biochemical characterization and growth features of the Egfp-HA9801 recombinant were highly similar to that of the parent HA9801. We did not find significant differences in lethality (50% lethal dose), morbidity and mortality between the two strains. Furthermore, the bacterial counts in each various tissues of Egfp-HA9801-infected mice displayed similar dynamic compared with the HA9801-infected mice. Our results also showed that the Egfp-HA9801 cells grown at 37°C for 36 h displayed greater green fluorescence signals than the cells grown at 28°C for 36 h and 37°C for 24 h. The fluorescence in the tissue cryosections of Egfp-HA9801-injected mice was also stronger than that of the HA9801 group. Together, these results indicate that the *egfp* and *spc* insertions into the Egfp-HA9801 recombinant did not significantly change the virulence when compared with HA9801, and this EGFP labeled strain can be used for future *S. suis* 2 pathogenesis research.

**Citation:** Chen T, Huang Q, Li Z, Zhang W, Lu C, et al. (2012) Construction and Characterization of a *Streptococcus suis* Serotype 2 Recombinant Expressing Enhanced Green Fluorescent Protein. PLoS ONE 7(7): e39697. doi:10.1371/journal.pone.0039697

**Editor:** Indranil Biswas, University of Kansas Medical Center, United States of America

**Received:** January 30, 2012; **Accepted:** May 29, 2012; **Published:** July 20, 2012

**Copyright:** © 2012 Chen et al. This is an open-access article distributed under the terms of the Creative Commons Attribution License, which permits unrestricted use, distribution, and reproduction in any medium, provided the original author and source are credited.

**Funding:** This work was supported by The Foundation of National Natural Science Foundation of China (No. 30671558), and The Priority Academic Program Development of Jiangsu Higher Education Institutions. The funders had no role in study design, data collection and analysis, decision to publish, or preparation of the manuscript.

**Competing Interests:** The authors have declared that no competing interests exist.

\* E-mail: yaohch@njau.edu.cn

## Introduction

*Streptococcus suis* is a Gram-positive coccus that is considered an important swine pathogen and a zoonotic agent causing meningitis, arthritis, septicemia and even sudden death in swine and humans [1,2]. Thus far, 35 different serotypes of *S. suis* have been described. Serotype 2 is the most virulent and the most frequently isolated from both diseased swine and humans [3]. *S. suis* 2 is widely distributed around the world, and not only bring large losses to the pig industry, but it also threatens the public health. In China, *S. suis* 2 was first isolated in Guangdong Province and did not attract wide attention as the cause of an emerging infectious disease until an outbreak occurred in Sichuan province, China where many people were infected, and some of them died in 1998 [4]. In July, 2005, the largest outbreak of human *S. suis* infection occurred in Sichuan province, China, where 204 people were infected, and 38 of them died [5]. The repeated intensive outbreaks of human *S. suis* infection have raised great public concern worldwide regarding the pathogenic mechanisms of this bacteria.

There have been increasing numbers of studies on virulence factors and pathogenesis of *S. suis* 2, and several molecules have been implicated as virulence factors, including the capsule polysaccharide (CPS) [6], a hemolysin (suisysin) [7,8], a 136-kDa

muramidase-released protein (MRP), and a 110-kDa extracellular factor (EF) protein [9]. In addition, it was shown recently that a fibronectin and fibrinogen-binding protein plays an important role in the colonization of affected organs after experimental infection [10]. *S. suis* 2 is usually transmitted by secretions of the oral or nasal mucosa and colonizes the palatine tonsil of both clinically ill and apparently healthy pigs [1]. The entry of *S. suis* into blood from tonsils, uptake by and travel within monocytes and entry into the brain as part of the normal circulation of monocytes play important roles in pathogenesis [11]. Hence, the outcome of the interaction between bacteria and blood phagocytes is considered a key step in the pathogenesis of *S. suis* infections [12].

Studies using chemi-fluorescent dyes (fluorochrome) for labeling bacteria have been described [13,14]. However, because of non-specificity of the chemicals, the extrinsic labeling compounds may leak from the bacteria to phagocytes. Additionally, these approaches can be of limited value for following bacterial pathogens within live host cells. Moreover, the bacteria may be damaged by the dye and bacterial division dilutes the fluorescence signal during infection [15].

Green fluorescent protein (GFP) from jellyfish *Aequoria victoria* is a fluorescent marker that is used for studying the localization, structure, and dynamics of living cells. The fluorescent protein is soluble in a wide variety of species, can be monitored non-

invasively by external illumination, and needs no external substrates [16]. The *gfp* gene, as a potential visible marker for tracking lactic acid bacteria, has been expressed by placement downstream of the constitutive *Lactococcus lactis* P32 promoter [17]. GFP has also been expressed in a number of different bacterial species, including *Escherichia coli*, *L. lactis* and *Streptococcus gordonii* [18]. Expression of GFP did not alter bacterial interactions with host cells, and bacteria producing GFP could be visualized within live mammalian cells [15]. Furthermore, a number of GFP mutant forms have been developed that exhibit enhanced fluorescence emission or altered fluorescence spectra such as enhanced GFP (EGFP).

In this study, we constructed the *S. suis* 2 Egfp-HA9801 recombinant which expresses the EGFP protein. Egfp-HA9801 was labeled successfully by inserting the *egfp* and *spc'* genes into the SS2 HA9801 genome through homologous recombination. The EGFP labeled Egfp-HA9801 was then compared with the parent strain HA9801 by analysis of biochemical characteristics, growth features, experimental infections and EGFP expression.

## Materials and Methods

### i. Ethics Statement

All animals used in this study, and animal experiments, were approved by Department of Science and Technology of Jiangsu Province.

### ii. Bacterial Strains, Plasmids, and Culture Conditions

The bacterial strains and plasmids used in this study are listed in Table 1. *S. suis* cells were grown on agar plates made with Todd-Hewitt (TH) broth containing 2% agar (Bacto) or in liquid cultures of TH broth. *E. coli* cells were grown on Luria-Bertani (LB) agar plates or in liquid LB broth. When necessary, antibiotics were added to the plate or broth at the following concentrations: spectinomycin (spc), 100 mg/ml for *S. suis* 2, 50 mg/ml for *E. coli* TOP 10 strain.

### iii. Construction of the *S. suis* 2 Recombinant Egfp-HA9801

The recombinant plasmid (pESEB) was constructed by cloning four flanking gene fragments into the pEVP3 plasmid. First, the flanking DNA sequences to *sly* and *bsly* were amplified from the chromosomal DNA of *S. suis* 2 HA9801 using PCR with two

pairs of specific primers (SLY-F/SLY-R and BSLY-F/BSLY-R) carrying *Sph* I/*Sma* I and *Sac* I/*Aat* II restriction enzyme sites, respectively (Table 2). Following digestion with the corresponding restriction enzymes, the DNA fragments were cloned into a pEVP3 vector directionally. Then, the *egfp* gene (from pEGFP-N1) was inserted at the *Sna* I/*Bam* H I sites, and the *spc'* gene cassette (from pSET2) was inserted at the *Bam* H I/*Sac* I sites (Fig. 1 A). Finally, the resulting recombinant plasmid (pESEB) was confirmed by PCR and restriction enzyme digestion. To obtain the recombinant strain, the pESEB plasmid was introduced into *S. suis* HA9801 competent cells by electroporation. For preparation of *S. suis* competent cells, wild-type *S. suis* was grown in TH broth containing 40 mmol/L D-L-threonine to OD600 of 0.4 at 37°C and washed twice with sterile water after incubation on ice for 30 min. Subsequently, the cells were resuspended in a mixture containing 15% glycerol and 0.3 mol/L sucrose and stored at -75°C. The electroporation settings were: resistance 250 Ω; voltage: 2.3 kV (cuvette gap: 2.0 mm) and time constant: 4.9 ms. The transformed cells were incubated at 37°C for 120 min and then plated on TH agar plates containing 200 μg/ml spectinomycin and incubated for 48 h at 37°C. A single colony was picked and inoculated in 5 ml TH broth containing 200 μg/ml spectinomycin and incubated overnight at 37°C. The resulting recombinant strain was verified by PCR and RT-PCR amplification and by direct DNA sequencing of the recombination sites using genomic DNA preparations of the recombinant strains.

### iv. Biochemical Characterization of the Recombinant *S. suis* 2 Egfp-HA9801

Single colonies from the parent HA9801 and Egfp-HA9801 strains, grown on TH broth agar containing 5% (v/v) sheep blood at 37°C for 24 h, were picked and inoculated into fresh 5 ml THB medium. Then the parent HA9801 and Egfp-HA9801 cells were continually passaged 20 times in 5 ml THB medium, and the biochemical characterizations of the F1, F10 and F20 passage were performed using the automatic biochemistry analyzer (bioMérieux VITEK 2 System).

### v. Growth of the Recombinant *S. suis* 2 Egfp-HA9801

Inoculations of  $1.0 \times 10^9$  CFU bacteria, equal to 1% (v/v) of 100 ml of THB medium, were incubated in fresh THB at 37°C for 18 h. During the 18 h period, aliquots of 2 ml of cultures were

**Table 1.** Bacterial strains, and plasmids used in this study.

Strains, plasmids and primers	Description	Reference or source
<b>Strains</b>		
<i>S. suis</i> HA9801	Virulent strain of SS2	Virulent strain of SS2 isolated from dead pig
Egfp-HA9801	The insertion mutant of <i>egfp</i> and <i>spc'</i> with background of HA9801, <i>Spc'</i>	Collected in our laboratory
<i>E. coli</i> TOP 10	Cloning host for maintaining the recombinant plasmids	In this study
<b>Plasmids</b>		
pEVP3	A suicide vector, <i>Cm</i> <sup>r</sup>	Collected in our laboratory
pESEB	A recombinant vector with the background of HA9801, designed for insertion of <i>egfp</i> gene; <i>Spc'</i> , <i>Cm</i> <sup>r</sup>	Collected in our laboratory
pEGFP-N1	A green-fluorescence protein vector	Clontech, Palo Alto, CA
pSET2	A plasmid containing <i>Spc'</i> gene	[20]

*Cm*<sup>r</sup>, chloramphenicol resistant; *Spc'*, spectinomycin resistant.  
doi:10.1371/journal.pone.0039697.t001

**Table 2.** Primers used for PCR amplification and detection.

Primers	Sequence of primers (5'-3')	Restriction sites	Functions
Sly-F	ACATGCATGCATGAGAAAAAGTTCGCAC	<i>Sph</i> I	sly gene(1510 bp)
Sly-R	TCCCCGGGCTCTATCACCTCATCCGC	<i>Sma</i> I	
BSly-F	CGAGCTCTCTGGCAATGTATTAT	<i>Sac</i> I	bsly gene,downstream fragment of sly (1165 bp)
BSly-R	GGGGACGTCCTTATCAGCAAAAAGA	<i>Aat</i> II	
SPC-F	GGATCCGTTTCGTGAATACATGTTAT	<i>Bam</i> HI	<i>Spc</i> <sup>R</sup> gene cassette(1031 bp)
SPC-R	GAGCTCGTTTTCAAAATCTGATTA	<i>Sac</i> I*	
EGFP-F	TCCCCCGGGATGGTGAGCAAGGGC	<i>Sma</i> I	egfp gene(749 bp)
EGFP-R	CGCGGATCCTTACTTGTACAGCTCGT	<i>Bam</i> HI	
Rtest	AGCTCGTTCCTTGT		

The restriction sites are in bold.

doi:10.1371/journal.pone.0039697.t002

removed every hour to measure the optical density at 600 (OD600) indicating the bacterial concentration.

#### vi. Experimental Infections of Balb/C Mice

A total of 155 female Balb/C mice at 6 weeks of age (Experimental Animal Center of Yangzhou University) were included in the study. All experiments involving mice were repeated twice and were conducted in accordance with the International Guiding Principles for Biomedical Research Involving Animals—1985. The mice were acclimatized to standard laboratory conditions of 12-h light/12-h dark cycle with free access to rodent chow and water. For all groups, mice showing severe clinical signs and considered moribund were humanely euthanized. Bacterial working cultures were prepared as previously described [21]. Stationary phase bacteria were washed twice in PBS (pH 7.4). Bacterial pellets were then resuspended and serially diluted in THB to appropriate concentrations. The final suspensions of the inoculum for experimental infection were plated onto THB agar to accurately determine the titer and recorded as colony forming units (CFU)/ml.

#### vii. Determination of the 50% Lethal Dose (LD50)

Six-week-old female Balb/C mice (six mice in each group) were infected by intraperitoneal (IP) injection with 500  $\mu$ l of either the HA9801 parent or Egfp-HA9801 recombinant with the dilutions ranging from  $1.2 \times 10^8$  to  $6.0 \times 10^8$  CFU in THB. Mice infected with sterile THB were used as controls. The 50% lethal doses (LD50) of both strains were calculated according to the Karber method [22].

#### viii. Mouse Survival and Mortality Studies

A total of 30 female Balb/C 6-week-old mice were infected by IP injection with 1 ml of either HA9801 parent or the Egfp-HA9801 recombinant at approximately  $6.0 \times 10^8$  CFU in THB. Mice infected with sterile THB were used as controls. The mortality and clinical signs of infection such as depression, swollen eyes, rough hair coat, lethargy, and neurological signs were recorded daily post-infection (p.i.) over a 7-day (d) period as previously described [23].

#### ix. Determination of Viable Bacteria in Organs

A total of 50 female Balb/C 6-week-old mice were infected by IP injection with 500  $\mu$ l of either HA9801 parent or the Egfp-HA9801 recombinant at approximately  $6.0 \times 10^8$  CFU in THB.

Mice infected with sterile THB were used as controls. At each designated time, three infected and one non-infected mice were sacrificed by cervical dislocation. The presence of HA9801 or the Egfp-HA9801 in blood (1 ml) and homogenized organ (0.05 g/organ) samples was determined by plating on THB agar plates.

#### x. Epifluorescence Microscopy

Egfp-HA9801 and HA9801 cells in liquid culture were washed once with 0.1 M PBS (pH 7.4) and resuspended in 30% glycerol. Fluorescence was observed by applying 4  $\mu$ l of the cell suspension on a microscope slide followed by examination using a Carl Zeiss Observer Z1 inverted epifluorescence microscope. The objective was a 40 $\times$ 10.6 LD Plan-Neofluar and a 100 $\times$ 1.40 Oil Plan-Apochromat. The excitation source was a 100 W HBO bulb, and digital images were captured with a 14 bit cooled standard-scan charge coupled-device camera (AxioCam MR3; Carl Zeiss) with resolution set at 1388 $\times$ 1040. The charge-coupled-device camera was controlled by the AxioVision software (version Rel.4.6, Carl Zeiss), and a FITC filter set (exciter: HQ480/40; emitter: HQ 535/50) was used for the excitation and detection of EGFP. The tissue cryosections from the dead mice, which were IP inoculated with  $6.0 \times 10^8$  CFU Egfp-HA9801 or HA9801 bacteria, were also checked immediately by epifluorescence microscopy.

#### xi. Statistical Analysis

Unless otherwise specified, all data are expressed as means  $\pm$  SD and analyzed by a two-tailed, unpaired Student's t-test. A *P* value <0.05 is considered statistically significant.

## Results

### i. Construction and Characterization of the *S. suis* 2 Egfp-HA9801 Recombinant

The recombinant strain was first screened on THB agar plates under the selective pressure of spectinomycin and then confirmed by PCR (Fig. 1 B) and RT-PCR (Fig. 1 C). The direct DNA sequencing result of the recombination sites also indicated that the *egfp* and *spc*<sup>R</sup> gene had been inserted into HA9801 genome successfully.

### ii. Biochemical Characterization of Egfp-HA9801

The results of the biochemical parameters of Egfp-HA9801 are shown in Table 3. The parameters of Egfp-HA9801 were the same as that of the parent HA9801 strain, except for arginine



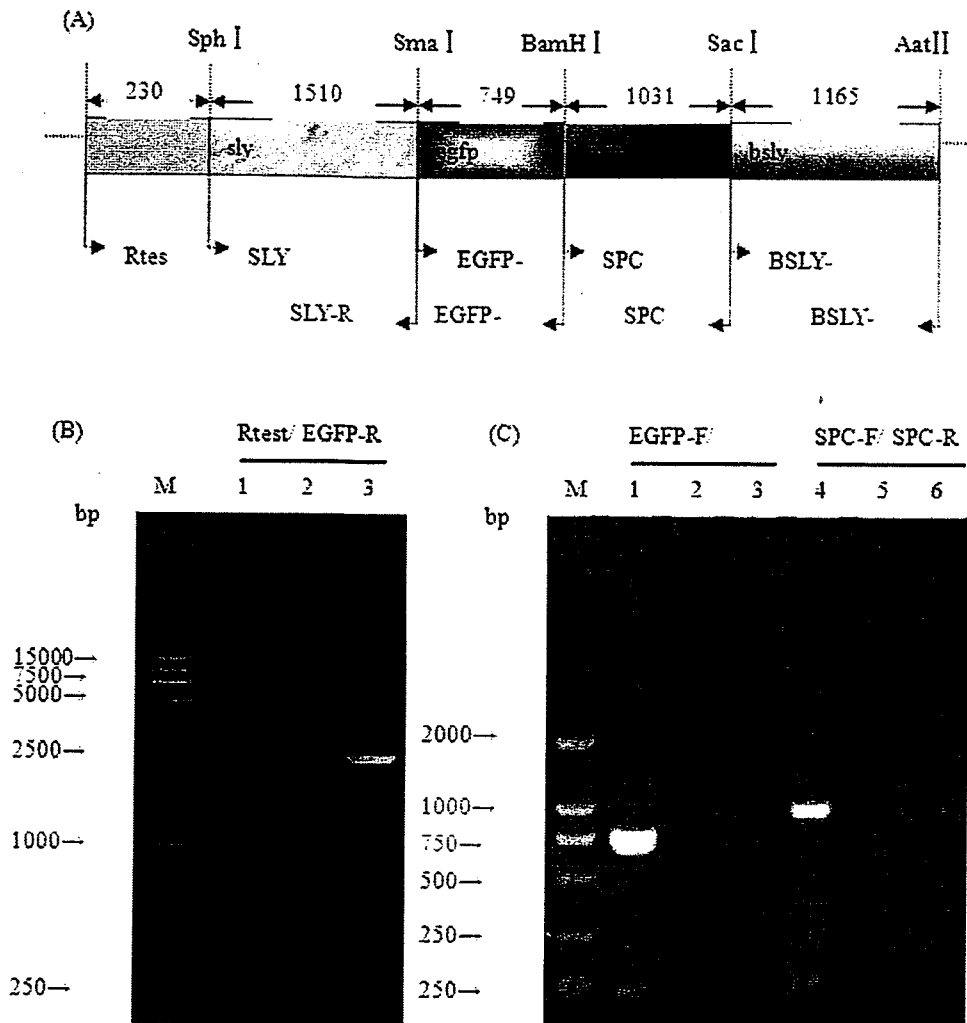


**Figure 1. Genomic organization of the double crossover recombination locus in *S. suis* 2 Egfp-HA9801 and confirmation analysis of the recombinant strain Egfp-HA9801.** (A) Genomic organization of the double crossover recombination locus and its flanking genes in *S. suis* 2 Egfp-HA9801. Dashes above the gene indicate restriction sites. The numbers above the gene and between the solid arrows indicate the size (bps) of the known gene fragments. The different color boxes represent *sly*, *egfp*, *spc* and *bsly* genes. The location of the primers used in PCR and RT-PCR detection are indicated by inverted arrowheads. (B) PCR analysis of the Egfp-HA9801 recombinant strain. The PCR primer combinations are shown over the lanes. Genomic DNA from the parent strain HA9801 (lane 2) and Egfp-HA9801 recombinant (lane 2) were used as templates. Lane 1 is the negative control. The 15 kb DNA ladder marker is shown to the left (M). (C) RT-PCR analysis of the Egfp-HA9801 recombinant strain. The primer combinations used in RT-PCR are shown over the lanes. Total RNA extracted from mid-exponential-phase cultures of the following strains were used as templates: parent strain HA9801 (lane 2, 5) and Egfp-HA9801 recombinant (lane 1, 4). Lane 3 and lane 6 are negative controls. The 15 kb DNA ladder marker is shown to the left (M). Theoretical size (bp) of each of the PCR and RT-PCR products generated with the primer combinations are shown in (A).

doi:10.1371/journal.pone.0039697.g001

dihydrolase 1, D-Galactose, and pyroglutamate enzyme aromatic amine. There was also no difference between the different passages of Egfp-HA9801. These results indicate that the biological characteristics of Egfp-HA9801 were stable and similar to HA9801, and had not been influenced by inserting the *egfp* and *spc* genes into the *S. suis* 2 genome.

iii. Growth Features of Egfp-HA9801

Cultures of both Egfp-HA9801 and the parent HA9801 strains at different times were used to measure their bacterial concentra-

tion (Fig. 2). The growth curve of Egfp-HA9801 was similar to that of HA9801.

iv. Experimental Infections of Balb/C Mice

To study the effect of *egfp* and *spc* insertions on the pathogenesis of *S. suis* 2, the virulence of the Egfp-HA9801 recombinant and parent HA9801 was assessed in a Balb/C mouse infection model. Results of the trial showed that the LD50 of Egfp-HA9801 and HA9801 were  $3.200 \times 10^8$  CFU and  $3.259 \times 10^8$  CFU, respectively (Table 4), indicating that there were no significant differences between the two strains ( $P > 0.05$ ).

**Table 3.** Biochemical characteristics of the *S. suis* 2 (SS2) parent strain and recombinant obtained using a automatic biochemistry analyzer.

Parameters	SS2 HA9801 parent strain			SS2 Egfp-HA9801 recombinant		
	F1	F10	F20	F1	F10	F20
Amygdalin	-	-	-	-	-	-
Phosphatidylinositol:phospholipase.C	-	-	-	-	-	-
D-Xylose	-	-	-	-	-	-
Arginine dihydrolase:1	+	(+)	+	(-)	-	-
β-D-galactosidase	-	-	-	-	-	-
α-glucosidase	+	+	+	+	+	+
Ala-Phe-Pro aromatic amines enzyme	+	+	+	+	+	+
β-Gal-pyran: glycosidase	-	-	-	-	-	-
α-Mannosidase	-	-	-	-	-	-
β-glucuronidase	+	(+)	(+)	+	+	+
α-galactosidase	+	+	+	+	+	+
Pyroglutamate-enzyme aromatic amine	(-)	-	(-)	(+)	+	+
β-D-Glucuronidase	-	-	-	-	-	-
Enzyme alanine aromatic amines	+	+	+	+	+	+
Tyrosinase enzyme aromatic amine	+	+	+	+	+	+
D-galactose	+	+	+	-	-	(-)
Lactose	+	+	+	+	+	+
N-acetyl-D-glucosamine	+	+	(+)	+	+	+
D-Maltose	+	+	+	+	+	+
Bacitracin tolerance	-	-	-	-	-	-
Methyl-B-D-glucose pyran-glucoside	+	+	+	+	+	+
Sucrose	+	+	+	+	+	+

+: Positive; -: Negative; (): Results Weak.  
doi:10.1371/journal.pone.0039697.t003

During the course of infection, all the mice infected with HA9801 at approximately  $6.0 \times 10^8$  CFU showed clear clinical signs, such as depression, swollen eyes, weakness and prostration post-inoculation. Five mice died in this group during the 24 h post-inoculation. From day 4 p.i., surviving mice in the HA9801

group developed clinical signs associated with *S. suis* 2 meningitis such as hyperexcitation, opisthotonus, bending of the head and walking in circles. Meanwhile, mice infected with Egfp-HA9801 had an 80% mortality rate, and all of them showed clear clinical signs (Table 5 and Fig. 3). All the results indicated that no significant differences were found between the Egfp-HA9801 group and the HA9801 group.

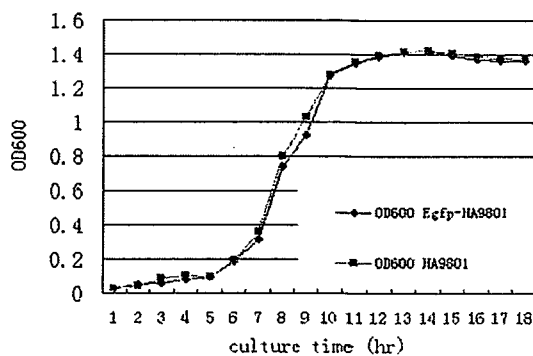


**Figure 2.** Growth curve of Egfp-HA9801 and parent HA9801. Both Egfp-HA9801 and HA9801 were incubated in 100 ml of fresh THB at 37°C for 18 h. During the 18 h period, aliquots of 2 ml of cultures were used to monitor the bacterial concentration every hour. No significant differences were found between the two strains throughout the experiment ( $P > 0.05$ ).  
doi:10.1371/journal.pone.0039697.g002

To further investigate the virulence of the Egfp-HA9801 recombinant, *in vivo* colonization experiments were carried out. According to the results of LD50 assessment, mice were IP inoculated with about  $6.0 \times 10^8$  CFU in 1 ml THB of the recombinant or parental strains. The live bacteria were recovered from the lung, liver, kidney, spleen, brain and blood at each designated timepoint. As shown in Fig. 4, bacterial counts from each specific tissue of Egfp-HA9801-infected mice were not significantly different from that of the HA9801-infected mice ( $P > 0.05$ ). These results suggested that the colonization of Egfp-HA9801 had not been obviously influenced by inserting *egfp* and *spc'* gene into the *S. suis* 2 genome. Together with the above results, this shows that Egfp-HA9801 was very similar with HA9801 in terms of virulence, presentation of symptoms and infection process. Therefore, the recombinant strain can be used as an EGFP labeled strain for SS2 pathogenesis research under natural conditions.

**Table 4.** LD50 of *S. suis* type 2 HA9801 strains and recombinant SS2 Egfp-HA9801 strains in Balb/C mice.

Strain	Infection dose (CFU)	Amount of mouse	Mortality	LD50 (CFU)
HA9801	6.0×10 <sup>8</sup>	6	6/6	3.259×10 <sup>8</sup>
	4.8×10 <sup>8</sup>	6	5/6	
	3.6×10 <sup>8</sup>	6	3/6	
	2.4×10 <sup>8</sup>	6	2/6	
	1.2×10 <sup>8</sup>	6	0/6	
Egfp-HA9801	6.0×10 <sup>8</sup>	6	6/6	3.200×10 <sup>8</sup>
	4.8×10 <sup>8</sup>	6	5/6	
	3.6×10 <sup>8</sup>	6	4/6	
	2.4×10 <sup>8</sup>	6	1/6	
	1.2×10 <sup>8</sup>	6	0/6	
Blank control		6	0/6	

The LD50 of both strains were calculated according to the Karber method.  
doi:10.1371/journal.pone.0039697.t004

**v. Expression of EGFP in *S. suis* Recombinant Egfp-HA9801 as Detected by Epifluorescence Microscopy**

*S. suis* recombinant Egfp-HA9801 cells were clearly fluorescent under the epifluorescent microscope, whereas no fluorescent signals from the HA9801 cells were observed (Fig. 5). In particular, the Egfp-HA9801 cells which were grown at 37°C for 36 h showed brighter fluorescent signals than the cells grown at 28°C for 36 h and 37°C for 24 h. Furthermore, the fluorescence of tissue cryosections of the Egfp-HA9801-injected mice was stronger than that of the HA9801 group (Fig. 6).

**Discussion**

*S. suis* 2 is considered as one of the most important swine pathogens and is an emerging, life-threatening zoonotic agent in both pigs and humans. Although a series of virulence factors associated with *S. suis* 2 were identified recently [6,24], the specific function of these virulence factors in the pathogenicity of *S. suis* 2 is still unknown, and the pathogenesis of the infection caused by *S. suis* is still poorly understood.

In this study, the EGFP labeled recombinant Egfp-HA9801 was constructed via homologous recombination and the impact of *egfp* and *spc* gene insertion on biochemical characteristics and virulence of *S. suis* 2 was assessed. The results of this study demonstrated that the EGFP labeled Egfp-HA9801 is a promising

and useful tool for the study of *S. suis* 2 pathogenesis both *in vitro* and *in vivo*.

The target organism can be labeled with GFP through plasmid-based *gfp* vectors or chromosomal marker. Although plasmid-based *gfp* vectors have been used in eukaryotic systems, and some *gfp*-broad host-range plasmids have been successfully used to label certain species of bacteria, there are two limitations to applying these vectors for bacterial strains used in environmental studies. First, due to concerns about plasmid stability under natural environmental conditions, bacterial strains used in pathogenesis studies should be chromosomally marked with a single copy of the *gfp* gene to maximize genetic stability as well as reduce the risk of transfer of the genetic marker to other microorganisms. The second limitation is the sensitivity required for detection of individual cells containing a single copy of the *gfp* marker. To circumvent these limitations, a Tn10- [25] and several Tn5-based

**Table 5.** Virulence of the *S. suis* parent strain HA9801 and Egfp-HA9801 recombinant in Balb/C mice.

	No. of Balb/C mice	Morbidity <sup>a</sup> (%)	Mortality <sup>b</sup> (%)
HA9801	10	100	90
Egfp-HA9801	10	100	80
Blank control	10	0	0

These measurements were performed over a period of 7-day post-infection.

<sup>a</sup>Percentage of mice with clinical symptoms.

<sup>b</sup>Percentage of mice that died due to infection.

doi:10.1371/journal.pone.0039697.t005

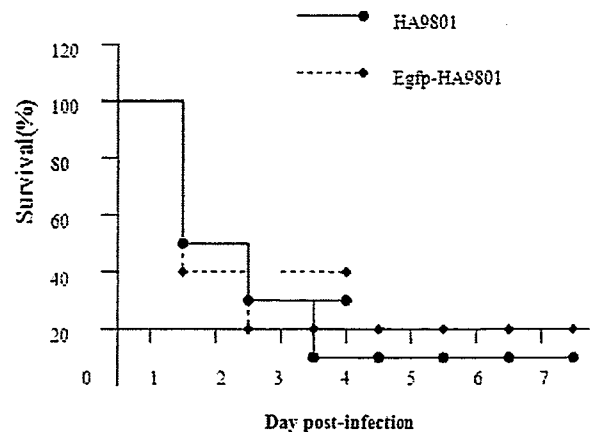


**Figure 3.** Survival curves for Balb/C mice infected with Egfp-HA9801 and HA9801 strains. Six-week-old Balb/C mice were inoculated i.p. with 6.0×10<sup>8</sup> CFU bacteria; mice survival was monitored over a 7-day period. Data are expressed as mean percentage of live animals in each group (n=10).

doi:10.1371/journal.pone.0039697.g003

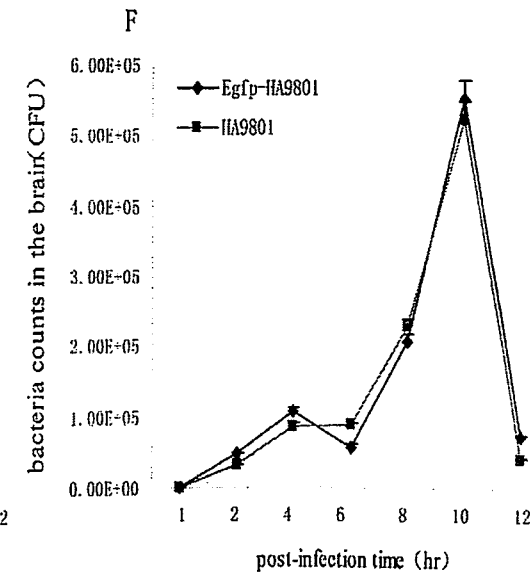
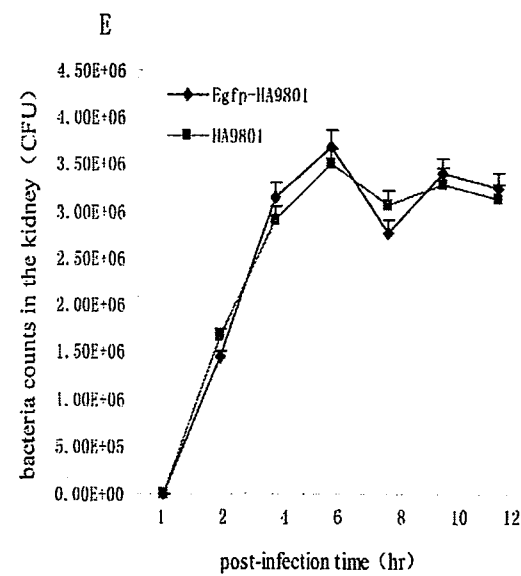
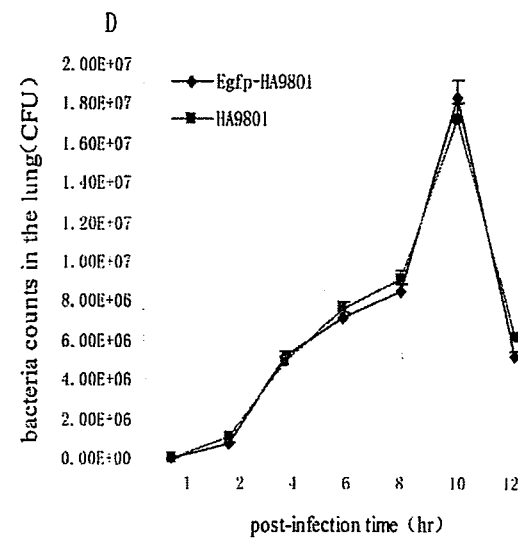
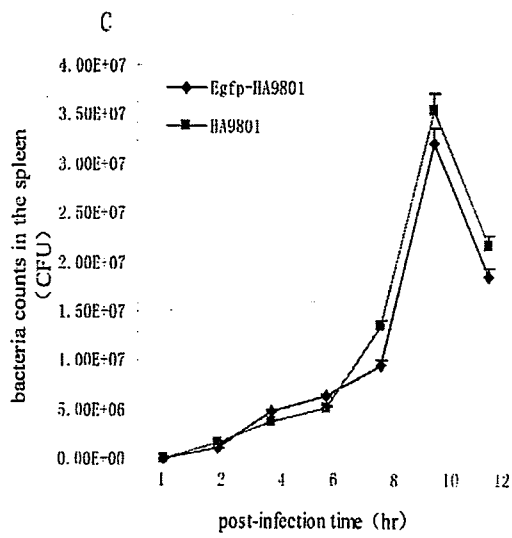
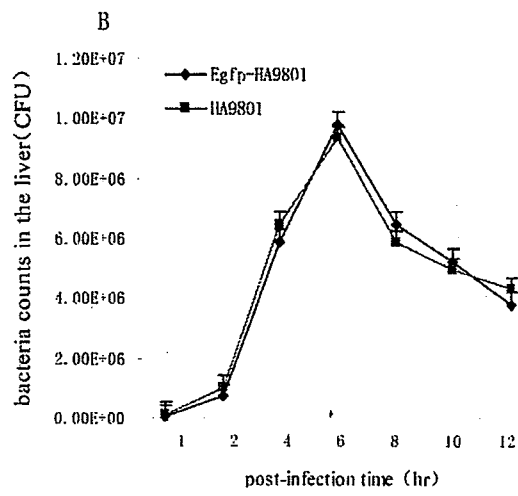
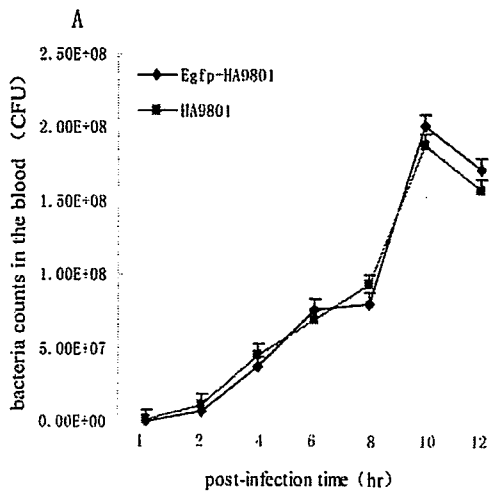


**Figure 4. Bacterial distribution in different organs from mice infected i.p. with HA9801 parent and Egfp-HA9801 recombinant strains.** Bacterial loads in the blood (A) are expressed as CFU/ml, and in the liver (B), spleen(C), lung (D), kidney (E) and brain (F) as CFU/0.05 g of tissue. Results are expressed as mean  $\pm$  SEM of at least three infected mice per p.i. time point. No significant differences were found between the two strains throughout the experiment ( $P>0.05$ ).  
doi:10.1371/journal.pone.0039697.g004

[26,27] transposon suicide gene delivery vectors have been developed. They have been used to mark various Gram-negative bacteria including, *Agrobacterium tumefaciens*, *Alcaligenes eutrophus*, *Moraxella sp.*, and *Vibrio sp.* However, there have not been any studies on Gram-positive bacteria chromosomally engineered with

a *gfp* genetic marker. In this study, the SS2 Egfp-HA9801 recombinant was chromosomally marked via homologous recombination, and the biochemical characterization and growth features of the Egfp-HA9801 recombinant were extremely similar to that of the parent HA9801. In the present work, we did not find

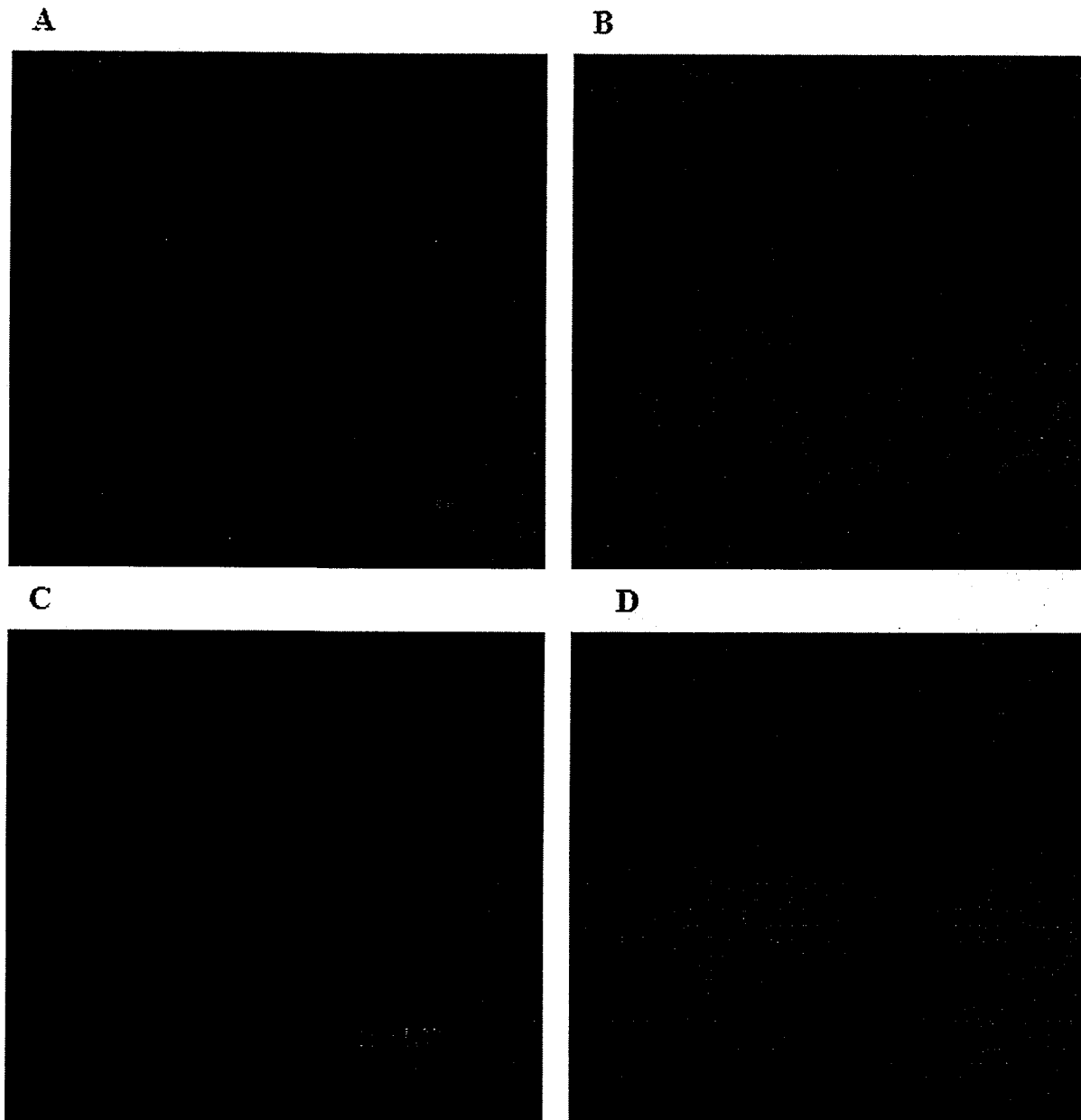


**Figure 5. Epifluorescence microscopy analysis of bacteria cultured *in vitro*.** A: Egfp-HA9801(10x40); B: HA9801(10x40); C: Egfp-HA9801(10x100); D: HA9801(10x100).  
doi:10.1371/journal.pone.0039697.g005

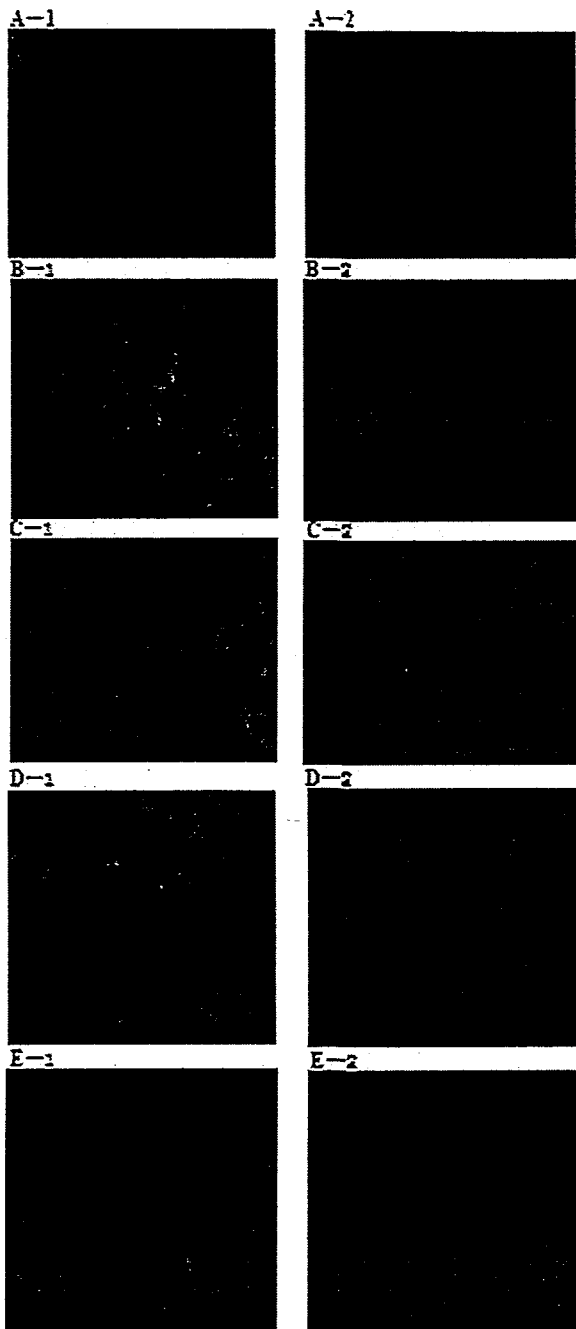


**Figure 6. Epifluorescence microscopy analysis of the cryosections of the tissues obtained from the mice infected with Egfp-HA9801 or HA9801.** The cryosections of liver (A-1), lung (B-1), kidney (C-1), spleen (D-1) and brain (E-1) from the Egfp-HA9801-infected mice were detected under epifluorescent microscope and the FITC images are shown in the left column. The FITC images of the cryosections of liver (A-2), lung (B-2), kidney (C-2), spleen (D-2) and brain (E-2) from the HA9801-infected mice, are showed in the right column.  
doi:10.1371/journal.pone.0039697.g006

significant differences in LD50, morbidity and mortality between the two strains, indicating that the insertion of *egfp* and *spc* had no effect on bacterial virulence. Furthermore, the bacterial counts in

each tissue of Egfp-HA9801-infected mice displayed similar dynamic variations compared with the HA9801-infected mice. These findings suggest that the *egfp* and *spc* insertion did not render any significant changes in the Egfp-HA9801 recombinant when compared with HA9801. Therefore, the recombinant can be used as EGFP labeled strain for SS2 pathogenesis research under natural conditions.

Overall, the expression of GFP protein is stable, but GFP protein folding is thermosensitive. Moreover, the chromophore formation requires sufficient time; hence, the principal limiting factors of GFP expression include environmental temperature and expression time [16,28]. Jin Zou *et al.* [29] reported that 72 h of expression at 30°C is appropriate for chromophore formation of the GFP variants in HeLa cells. Surprisingly, the same GFP variants could not be detected with either the fluorescence spectrophotometer or fluorescence microscope in HeLa cells when grown at 37°C after transfection. For *S.suis* 2 SX332 cells, GFP expression peaked at 48 h and 30°C [30]. Our results showed that the Egfp-HA9801 cells grown at 37°C for 36 h showed more obvious green fluorescence than the cells grown for other culture temperatures and time periods, indicating that 36 h of expression at 37°C is optimal for expression of EGFP in our recombinant strain. One possible reason is that the expression of GFP at 37°C proceeds too fast to process the necessary post-translational modification in the other GFP mutant strains but this temperature is appropriate for EGFP. Furthermore, the labeling method based on chromosomal marking may affect the optimum condition of GFP expression.

In this study, the fluorescence of tissue cryosections of Egfp-HA9801-innoculated mice was stronger than that of the HA9801 group, but the green fluorescence of the bacteria in the cryosections were not clearly seen because of the high fluorescence background of the tissue. Autofluorescence is often seen in many species and is due to various factors, including metabolites and structural components. However, the emission and excitation characteristics of autofluorescence are very different from GFP; hence, further optimization of standard filter sets may simply be made to reduce or eliminate the autofluorescence in the tissues [31]. Schnell *et al.* [32] studied the effect of chemical treatments on tissue sections from monkey, rat, and human neural tissue. They revealed that lipofuscin-like autofluorescence in these tissues could be significantly reduced or eliminated by treatment with 1–10 mmol/L CuSO<sub>4</sub> in a 50 mmol/L ammonium acetate buffer (pH 5) or 1% Sudan black B in 70% ethanol. Further optimization studies are needed to reduce or eliminate the autofluorescence in the tissues.

In conclusion, our study demonstrated, for the first time, that the Egfp-HA9801 recombinant, labeled with *egfp* gene basing on chromosomal marking, is a promising and useful tool for the study of *S. suis* 2 pathogenesis both *in vitro* and *in vivo*.

**Acknowledgments**

We are grateful to Dr. Sekizaki (National Institute of Animal Health, Japan) for supplying plasmid pSET2 and Dr.morrison (University of Illinois, USA) for providing us plasmid pEVP3and their precious guiding for correctly using these plasmids. We thank Jie Rong Shujian Zhang and Dr. Zongfu Wu for excellent technical assistance.

**Author Contributions**

Conceived and designed the experiments: TC QH ZL WZ CL HY. Performed the experiments: TC QH ZL. Analyzed the data: TC QH HY. Contributed reagents/materials/analysis tools: TC QH WZ HY. Wrote the paper: TC.

## References

- Staats JJ, Feder I, Okwumabua O, Chengappa MM (1997) Streptococcus suis: past and present. *Vet Res Commun*, 21(6): 381–407.
- Lun ZR, Wang QP, Chen XG, Li AX, Zhu XQ (2007) Streptococcus suis: an emerging zoonotic pathogen. *Lancet Infect Dis*, 7(3): 201–209.
- Gotschalk M, Segura M, Xu J (2007) Streptococcus suis infections in humans: the Chinese experience and the situation in North America. *Anim Health Res Rev*, 8(1): 29–45.
- Normile D (2005) Infectious diseases. WHO probes deadliness of China's pig-borne disease. *Science*, 309(5739): 1308–1309.
- Yu H, Jing H, Chen Z, Zheng H, Zhu X, et al. (2006) Human Streptococcus suis outbreak, Sichuan, China. *Emerg Infect Dis*, 12: 914–920.
- Smith HE, Damman M, van der VJ, Wagenaar F, Wisselink HJ, et al. (1999) Identification and characterization of the cps locus of Streptococcus suis serotype 2: the capsule protects against phagocytosis and is an important virulence factor. *Infection and Immunity*, 67: 1750–1756.
- Gotschalk MG, Lacouture S, Dubreuil JD (1995) Characterization of Streptococcus suis capsular type 2 haemolysin. *Microbiology*, 141 (Pt 1): 189–195.
- Jacobs AA, Loeffen PL, van den Berg AJ, Storm P K (1994) Identification, purification, and characterization of a thiol-activated hemolysin (sullysin) of Streptococcus suis. *Infect Immun*, 62(5): 1742–1748.
- Vecht U, Wisselink HJ, Jellema ML, Smith HE (1991) Identification of two proteins associated with virulence of Streptococcus suis type 2. *Infect Immun*, 59(9): 3156–3162.
- de Greeff A, Buys H, Verhaar R, Dijkstra J, van Alphen L, et al. (2002) Contribution of fibronectin-binding protein to pathogenesis of Streptococcus suis serotype 2. *Infect Immun*, 70(3): 1319–1325.
- Williams AE (1990) Relationship between intracellular survival in macrophages and pathogenicity of Streptococcus suis type 2 isolates. *Microb Pathog*, 8(3): 189–196.
- Chanter N, Jones P, Alexander T (1993) Meningitis in pigs caused by Streptococcus suis—a speculative review. *Vet Microbiol*, 36: 39–55.
- Heinzelmann M., Gardner S, Mercer JM, Roll A, Polk HJ (1999) Quantification of phagocytosis in human neutrophils by flow cytometry. *Microbiol. Immunol*, 43: 505–512.
- Rodriguez M, Van der PW, Van de WJ (2001) Flowcytometry-based phagocytosis assay for sensitive detection of opsonic activity of pneumococcal capsular polysaccharide antibodies in human sera. *J. Immunol. Methods*, 252: 33–44.
- Valdivia R., Hromockyj A, Monack D, Ramakrishnan L, Falkow S (1996) Applications for green fluorescent protein (GFP) in the study of host-pathogen interactions. *Gene*, 173: 47–52.
- Zimmer M (2002) Green fluorescent protein (GFP): applications, structure, and related photophysical behavior. *Chem. Rev*, 102: 759–781.
- Scott K, Mercer D, Glover L, Flint H (1998) The green fluorescent protein as a visible marker for lactic acid bacteria in complex ecosystems. *FEMS Microbiol. Ecol*, 26: 219–230.
- Hansen M, Palmer RJ, Udsen C, White D, Molin S (2001) Assessment of GFP fluorescence in cells of Streptococcus gordonii under conditions of low pH and low oxygen concentration. *Microbiology*, 147: 1383–1391.
- Jean PC, Agnes D, Ekaterina VP, Bernard M, Donald AM (1995) Construction and evaluation of new drug-resistance cassettes for gene disruption mutagenesis in Streptococcus pneumoniae, using an ami test platform. *Gene*, 164: 123–128.
- Takamatsu D, Osaki M, Sekizaki T (2001) Construction and characterization of Streptococcus suis-Escherichia coli shuttle cloning vectors. *Plasmid*, 45: 101–113.
- Dominguez-Punaro MC, Segura M, Plante MM, Lacouture S, Rivest S, et al. (2007) Streptococcus suis serotype 2, an important swine and human pathogen, induces strong systemic and cerebral inflammatory responses in a mouse model of infection. *Journal of Immunology*, 179: 1842–1854.
- Li L, Zhou R, Li T, Kang M, Wan Y, et al. (2008) Enhanced biofilm formation and reduced virulence of Actinobacillus pleuropneumoniae luxS mutant. *Microbial Pathogenesis*, 45: 192–200.
- Vanier G, Fittipaldi N, Slater JD, Dominguez-Punaro ML, Rycroft AN, et al. (2009) New putative virulence factors of Streptococcus suis involved in invasion of porcine brain microvascular endothelial cells. *Microbial Pathogenesis*, 46: 13–20.
- Berthelot-Herault F, Morvan H, Keribin AM, Gotschalk M, Kobisch M (2000) Production of muraminidase-released protein (MRP), extracellular factor (EF) and sullysin by field isolates of Streptococcus suis capsular types 2, 1/2, 9, 7 and 3 isolated from swine in France. *Veterinary Research*, 31: 473–479.
- Stretton S, Techakarnjanak S, McLennan AM, Goodman AE (1998) Use of green fluorescent protein to tag and investigate gene expression in marine bacteria. *Appl. Environ. Microbiol*, 64: 2554–2559.
- Suarez A, Guttler A, Stratz M, Staendner LH, Timmis KN, et al. (1997) Green fluorescent protein-based reportersystems for genetic analysis of bacteria including monocopy applications. *Gene*, 196: 69–74.
- Tombolini R, Unge A, Davy ME, de Bruijn FJ, Jansson J (1997) Flow cytometric and microscopic analysis of GFP-tagged Pseudomonas fluorescens bacteria. *FEMS Microbiol. Ecol*, 22: 17–28.
- Tsien R. (1998) The green fluorescent protein. *Ann. Rev. Biochem*, 67: 509–544.
- Jin Z, Jenny JY, Kristy W, Monica L, April LE, et al. (2005) Expression and optical properties of green fluorescent protein expressed in different cellular environments. *Journal of Biotechnology*, 119: 368–378.
- Shichun L, Willson PJ (2004) Expression of green fluorescent protein and its application in pathogenesis studies of serotype 2 Streptococcus suis. *Journal of Microbiological Methods*, 56: 401–412.
- Nicholas B, Andrew WK (2001) Seeing the wood through the trees: a review of techniques for distinguishing green fluorescent protein from endogenous autofluorescence. *Analytical Biochemistry*, 291: 175–197.
- Schnell SA, Staines WA, Wessendorf MW (1999) Reduction of lipofuscin-like autofluorescence in fluorescently labeled tissue. *J Histochem Cytochem*, 47: 719–73.

# Genomic and Epidemiological Characteristics Provide New Insights into the Phylogeographical and Spatiotemporal Spread of Porcine Epidemic Diarrhea Virus in Asia

Min Sun,<sup>a,b</sup> Jiale Ma,<sup>a,b</sup> Yanan Wang,<sup>a,b</sup> Ming Wang,<sup>a,b</sup> Wenchao Song,<sup>a</sup> Wei Zhang,<sup>a,b</sup> Chengping Lu,<sup>a,b</sup> Huochun Yao<sup>a,b</sup>

College of Veterinary Medicine, Nanjing Agricultural University, Nanjing, China<sup>a</sup>; Key Lab of Animal Bacteriology, Ministry of Agriculture, Nanjing, China<sup>b</sup>

Porcine epidemic diarrhea has become pandemic in the Asian pig-breeding industry, causing significant economic loss. In the present study, 11 complete genomes of porcine epidemic diarrhea virus (PEDV) field isolates from China were determined and analyzed. Frequently occurring mutations were observed, which suggested that full understanding of the genomic and epidemiological characteristics is critical in the fight against PEDV epidemics. Comparative analysis of 49 available genomes clustered the PEDV strains into pandemic (PX) and classical (CX) groups and identified four hypervariable regions (V1 to V4). Further study indicated key roles for the spike (S) gene and the V2 region in distinguishing between the PX and CX groups and for studying genetic evolution. Genotyping and phylogeny-based geographical dissection based on 219 S genes revealed the complexity and severity of PEDV epidemics in Asia. Many subgroups have formed, with a wide array of mutations in different countries, leading to the outbreak of PEDV in Asia. Spatiotemporal reconstruction based on the analysis suggested that the pandemic group strains originated from South Korea and then extended into Japan, Thailand, and China. However, the novel pandemic strains in South Korea that appeared after 2013 may have originated from a Chinese variant. Thus, the serious PED epidemics in China and South Korea in recent years were caused by the complex subgroups of PEDV. The data in this study have important implications for understanding the ongoing PEDV outbreaks in Asia and will guide future efforts to effectively prevent and control PEDV.

Porcine epidemic diarrhea (PED) is an acute enteric tract infectious disease characterized by thin-walled intestines with severe villus atrophy and congestion, which can rapidly lead to death from acute watery diarrhea and vomit, especially in piglets (1–3). Porcine epidemic diarrhea virus (PEDV), the etiological agent (4, 5), is an alphacoronavirus from the family *Coronaviridae* of the order *Nidovirales* (6).

The PEDV genome is approximately 28 kb in length and comprises seven open reading frames (ORFs) (7, 8). The spike (S) gene of PEDV encodes the spike glycoprotein and can be divided into S1 and S2 domains, just as in other coronaviruses (9–11). The S glycoprotein interacts with the cellular receptor to regulate viral entry and contains neutralizing epitopes to induce neutralizing antibodies (12, 13). In addition, the S gene shows a high degree of genetic diversity (14), especially in the S1 domain or the N-terminal region of the S1 domain (15–17), and is considered an important gene marker in understanding genetic variations of PEDV strains in the field (16, 18, 19).

The first PEDV strain, CV777, was recognized in Belgium in 1977 (4, 5). Postemergence, several European nations reported disease outbreaks (20, 21). Currently, PED disease is causing serious losses in the pig industry in many Asian nations, including South Korea (14, 22, 23), Thailand (9, 18), and China (24). At present, strains of PEDV cause more severe clinical symptoms than previous strains; pigs of all ages are affected and exhibit different degrees of diarrhea and loss of appetite (2, 18, 23). The strains emerging in Asia are distinct from previous endemic PEDV strains and may have been introduced from overseas (9, 23).

In the present study, 11 complete genomic sequences of Chinese field strains collected from 2011 to 2014 were determined. Together with 38 other available PEDV genomes, they were used to analyze genome characteristics and evaluate the genetic stability of the virus. Furthermore, we analyzed the epidemic regularity of

219 PEDV field strains, determined the relationship among PEDV strains more precisely, and revealed the phylogeography and spatiotemporal spread of PEDV in Asia.

## MATERIALS AND METHODS

**Sample collection and treatment.** From April 2011 to March 2014, nine intestinal homogenates and two feces samples were collected from pigs that had severe diarrhea and a high mortality rate at 11 farms (Table 1). PEDV infection was confirmed by a PEDV membrane (M) gene-based reverse transcription-PCR (RT-PCR) (25) and by sequencing. The 11 positive PEDV samples were from large-scale commercial swine farms (>50,000 pigs) and were inoculated with PEDV vaccine. In each outbreak, intestinal or feces samples collected from 3- to 4-day-old piglets displayed the clinical features associated with PED, including watery diarrhea, loss of appetite, vomiting, and dehydration.

These samples were collected individually and placed in separate sterile specimen containers. The minced intestinal and blended feces were used to generate a 10% (g/ml) homogenate in phosphate-buffered saline (PBS). The homogenate was freeze-thawed three times, vortexed, and

Received 11 October 2014 Returned for modification 7 November 2014

Accepted 7 February 2015

Accepted manuscript posted online 18 February 2015

Citation Sun M, Ma J, Wang Y, Wang M, Song W, Zhang W, Lu C, Yao H. 2015. Genomic and epidemiological characteristics provide new insights into the phylogeographical and spatiotemporal spread of porcine epidemic diarrhea virus in Asia. *J Clin Microbiol* 53:1484–1492. doi:10.1128/JCM.02898-14.

Editor: B. W. Fenwick

Address correspondence to Huochun Yao, yaohch@njau.edu.cn.

Supplemental material for this article may be found at <http://dx.doi.org/10.1128/JCM.02898-14>.

Copyright © 2015, American Society for Microbiology. All Rights Reserved.

doi:10.1128/JCM.02898-14



TABLE 1 Eleven PEDV isolates obtained from different farms in China during outbreaks in 2011 to 2014

Strain name	Sample origin	GenBank accession no.	Nations	Collection date
PEDV-1C	Small intestine	KM609203	China	March 2012
PEDV-7C	Small intestine	KM609204	China: JiangXi	June 2011
PEDV-8C	Small intestine	KM609205	China	Unknown
PEDV-10F	Feces	KM609206	China: JiangSu	January 2012
PEDV-14	Small intestine	KM609207	China: Zhejiang	April 2011
PEDV-15F	Feces	KM609208	China: ChongQing	March 2012
PEDV-CHZ	Small intestine	KM609209	China: JiangSu	March 2013
PEDV-LY	Small intestine	KM609210	China: ShanDong	January 2014
PEDV-LS	Small intestine	KM609211	China: ShanDong	January 2014
PEDV-LYG	Small intestine	KM609212	China: JiangSu	March 2014
PEDV-WS	Small intestine	KM609213	China: Zhejiang	March 2014

centrifuged at 5,000 rpm for 10 min at 4°C. The supernatant was removed and centrifuged at 10,000 rpm for 10 min at 4°C. The final supernatants were used immediately or stored at -20°C.

**RNA extraction and RT-PCR.** The primers (see Table S1 in the supplemental material) were designed based on the highly conserved sites of the PEDV reference strain CHGD-01 (GenBank accession no. JX261936.1), using Oligo 6.0. Six overlapping DNA fragments were amplified by RT-PCR.

Viral RNA extraction, RT-PCR amplification, and cloning were performed according to conventional protocols, with some modifications (26). In brief, viral RNA was extracted from the supernatants of the homogenized positive samples using an RNeasy minikit (Qiagen, Hilden, Germany), according to the manufacturer's instructions. Viral RNA was eluted into 50 µl of RNase-free water. HiScript reverse transcriptase (HiScript II 1st Strand cDNA synthesis kit; Vazyme, China) was used to synthesize cDNA from the extracted RNA and stored at -20°C. The amplifications for the six overlapping DNA fragments were performed using LAMP DNA polymerase (Vazyme, Nanjing, China). A SMARTer rapid amplification of cDNA ends (RACE) kit (Clontech, Japan) confirmed the 5' and 3' ends of the genome, according to the manufacturer's instructions.

**Whole-genome sequence and assembly.** In brief, bands of corresponding size of the RT-PCR products were excised, and a QIAquick gel extraction kit (TaKaRa, Shanghai, China) was used to purify the synthesized DNA, according to the manufacturer's instructions. The Shanghai Sunny Biotechnology Co, Ltd. (Shanghai, China) sequenced the purified products. Each nucleotide was identified from the replicates that gave identical results. The DNASTar software package (DNASTar Inc., Madison, WI, USA) was used to assemble and analyze the sequencing data. The complete genome sequences of the 11 Chinese PEDV strains were submitted to the GenBank database with the accession numbers shown in Table 1.

**Variation analysis of 49 whole PEDV genomes.** The method of calculating the variation coefficient is shown in Fig. S1A in the supplemental material. One hundred base pairs at a time were extracted from the alignment of 49 whole PEDV genomes (Table 1; see also Table S2 in the supplemental material) constructed by MEGA (v5.0.3) software (27), which contained a total of 4,900 points, and analyzed. If the nucleotide at one point was dissimilar to the common one, it was defined as a variable point. The variation coefficient was the number of variable points in every 100 bp, and the maximum value was 2,400. The analysis was repeated by sliding the analysis window forward by 20 bp and analyzing the next 100 bp. A total of 1,404 variation coefficients were calculated by our procedure (<http://www.chinasscontrol.com/biosystem/index.php>). A vertical value of >100 was considered a dissimilar region. Prism 5 (GraphPad Software, La Jolla, CA, USA) was used to construct a graph of the variation coefficients with a window size of 100 bp and a step of 20 bp.

**Multiple-sequencing alignments and phylogenetic analysis.** Phylogenetic analysis was performed following the procedures outlined by

Chen et al. (15). ClustalW alignments with default parameters were produced for the whole genome, the entire spike gene, the N-terminal domain (NTD) of the S gene (corresponding to nucleotides [nt] 20635 to 21813 [covering 1,179 bp] of the strain AH2012), and the four most variable regions (V1 to V4; Fig. 1A). Phylogenetic trees were constructed separately with the molecular evolutionary genetics analysis (MEGA) software package (v.5.0.3) (27) using the neighbor-joining method, with *p*-distance, complete gap deletion, and bootstrapping (*n* = 1,000) parameters.

**Analysis of nucleotide positions distinguishing PEDV classical and pandemic groups (DCP).** The calculation method for the DCP values is shown in Fig. S1B in the supplemental material. Some DCP nucleotide positions are indicated by blue boxes as typical examples. The number of DCP positions defined the DCP value, which was calculated with a window size of 100 bp and a step of 20 bp. The baseline of the value was 6. Prism 5 (GraphPad Software, La Jolla, CA) was used to draw the graph of the DCP values (window size of 100 bp, step of 20 bp).

**Antigenic index and hydrophilicity plots.** Four strains were subjected to antigenic index and hydrophilicity analysis, based on the NTD region of the S protein. The antigenic index and hydrophilicity plots were obtained using the Jameson-Wolf and Kyte-Doolittle algorithms (28–30), respectively, with the aid of the DNASTar package (DNASTar Inc., Madison, WI, USA). The Kyte-Doolittle method predicts regions of hydrophilicity by summing hydrophilicities over a specified range of amino acids, with an average of nine residues. The Jameson-Wolf method predicts the antigenic index, which produces an index of antigenicity by combining the values for hydrophilicity.

**Phylogeography and spatiotemporal analysis.** A total of 219 available and background-clear Asian complete S gene sequences of PEDV were downloaded from GenBank (see Table S3 in the supplemental material). A geographical dissection of the Asian PEDV strains was performed based on the phylogenetic tree of 219 complete S genes. Some PEDV strains had no basic information or available whole-genome or S gene sequences (e.g., some strains from Taiwan and Vietnam) and were not included in this count. The strains were located in the isolated provinces or countries shown on the map in Fig. 4. Note that for strains from China, the location was accurate at the province level, whereas for the others, only the country of origin was known. A time-based geographical dissection of Asian PEDV strains was conducted. On the map, we used four colored spots to distinguish the pandemic group strains, the classic group strains, and the newly sequenced cases of PEDV.

**Nucleotide sequence accession numbers.** The sequences determined in this study were deposited in GenBank under accession numbers KM609203 to KM609213.

## RESULTS

**Whole-genome sequencing.** To reveal the characteristics of this virus and determine more precisely the relationships among the PEDV strains currently circulating in China and other nations, 11 whole genomes of Chinese PEDV isolates collected from different districts at different times were sequenced. All of the whole genomes were 28,038 nucleotides in length, excluding the poly(A) tail. The 11 whole genomes exhibited nucleotide sequence identities ranging from 97.5% to 99.7%, with no insertions or deletions. Their genomic organization was typical of all previously sequenced PEDV strains and was summarized as 5'UTR-ORF1a/1b-S-ORF3-E-M-N-3'UTR (Fig. 1B). The lengths of the seven ORFs were 12,309 bp, 7,638 bp, 4,161 bp, 675 bp, 231 bp, 681 bp, and 1,326 bp, respectively.

**Identification of hypervariable regions by whole-genome analysis.** To comprehensively investigate the heterogeneity of PEDV, we performed variation analysis of 49 PEDV whole genomes (11 determined in this study and 38 other available PEDV complete genomes). We identified the four most dissimilar re-

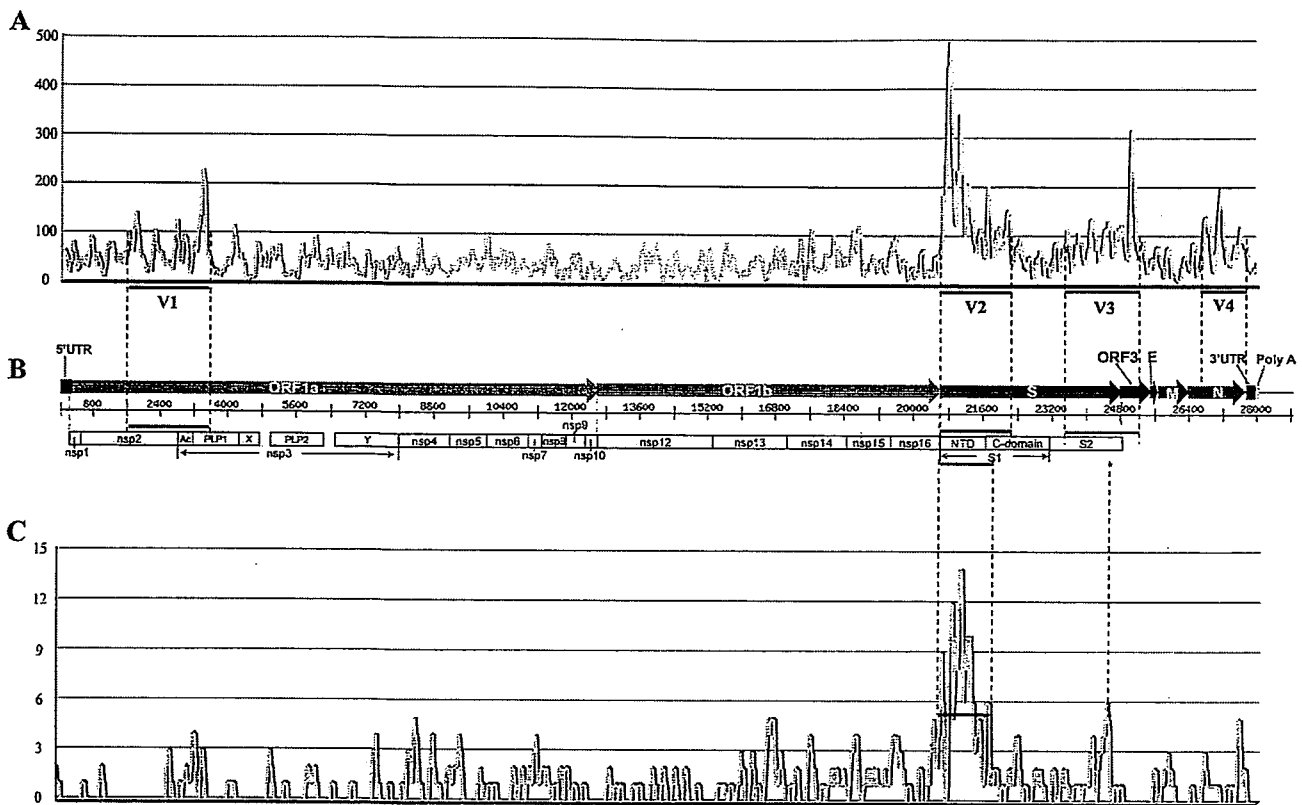


**FIG 1** (A) Variation analysis of 49 whole PEDV genomes from NCBI. The graph shows the variation coefficient (window size = 100 bp, step = 20 bp) in the alignment of 49 whole PEDV genomes. The detailed calculation method of the variation coefficient is shown in Fig. S1A in the supplemental material. Dashed and thick red lines, positions of four high mutation regions (V1, V2, V3, and V4) containing more nucleic acid deletions/insertions/mutations. (B) Organization of the PEDV genome. The approximate positions and sizes of genes in the PEDV genome correspond to the scale bar. The putative S1-S2 boundary (amino acid positions) of the S protein is also shown. (C) Analysis of nucleotide positions distinguishing classical and pandemic pathotypes (DCP). Graph showing the DCP position content (window size = 100 bp, step = 20 bp) in the alignment of 49 whole PEDV genomes. The detailed calculation method of DCP position is shown in Fig. S1B in the supplemental material. Dashed and green thick line, the major regions containing abundant DCP positions.

gions, named V1, V2, V3, and V4, respectively (Fig. 1A). In Fig. 1B, the putative variant regions corresponding to functional domains in the PEDV genome are shown below the sequence. V1 comprises the region encoding the C-terminal domain (CTD) of nonstructural protein 2 (nsp2) plus the N-terminal domain (NTD) of nsp3, V2 is in the S1 gene, V3 spans the CTD of the S gene with most of ORF3, and V4 is located in the nucleocapsid (N) gene. V1, V2, V3, and V4 are located on the whole genome of the AH2012 strain (GenBank accession no. KC210145.1) at 1,721 to 3,500 bp, 20,661 to 22,300 bp, 23,541 to 25,200 bp, and 26,741 to 27,700 bp, respectively. Note that the NTDs of the S gene and the ORF3 gene were the most obviously different among the four regions.

**Whole-genomic phylogenetic analysis identified the classical and pandemic groups.** The phylogenetic tree of 49 PEDV genomes indicated that the PEDV isolates could be divided into two clusters, designated the pandemic group and the classical group (Fig. 2A). Thirty-nine Chinese and American strains isolated after 2008 comprised the pandemic group. The classical group comprised 10 strains, including 3 Korean strains (SM98, DR13, and attenuated DR13), 6 Chinese strains (CH/S, LZC, SD-M, attenuated vaccine, JS2008, and JS2008 new), and 1 European strain (CV777). All the strains were isolated before 2008, except strain SD-M (5, 14, 31, 32), and had a rather distant phylogenetic rela-

tionship with pandemic group field strains. The 11 isolates first reported in the present study were all clustered into the pandemic group and had a close relationship with Chinese strains isolated after 2008. Among them, the PEDV-LYG and WS strains, collected in 2014, were most closely related to the CH/FJND-3/2011 strain, which was reported as a PEDV variant (33). Only the PEDV-7C strain was closely clustered with the CHGD-01 (26), GD-1 (34), CH/GDGZ/2012 (35), and GD-A (36) strains, which were all isolated in Guangdong province, China.

**Identification of regions that distinguished between the classical and pandemic groups (DCP).** To recognize the characteristic gene differences between the classical and pandemic groups, we analyzed the 49 whole-genome sequences. Ultimately, we identified a total of 322 distinctive nucleotides between the pandemic group strains and the classical group strains, based on whole-genome sequencing (data not shown). Among the 322 nt, 79 nt (24.5%) were located in the 1- to 1,179-bp region of the S gene (located on the whole genome of the AH2012 strain at 20,635 to 21,813 bp), and it was the major region that distinguished between the classical and pandemic groups (Fig. 1C). This region, which is included in the V2 region (Fig. 1C), resulted in 49 amino acid changes (see Fig. S2 in the supplemental material).

**Phylogenetic tree analysis of the whole S gene and the NTD region.** The phylogenetic trees for the full-length S gene and NTD

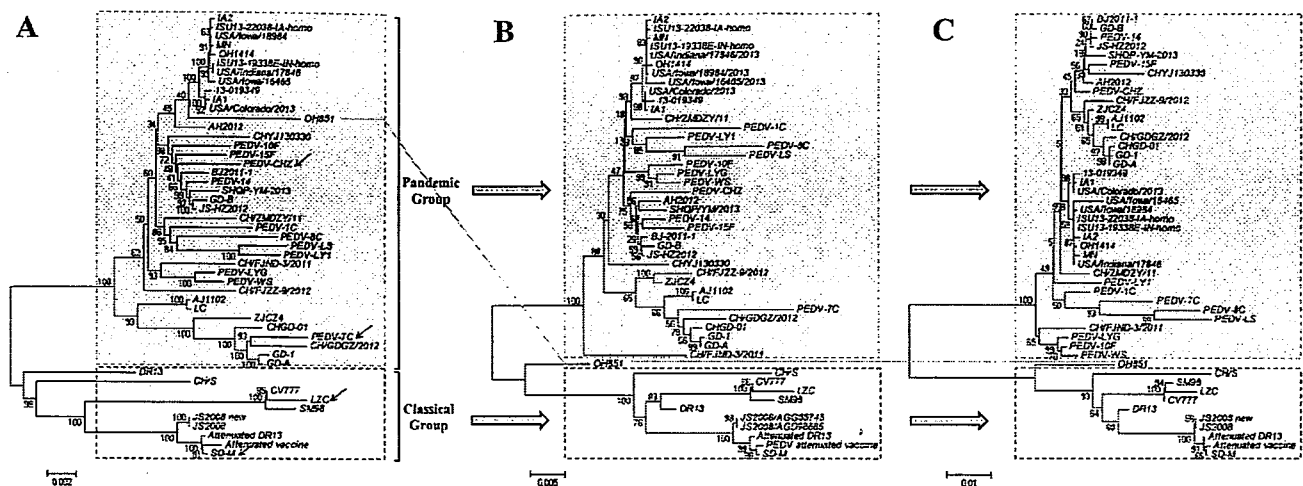


FIG 2 Phylogenetic trees of whole PEDV genomes (A), complete S genes encoded in the 49 whole PEDV genomes (B), and the corresponding N-terminal domain (NTD) sequences (C). The three neighbor-joining trees (bootstrap  $n = 1,000$ ;  $p$ -distance) were constructed based on ClustalW alignments of their respective nucleic acid sequences. The sequences in red and branches were revealed for the first time in this study. All three phylogenetic trees were divided into two deep branches, a pandemic branch and a classical branch. The only exception was PEDV isolate OH851, which is linked by blue lines among the three phylogenetic trees.

region collectively showed the same grouping structure as the tree generated from the PEDV whole genomes, except for the U.S. strain OH851, which was clustered differently in the trees of the S gene and the NTD region compared with the entire genome tree (Fig. 2). This agreed with a previous study (37). Between the complete genome and the entire S gene tree, there was also some small dissimilarity in the pandemic group, including the AH2012, CH/ZMDZY/11, CH/FJND-3/2011, CH/FJZZ-9/2012, and PEDV-10F strains, whose subgroup distribution changed. The NTD region tree was very similar to the entire S gene tree, except for strain PEDV-7C in the pandemic group. Even though PEDV evolution was not entirely reflected in the analysis of the S gene or NTD region, clustering based on these regions remained an efficient approach for PEDV. Phylogenetic trees based on the V1, V3, and V4 regions did not indicate two distinct genogroups (see Fig. S3 in the supplemental material), which further showed that the S gene was the best candidate to evaluate the evolutionary relationships of PEDV strains.

**Antigenic index and the hydrophilicity plot analysis of the two PEDV groups.** Four strains (CHZ, 7C, SD-M, and LZC), as representatives, were subjected to further analysis of their antigenic index and the hydrophilicity plot for the NTD (1 to 360 amino acids) of the S protein (Fig. 3). The first two strains were clustered into the pandemic group, and the latter two strains were in the classical group (Fig. 2A). The main antigenic index differences were located at amino acids 53 to 73 and 118 to 179 (Fig. 3A). In addition, the major differences on the hydrophilicity plot were for amino acids 53 to 73 and 118 to 165 (Fig. 3B). These dissimilar regions showed certain point mutations and deletions that differentiated the pandemic group from the classical group.

**Genotyping and phylogeny-based geographical dissection of PEDV strains in Asia.** We used 219 available complete S gene sequences, which were isolated from Japan (4 strains), South Korea (39 strains), Thailand (12 strains), and China (204 strains) (see Table S3 in the supplemental material). The PEDV strains fell into two distinct groups. The group that included all the strains in the

whole-genome pandemic cluster remained and was termed the pandemic group (PX). Similarly, the classical group was termed CX (Fig. 4 left). The PX was further divided into subgroups 1a, 1b, 1c, 2a, 2b, and 2c; and the CX was divided into 1a, 1b, and 1c (Fig. 4 left). From the phylogenetic tree, four subgroups (PX1a, PX1c, CX1a, and CX1b) contained only Chinese field strains. Thai strains were clustered into two subgroups with Chinese or South Korean strains in the pandemic group. The strains in Japan formed subgroups PX2c and CX2c with South Korean or Chinese strains, whereas the South Korean strains were grouped into four subgroups (PX1b, PX2b, PX2c, and CX1c), and the Chinese strains clustered into every subgroup, except PX2b and PX2c (see Fig. S4 in the supplemental material). The clinical strains from PX1a were the main epidemic subgroup of PEDV outbreaks in China, and PX1b was the main subgroup responsible for outbreaks in South Korea. Interestingly, CX1c contained strains isolated from South Korea, Japan, and China from 1986 to 2013 (see Fig. S4) and was the most complex subgroup.

The possible geographical origins of the 219 PEDV strains were plotted to obtain clues regarding the spread tendency of the emergent PEDV strains in Asia (Fig. 4 right). From the geographical locations, we found that in Japan and Thailand, the common strains were relatively simple, whereas in China, PEDV had spread into every province around the coastal regions, even into Sichuan province or northeast China, since the CH/S strain was isolated in 1986 in Shanghai (31). South Korea also suffered continuous and large-scale outbreaks. Since late 2013, several outbreaks of PEDV infection emerged in Taiwan (38) and Vietnam (39); however, the information on the epidemics was not detailed enough to be analyzed in this study.

**Spatiotemporal reconstruction of PEDV strains in Asia.** Combining the molecular sequence data with the isolation times and geographical coordinates allowed a spatiotemporal distribution of PEDV to be inferred (Fig. 5; see also Fig. S4 in the supplemental material). By 2005, several occasional epidemics had been reported. All four from China, one from Japan, and three from

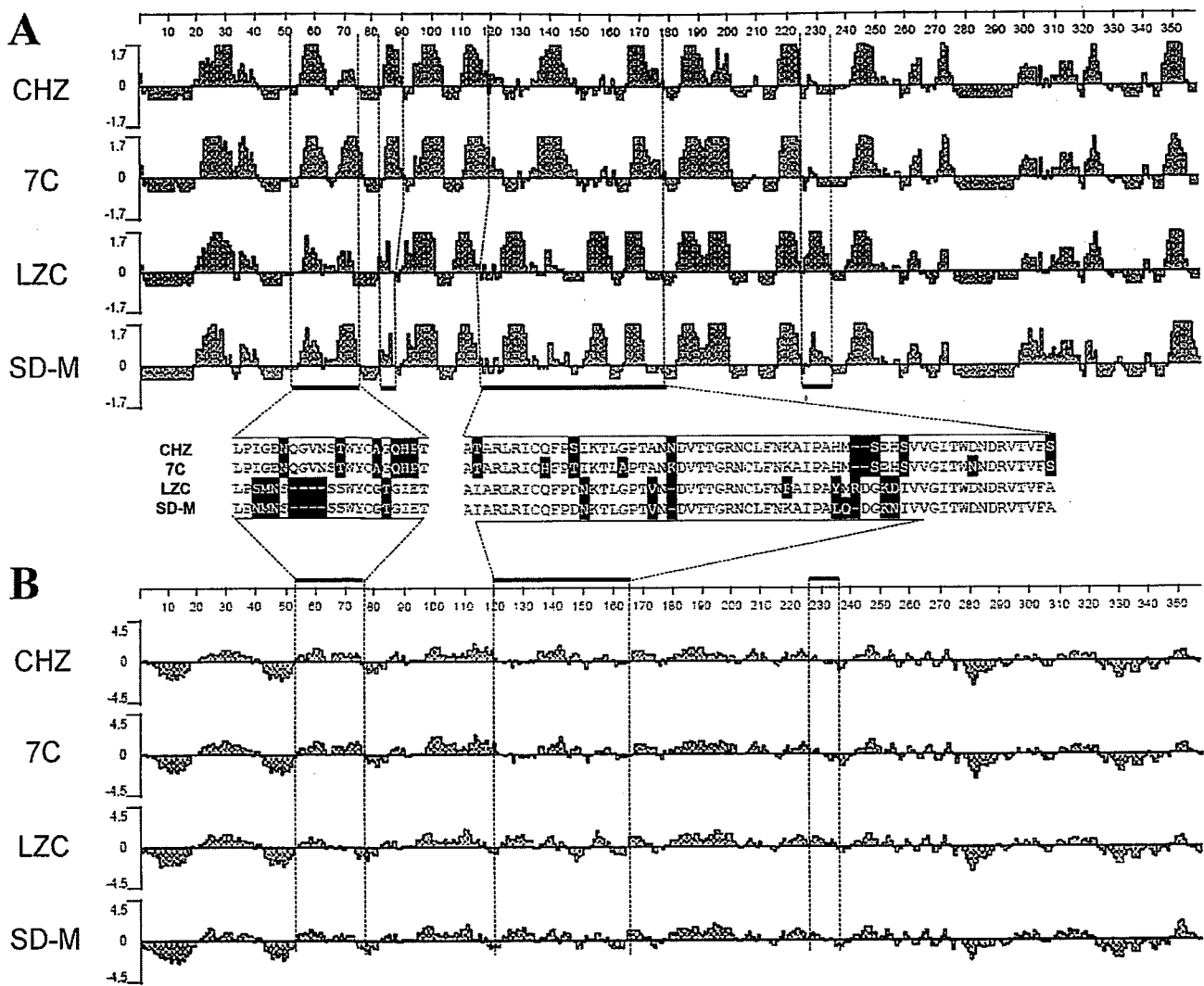


FIG 3 Comparison of the antigenic index (A) and hydrophilicity plot (B) of the NTD of S protein fragments between classical and pandemic pathotypes. Dashed and green thick lines, the positions of several regions containing significant differences between classical and pandemic pathotypes. Red shading, mismatched amino acids. PEDV isolates CHZ and 7C belong to the pandemic group, whereas LZC and SD-M isolates are from the classical group.

South Korea were clustered into the classical group. However, two from South Korea were clustered into the pandemic group (Fig. 5), which indicated that the pandemic PEDV in Asia might have originated from South Korea. As of 2010, PEDV was widespread, pandemic group strains emerged in South Korea, and Japan added two pandemic group strains and one classical group strain, whereas China only added four classical group strains (Fig. 5). In addition, there were two pandemic group strains first reported in Thailand (9).

Between 2010 and 2011, PEDV was continuously detected in various areas in Thailand, and the prevalence of PEDV infections was low and only sporadic outbreaks occurred in South Korea. However, for unclear reasons, a severe PED epizootic was affecting pigs of all ages in many provinces of China, extending into Sichuan and the northeast area of China (Fig. 5). Prevalent PEDV field strains in China were not only distributed in the pandemic group but also represented some clinical strains of the classical group. Between 2012 and 2014, PEDV caused widespread outbreaks in

Thailand, South Korea, and China, even extending to Taiwan (38) and Vietnam (39).

## DISCUSSION

In recent years, PEDV has continued to cause severe economic damage to the swine industry in Asia. The existing measures, including vaccination, biosecurity, and feedback, cannot effectively block the spread of this disease (2, 14, 40–42). The 11 complete genomes of PEDV field isolates from China determined in this study showed a wide range of genetic variation, which suggested a large risk of PEDV outbreak by novel variants. Comparisons and phylogenetic analysis of 49 PEDV whole genomes (including 12 emerging strains from the United States) confirmed that this issue is also present throughout Asia and in America. Several investigators have reported that the S gene is appropriate to study the genetic relatedness of this virus (14, 15). Here, we attempted to search for variations more accurately through whole-genome

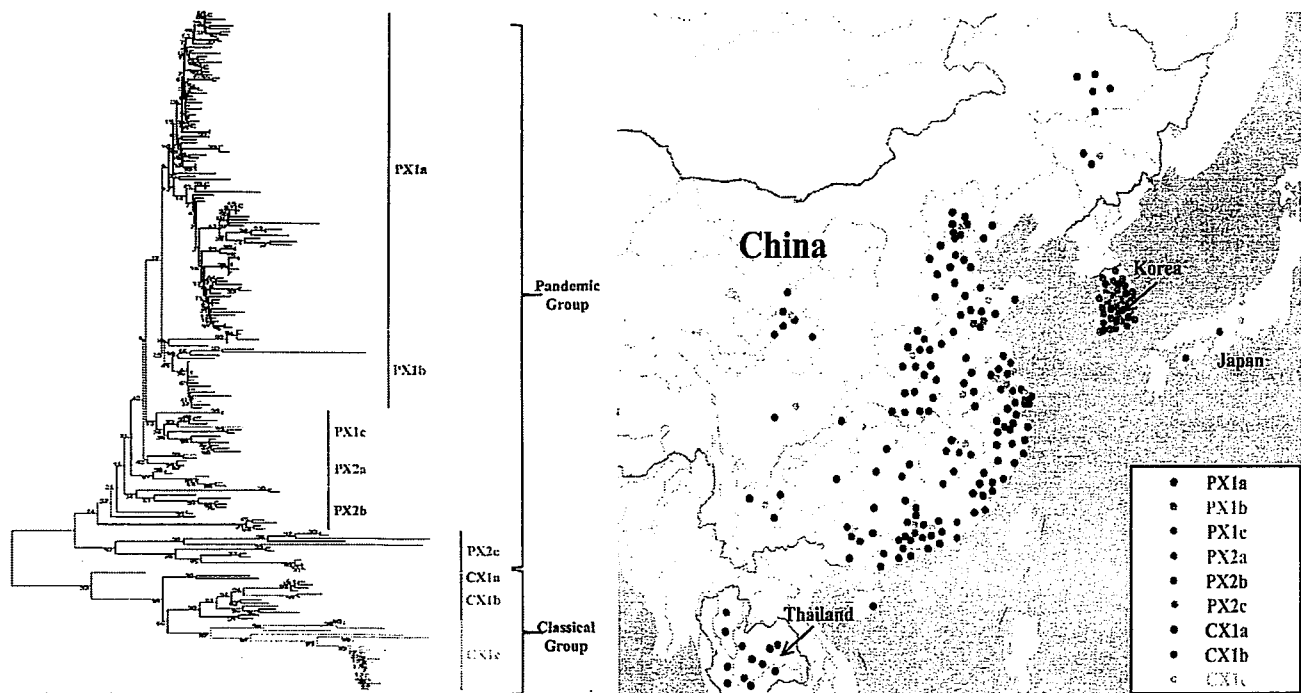


FIG 4 Map and phylogenetic tree of 219 PEDV S gene sequences. (Left) Phylogeny-based genotyping of 219 PEDV strains with available complete S gene sequences from Asia. The neighbor-joining tree (bootstrap  $n = 1,000$ ;  $p$ -distance) was constructed based on a ClustalW alignment of full-length nucleotide sequences of the S gene. The names of the strains, years, places of isolation, and GenBank accession numbers are shown in Table S3 in the supplemental material. The genogroups and subgroups were proposed according to the above phylogenetic analysis. The pandemic pathotype was divided into six subgroups (PX1a, PX1b, PX1c, PX2a, PX2b, and PX2c) and the classical pathotype into three groups (CX1a, CX1b, and CX1c). (Right) Phylogeny-based geographical dissection of PEDV strains from Asia. A map of Asia shows the districts where PEDV strains with available complete S gene sequences were isolated. The numbers in order and the colors for PEDV strains correspond to those labeled in the left panel.

analysis and hoped to provide clues to the PEDV evolutionary mechanism.

In this study, four hypervariable regions (V1 to V4) were identified in the whole PEDV genomes, which particularly associated with the PEDV evolutionary process. V1 is located between *nsp2* and *nsp3*, which is considered the putative region of possible recombination events of the US-AH lineage strains (43). V2 is located in the amino terminus of the S protein, which functions as a receptor-binding domain (44). V3 is distributed mainly in the ORF3 gene, which has been used to differentiate between field and vaccine-derived isolates and altered the virulence of PEDV (45). V4 is included in the N gene, which contradicts a previous report that implied that the N gene is highly conserved (46). These differences probably reflect the limited available sequences, small study samples, and analysis of the single N gene in the previous study.

Among the regions, the V2 region (included in the S gene) was the most appropriate to evaluate the evolutionary relationship of PEDV strains and to cluster PEDV strains into the pandemic and classical groups. Further analysis confirmed that the V2 region was suitable to analyze the significant differences in epidemiology between the two groups (2, 9, 47). Thus, the V2 region might play an important role in the genetic evolutionary process of PEDV and will be the focus of future research. The high degree of genetic heterogeneity in the V2 region might explain why the classical vaccine strains cannot effectively control the spread of the pandemic group strains at present. The antigenic index analysis of the

V2 region showed enhanced antigenicity in the pandemic group compared with the classical group (43), while none of the known antigen epitope motifs was included in the V2 region (48, 49). These results suggested that some novel neutralizing sites might have formed in the V2 region of the pandemic group strains, which might be associated with their rapid spread and strong pathogenicity (50, 51).

In the phylogenetic tree of the whole genome and the NTD region (included in the V2 region and S gene), the OH851 strain clustered in different groups, which was the only exception. In South Korea, another strain was clustered with strain OH851 (52). These new PEDV variants might originate from a genetic recombination event between pandemic group strains and classical group strains (37). We may still be able to use the S gene to evaluate the evolutionary relationship of PEDV strains and cluster these strains as OH851-like strains, which will require further analysis. Currently, several novel PEDV strains that showed large genomic deletions in the S gene have been isolated in the United States (53) and South Korea (54). These observations suggested that it is critical to monitor PEDV molecular epidemiology continuously.

PEDV has spread into most nations with a swine industry in Asia (2, 9, 23), even being detected in Taiwan (38) and Vietnam (39). Thus, it has spread beyond its geographical limitation. According to the S gene sequences, the 219 PEDV strains in Asia were clustered into pandemic and classical groups. Further subgroup analysis indicated the significant regional differences in the spread

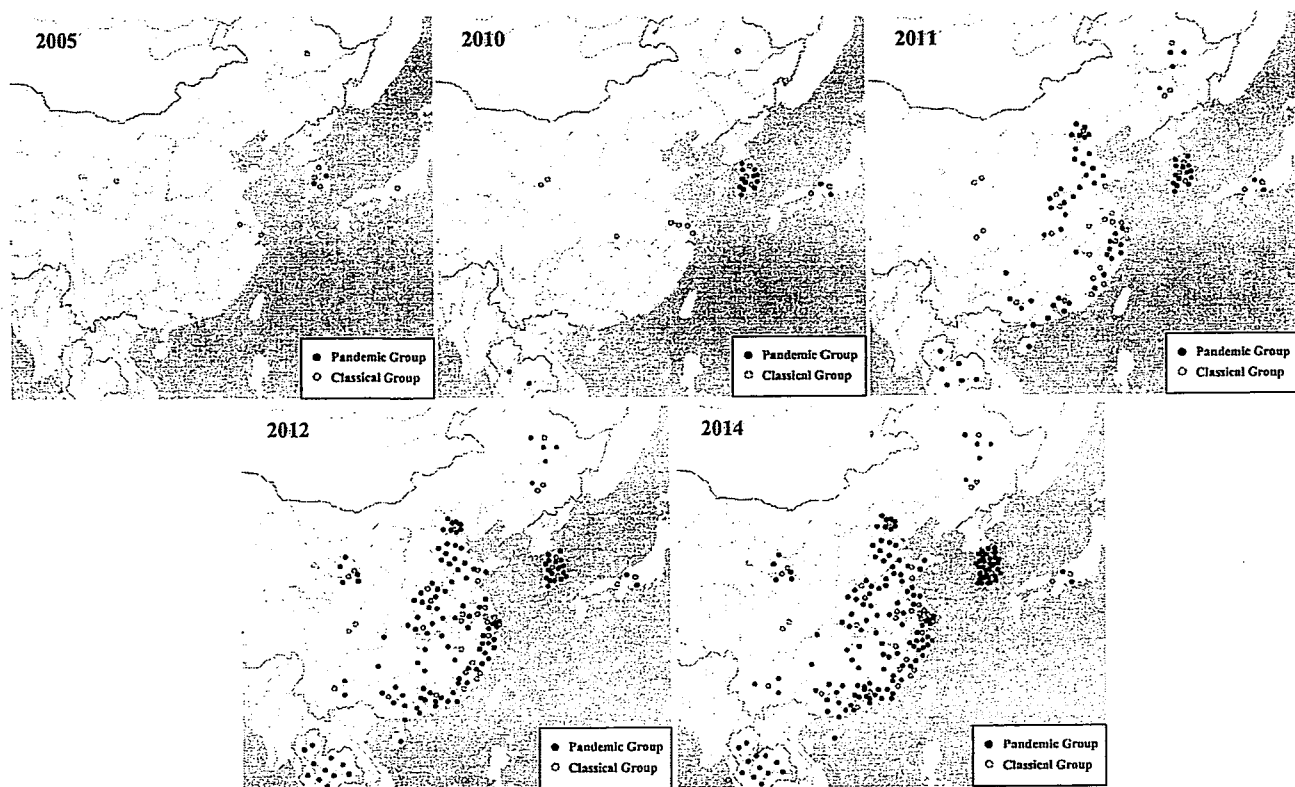


FIG 5 The reconstructed spatiotemporal diffusion of PEDV at different time points in east Asia. Note that strains in China were located accurately for every province, but the other data only provided the country of origin. Some PEDV strains had no basic information, had no available whole-genome or complete S gene sequence, and were not included in this count (such as some strains from Taiwan and Vietnam). Red and pink plots, newly added strains relative to the previous period.

of PEDV in different Asian countries. The PX1a, PX1c, CX1a, and CX1c strain subgroups were only epidemic in China, while the PX2b and PX2c subgroups were not detected. All strains isolated after 2013 in South Korea (except KNU/1301/2013 and KNU/1302/2013) were clustered into the PX1b subgroup and formed the main subgroup in South Korea. Notably, to date, a widespread outbreak has not occurred in Japan.

Spatiotemporal reconstruction of PEDV strains showed that South Korean Chinju99, isolated in 1999 (55), is the oldest PEDV pandemic group strain in Asia. The original strains of the pandemic group detected in Japan, Thailand, and China are all homologous with Chinju99, and their genomes have remained relatively stable (51), which implies that the pandemic group strains in Asian countries originated from South Korea. Before 2008, most PEDV field strains belonged to the classical group (Fig. S4 in the supplemental material), but subsequent acute outbreaks in Asia were caused by pandemic group PEDV strains, initially in South Korea (2008) (14) and then in Thailand (2008) (41) and China (2011) (2). Since 2013, the South Korean pandemic strains have become distinct from previous strains and are closely related to Chinese strains isolated after 2011 (see Fig. S4), which indicates that the currently emerging pandemic strains in the PX1b subgroup in South Korea originated from China.

In summary, South Korea and China have undergone the most complex PEDV epidemic situations in the past 5 years. The pandemic group strains in Asia likely originated from South Korea and then spread into Japan, Thailand, and China, successively.

However, the pandemic strains that emerged in South Korea after 2013 may have originated from a Chinese variant. In the process of spreading, PEDV underwent numerous genetic variations. In particular, the V2 region plays important roles in PEDV genetic evolution and pathogenicity, which should be investigated further in future research.

#### ACKNOWLEDGMENT

This work was supported by a grant from the Priority Academic Program Development of Jiangsu Higher Education Institutions (PAPD).

#### REFERENCES

1. Have P, Moving V, Svansson V, Uttenthal A, Bloch B. 1992. Coronavirus infection in mink (*Mustela vison*): serological evidence of infection with a coronavirus related to transmissible gastroenteritis virus and porcine epidemic diarrhoea virus. *Vet Microbiol* 31:1–10. [http://dx.doi.org/10.1016/0378-1135\(92\)90135-G](http://dx.doi.org/10.1016/0378-1135(92)90135-G).
2. Li W, Li H, Liu Y, Pan Y, Deng F, Song Y, Tang X, He Q. 2012. New variants of porcine epidemic diarrhoea virus, China, 2011. *Emerg Infect Dis* 18:1350–1353. <http://dx.doi.org/10.3201/eid1808.120002>.
3. Sueyoshi M, Tsuda T, Yamazaki K, Yoshida K, Nakazawa M, Sato K, Minami T, Iwashita K, Watanabe M, Suzuki Y, Mori M. 1995. An immunohistochemical investigation of porcine epidemic diarrhoea. *J Comp Pathol* 113:59–67. [http://dx.doi.org/10.1016/S0021-9975\(05\)80069-6](http://dx.doi.org/10.1016/S0021-9975(05)80069-6).
4. Chasey D, Cartwright SF. 1978. Virus-like particles associated with porcine epidemic diarrhoea. *Res Vet Sci* 25:255–256.
5. Pensaert MB, de Bouck P. 1978. A new coronavirus-like particle associated with diarrhoea in swine. *Arch Virol* 58:243–247. <http://dx.doi.org/10.1007/BF01317606>.

6. Vijaykrishna D, Smith GJ, Zhang JX, Peiris JS, Chen H, Guan Y. 2007. Evolutionary insights into the ecology of coronaviruses. *J Virol* 81:4012–4020. <http://dx.doi.org/10.1128/JVI.02605-06>.
7. Yang DQ, Ge FF, Ju HB, Wang J, Liu J, Ning K, Liu PH, Zhou JP, Sun QY. 2014. Whole-genome analysis of porcine epidemic diarrhea virus (PEDV) from eastern China. *Arch Virol* 159:2777–2785. <http://dx.doi.org/10.1007/s00705-014-2102-7>.
8. Kocherhans R, Bridgen A, Ackermann M, Tobler K. 2001. Completion of the porcine epidemic diarrhoea coronavirus (PEDV) genome sequence. *Virus Genes* 23:137–144. <http://dx.doi.org/10.1023/A:1011831902219>.
9. Temeeyasen G, Srijangwad A, Tripipat T, Tipsombathoon P, Piriyapongsa J, Phoolcharoen W, Chuanasa T, Tantituvanont A, Nilubol D. 2014. Genetic diversity of ORF3 and spike genes of porcine epidemic diarrhea virus in Thailand. *Infect Genet Evol* 21:205–213. <http://dx.doi.org/10.1016/j.meegid.2013.11.001>.
10. Jackwood MW, Hilt DA, Callison SA, Lee CW, Plaza H, Wade E. 2001. Spike glycoprotein cleavage recognition site analysis of infectious bronchitis virus. *Avian Dis* 45:366–372. <http://dx.doi.org/10.2307/1592976>.
11. Sturman LS, Holmes KV. 1984. Proteolytic cleavage of peplomer glycoprotein E2 of MHV yields two 90K subunits and activates cell fusion. *Adv Exp Med Biol* 173:25–35. [http://dx.doi.org/10.1007/978-1-4615-9373-7\\_3](http://dx.doi.org/10.1007/978-1-4615-9373-7_3).
12. Bosch BJ, van der Zee R, de Haan CA, Rottier PJ. 2003. The coronavirus spike protein is a class I virus fusion protein: structural and functional characterization of the fusion core complex. *J Virol* 77:8801–8811. <http://dx.doi.org/10.1128/JVI.77.16.8801-8811.2003>.
13. Chang SH, Bae JL, Kang TJ, Kim J, Chung GH, Lim CW, Laude H, Yang MS, Jang YS. 2002. Identification of the epitope region capable of inducing neutralizing antibodies against the porcine epidemic diarrhea virus. *Mol Cells* 14:295–299. <http://www.molcells.org/journal/view.html?year=2002&volume=14&number=2&spage=295>.
14. Lee DK, Park CK, Kim SH, Lee C. 2010. Heterogeneity in spike protein genes of porcine epidemic diarrhea viruses isolated in Korea. *Virus Res* 149:175–182. <http://dx.doi.org/10.1016/j.virusres.2010.01.015>.
15. Chen Q, Li G, Stasko J, Thomas JT, Stensland WR, Pillatzki AE, Gauger PC, Schwartz KJ, Madson D, Yoon KJ, Stevenson GW, Burroughs ER, Harmon KM, Main RG, Zhang J. 2014. Isolation and characterization of porcine epidemic diarrhea viruses associated with the 2013 disease outbreak among swine in the United States. *J Clin Microbiol* 52:234–243. <http://dx.doi.org/10.1128/JCM.02820-13>.
16. Park SJ, Moon HJ, Yang JS, Lee CS, Song DS, Kang BK, Park BK. 2007. Sequence analysis of the partial spike glycoprotein gene of porcine epidemic diarrhea viruses isolated in Korea. *Virus Genes* 35:321–332. <http://dx.doi.org/10.1007/s11262-007-0096-x>.
17. Lee S, Lee C. 2014. Outbreak-related porcine epidemic diarrhea virus strains similar to US strains, South Korea, 2013. *Emerg Infect Dis* 20:1223–1226. <http://dx.doi.org/10.3201/eid2007.140294>.
18. Puranaveja S, Poolperm P, Lertwatcharasarakul P, Kesdaengsakonwut S, Boonsoongnern A, Urairong K, Kitikoon P, Choojai P, Kedkovid R, Teankum K, Thanawongnuwech R. 2009. Chinese-like strain of porcine epidemic diarrhea virus, Thailand. *Emerg Infect Dis* 15:1112–1115. <http://dx.doi.org/10.3201/eid1507.081256>.
19. Spaan W, Cavanagh D, Horzinek MC. 1988. Coronaviruses: structure and genome expression. *J Gen Virol* 69:2939–2952. <http://dx.doi.org/10.1099/0022-1317-69-12-2939>.
20. Van Reeth K, Pensaert M. 1994. Prevalence of infections with enzootic respiratory and enteric viruses in feeder pigs entering fattening herds. *Vet Rec* 135:594–597.
21. Nagy B, Nagy G, Meder M, Mocsari E. 1996. Enterotoxigenic *Escherichia coli*, rotavirus, porcine epidemic diarrhoea virus, adenovirus and calicivirus in porcine postweaning diarrhoea in Hungary. *Acta Vet Hung* 44:9–19.
22. Kusanagi K, Kuwahara H, Katoh T, Nunoya T, Ishikawa Y, Samejima T, Tajima M. 1992. Isolation and serial propagation of porcine epidemic diarrhea virus in cell cultures and partial characterization of the isolate. *J Vet Med Sci* 54:313–318. <http://dx.doi.org/10.1292/jvms.54.313>.
23. Choi JC, Lee KK, Pi JH, Park SY, Song CS, Choi IS, Lee JB, Lee DH, Lee SW. 2014. Comparative genome analysis and molecular epidemiology of the reemerging porcine epidemic diarrhea virus strains isolated in Korea. *Infect Genet Evol* 26:348–351. <http://dx.doi.org/10.1016/j.meegid.2014.06.005>.
24. Jinghui F, Yijing L. 2005. Cloning and sequence analysis of the M gene of porcine epidemic diarrhea virus LJB/03. *Virus Genes* 30:69–73. <http://dx.doi.org/10.1007/s11262-004-4583-z>.
25. Ishikawa K, Selkiguchi H, Ogino T, Suzuki S. 1997. Direct and rapid detection of porcine epidemic diarrhea virus by RT-PCR. *J Virol Methods* 69:191–195. [http://dx.doi.org/10.1016/S0166-0934\(97\)00157-2](http://dx.doi.org/10.1016/S0166-0934(97)00157-2).
26. Pan Y, Tian X, Li W, Zhou Q, Wang D, Bi Y, Chen F, Song Y. 2012. Isolation and characterization of a variant porcine epidemic diarrhea virus in China. *Virol J* 9:195. <http://dx.doi.org/10.1186/1743-422X-9-195>.
27. Tamura K, Peterson D, Peterson N, Stecher G, Nei M, Kumar S. 2011. MEGA5: molecular evolutionary genetics analysis using maximum likelihood, evolutionary distance, and maximum parsimony methods. *Mol Biol Evol* 28:2731–2739. <http://dx.doi.org/10.1093/molbev/msr121>.
28. Jameson BA, Wolf H. 1988. The antigenic index: a novel algorithm for predicting antigenic determinants. *Comput Appl Biosci* 4:181–186.
29. Ie SI, Thedja MD, Roni M, Muljono DH. 2010. Prediction of conformational changes by single mutation in the hepatitis B virus surface antigen (HBsAg) identified in HBsAg-negative blood donors. *Virol J* 7:326. <http://dx.doi.org/10.1186/1743-422X-7-326>.
30. Kyte J, Doolittle RF. 1982. A simple method for displaying the hydropathic character of a protein. *J Mol Biol* 157:105–132. [http://dx.doi.org/10.1016/0022-2836\(82\)90515-0](http://dx.doi.org/10.1016/0022-2836(82)90515-0).
31. Chen J, Wang C, Shi H, Qiu HJ, Liu S, Shi D, Zhang X, Feng L. 2011. Complete genome sequence of a Chinese virulent porcine epidemic diarrhea virus strain. *J Virol* 85:11538–11539. <http://dx.doi.org/10.1128/JVI.06024-11>.
32. Zhao M, Sun Z, Zhang Y, Wang G, Wang H, Yang F, Tian F, Jiang S. 2012. Complete genome sequence of a Vero cell-adapted isolate of porcine epidemic diarrhea virus in eastern China. *J Virol* 86:13858–13859. <http://dx.doi.org/10.1128/JVI.02674-12>.
33. Chen J, Liu X, Shi D, Shi H, Zhang X, Feng L. 2012. Complete genome sequence of a porcine epidemic diarrhea virus variant. *J Virol* 86:3408. <http://dx.doi.org/10.1128/JVI.07150-11>.
34. Wei ZY, Lu WH, Li ZL, Mo JY, Zeng XD, Zeng ZL, Sun BL, Chen F, Xie QM, Bee YZ, Ma JY. 2012. Complete genome sequence of novel porcine epidemic diarrhea virus strain GD-1 in China. *J Virol* 86:13824–13825. <http://dx.doi.org/10.1128/JVI.02615-12>.
35. Tian Y, Su D, Zhang H, Chen RA, He D. 2013. Complete genome sequence of a very virulent porcine epidemic diarrhea virus strain, CH/GDGZ/2012, isolated in southern China. *Genome Announc* 1:p11=e00645-13. <http://dx.doi.org/10.1128/genomeA.00645-13>.
36. Fan H, Zhang J, Ye Y, Tong T, Xie K, Liao M. 2012. Complete genome sequence of a novel porcine epidemic diarrhea virus in south China. *J Virol* 86:10248–10249. <http://dx.doi.org/10.1128/JVI.01589-12>.
37. Wang L, Byrum B, Zhang Y. 2014. New variant of porcine epidemic diarrhea virus, United States, 2014. *Emerg Infect Dis* 20:917–919. <http://dx.doi.org/10.3201/eid2005.140195>.
38. Lin CN, Chung WB, Chang SW, Wen CC, Liu H, Chien CH, Chiou MT. 2014. US-like strain of porcine epidemic diarrhea virus outbreaks in Taiwan, 2013–2014. *J Vet Med Sci* 76:1297–1299. <http://dx.doi.org/10.1292/jvms.14-0098>.
39. Vui DT, Tung N, Inui K, Slater S, Nilubol D. 2014. Complete genome sequence of porcine epidemic diarrhea virus in Vietnam. *Genome Announc* 2:p11=e00753-14. <http://dx.doi.org/10.1128/genomeA.00753-14>.
40. Chae C, Kim O, Choi C, Min K, Cho WS, Kim J, Tai JH. 2000. Prevalence of porcine epidemic diarrhoea virus and transmissible gastroenteritis virus infection in Korean pigs. *Vet Rec* 147:606–608. <http://dx.doi.org/10.1136/vr.147.21.606>.
41. Olanratmanee EO, Kunavongkritt A, Tummaruk P. 2010. Impact of porcine epidemic diarrhea virus infection at different periods of pregnancy on subsequent reproductive performance in gilts and sows. *Anim Reprod Sci* 122:42–51. <http://dx.doi.org/10.1016/j.anireprosci.2010.07.004>.
42. Lowe J, Gauger P, Harmon K, Zhang J, Connor J, Yeske P, Loula T, Levis I, Dufresne L, Main R. 2014. Role of transportation in spread of porcine epidemic diarrhea virus infection, United States. *Emerg Infect Dis* 20:872–874. <http://dx.doi.org/10.3201/eid2005.131628>.
43. Huang YW, Dickerman AW, Pineyro P, Li L, Fang L, Kiehne R, Oppriensnig T, Meng XJ. 2013. Origin, evolution, and genotyping of emergent porcine epidemic diarrhea virus strains in the United States. *mBio* 4:e00737-13. <http://dx.doi.org/10.1128/mBio.00737-13>.
44. Belouvard S, Millet JK, Licitra BN, Whittaker GR. 2012. Mechanisms of coronavirus cell entry mediated by the viral spike protein. *Viruses* 4:1011–1033. <http://dx.doi.org/10.3390/v4061011>.
45. Park SJ, Moon HJ, Luo Y, Kim HK, Kim EM, Yang JS, Song DS,



- Kang BK, Lee CS, Park BK. 2008. Cloning and further sequence analysis of the ORF3 gene of wild- and attenuated-type porcine epidemic diarrhea viruses. *Virus Genes* 36:95–104. <http://dx.doi.org/10.1007/s11262-007-0164-2>.
46. Li Z, Chen F, Yuan Y, Zeng X, Wei Z, Zhu L, Sun B, Xie Q, Cao Y, Xue C, Ma J, Bee Y. 2013. Sequence and phylogenetic analysis of nucleocapsid genes of porcine epidemic diarrhea virus (PEDV) strains in China. *Arch Virol* 158:1267–1273. <http://dx.doi.org/10.1007/s00705-012-1592-4>.
  47. Vlasova AN, Marthaler D, Wang Q, Culhane MR, Rossow KD, Rovira A, Collins J, Saif LJ. 2014. Distinct characteristics and complex evolution of PEDV strains, North America, May 2013–February 2014. *Emerg Infect Dis* 20:1620–1628. <http://dx.doi.org/10.3201/eid2010.140491>.
  48. Cruz DJ, Kim CJ, Shin HJ. 2006. Phage-displayed peptides having antigenic similarities with porcine epidemic diarrhea virus (PEDV) neutralizing epitopes. *Virology* 354:28–34. <http://dx.doi.org/10.1016/j.virol.2006.04.027>.
  49. Sun D, Feng L, Shi H, Chen J, Cui X, Chen H, Liu S, Tong Y, Wang Y, Tong G. 2008. Identification of two novel B cell epitopes on porcine epidemic diarrhea virus spike protein. *Vet Microbiol* 131:73–81. <http://dx.doi.org/10.1016/j.vetmic.2008.02.022>.
  50. Tian Y, Yu Z, Cheng K, Liu Y, Huang J, Xin Y, Li Y, Fan S, Wang T, Huang G, Feng N, Yang Z, Yang S, Gao Y, Xia X. 2013. Molecular characterization and phylogenetic analysis of new variants of the porcine epidemic diarrhea virus in Gansu, China in 2012. *Viruses* 5:1991–2004. <http://dx.doi.org/10.3390/v5081991>.
  51. Sun R, Leng Z, Zhai SL, Chen, D, Song, C. 2014. Genetic variability and phylogeny of current Chinese porcine epidemic diarrhea virus strains based on spike, ORF3, and membrane genes. *ScientificWorldJournal* 2014:208439. <http://dx.doi.org/10.1155/2014/208439>.
  52. Lee S, Park GS, Shin JH, Lee C. 2014. Full-genome sequence analysis of a variant strain of porcine epidemic diarrhea virus in South Korea. *Genome Annou* 2:p11116–14. <http://dx.doi.org/10.1128/genomeA.01116-14>.
  53. Oka T, Saif LJ, Marthaler D, Esseili MA, Meulia T, Lin CM, Vlasova AN, Jung K, Zhang Y, Wang Q. 2014. Cell culture isolation and sequence analysis of genetically diverse US porcine epidemic diarrhea virus strains, including a novel strain with a large deletion in the spike gene. *Vet Microbiol* 173:258–269. <http://dx.doi.org/10.1016/j.vetmic.2014.08.012>.
  54. Park S, Kim S, Song D, Park B. 2014. Novel porcine epidemic diarrhea virus variant with large genomic deletion, South Korea. *Emerg Infect Dis* 20:2089–2092. <http://dx.doi.org/10.3201/eid2012.131642>.
  55. Yeo SG, Hernandez M, Krell PJ, Nagy EE. 2003. Cloning and sequence analysis of the spike gene of porcine epidemic diarrhea virus Chinju99. *Virus Genes* 26:239–246. <http://dx.doi.org/10.1023/A:1024443112717>.



# Novel Variant Serotype of *Streptococcus suis* Isolated from Piglets with Meningitis

Zihao Pan,<sup>a,b</sup> Jiale Ma,<sup>a,b</sup> Wenyang Dong,<sup>b</sup> Wenchao Song,<sup>b</sup> Kaicheng Wang,<sup>c</sup> Chengping Lu,<sup>a,b</sup> Huochun Yao<sup>a,b</sup>

Key Lab of Animal Bacteriology, Ministry of Agriculture, Nanjing Agricultural University, Nanjing, China<sup>a</sup>; OIE Reference Lab for Swine Streptococcosis, Nanjing, China<sup>b</sup>; China Animal Health and Epidemiology Center, Qingdao, China<sup>c</sup>

*Streptococcus suis* is an emerging zoonotic pathogen causing severe infections in pigs and humans. In previous studies, 33 serotypes of *S. suis* have been identified using serum agglutination. Here, we describe a novel *S. suis* strain, CZ130302, isolated from an outbreak of acute piglet meningitis in eastern China. Strong pathogenicity of meningitis caused by strain CZ130302 was reproduced in the BALB/c mouse model. The strain showed a high fatality rate (8/10), higher than those for known virulent serotype 2 strains P1/7 (1/10) and 9801 (2/10). Cell adhesion assay results with bEnd.3 and HEp2 cells showed that CZ130302 was significantly close to P1/7 and 9801. Both the agglutination test and its complementary test showed that strain CZ130302 had no strong cross-reaction with the other 33 *S. suis* serotypes. The multiplex PCR assays revealed no specified bands for all four sets used to detect the other 33 serotypes. In addition, genetic analysis of the whole *cps* gene clusters of all serotypes was performed in this study. The results of comparative genomics showed that the *cps* gene cluster of CZ130302, which was not previously reported, showed no homology to the gene sequences of the other strains. Especially, the *wzy*, *wzx*, and acetyltransferase genes of strain CZ130302 are phylogenetically distinct from strains of the other 33 serotypes. Therefore, this study suggested that strain CZ130302 represents a novel variant serotype of *S. suis* (designated serotype Chz) which has a high potential to be virulent and associated with meningitis in animals.

*Streptococcus suis* causes meningitis and septicemia in pigs and is also known as a zoonotic agent (1). Human infections of *S. suis* were first reported in Denmark in 1968 (2). Since then, this pathogen has spread all over the world. The human *Streptococcus suis* was epidemic in most Europe countries (3, 4), as well as in Asian countries, such as Vietnam and Thailand (5–7). In China, two outbreaks of human streptococcosis have occurred, affecting more than 100 people and causing 39 deaths (8). More and more *S. suis* infections from China, Thailand, Hong Kong, Taiwan, and Singapore have been reported, which indicates that *S. suis* has been an important cause of adult meningitis, endocarditis, septicemia, and arthritis in Asia (9).

The serotyping of *S. suis* isolates rests on the basis of the antigenicity of their capsular polysaccharides (CPs); 35 serotypes have been identified by agglutination tests (10). With the development of sequence analysis of 16S rRNA and *cpn60* genes in *S. suis*, the original *S. suis* serotypes 32 and 34 were reclassified as *Streptococcus orisratti* (11). Phylogenetic analyses of the *cps* gene cluster, conserved Wzy polymerase, Wzx flippase, and glycosyltransferase are all taken as important means of classifying a novel serotype (12). Multiplex PCR assays against the specific genes of the *cps* clusters have also been developed to identify serotypes in *S. suis* (13–15).

From March to May 2013, strain CZ130302 caused an outbreak of streptococcosis in piglets at multiple large-scale pig farms in Jiangsu Province, China. This pathogenic bacterium induced meningitis in 30-day-old piglets, with a total morbidity rate of 25% to 35%. The fatality rate of diseased piglets could reach 65%. We identified that the agent responsible for meningitis and septicemia in piglets as *S. suis* (CZ130302), and the strong pathogenicity of meningitis was reproduced successfully in a BALB/c mouse model. Follow-up identification and characteristic analysis of the serotype of the CZ130302 strain were performed. Interestingly, this strain did not belong to any known *S. suis* serotype. All the

results suggested that the strain was a novel serotype which was probably responsible for the new round of emerging zoonosis in the swine industry.

## MATERIALS AND METHODS

**Ethics statement.** Five-week-old male germfree BALB/c mice and New Zealand White rabbits were purchased from the Comparative Medicine Center of Yangzhou University. All animal experiments were approved by Department of Science and Technology of Jiangsu Province [license number SYXK (SU) 2010-0005].

**Bacterial strains and growth conditions.** The important strains used in this study are listed in Table 1. The new variant strain CZ130302 was isolated from an outbreak of acute piglet meningitis in 2013. The *S. suis* reference serotypes 1 to 5, 7 to 12, 16, 17, 20 to 24, 26, 32, 33, and 34 are stored in our laboratory; serotypes 6, 13, 15, 18, 19, 23, 25, 27, 30, and 31 are preserved in China Animal Health and Epidemiology Center. In addition, a total of 254 *S. suis* strains isolated from different sources and regions, at different times, and of different serotypes were included in this study. The bacteria were grown in Todd-Hewitt broth (THB; BD) and

Received 10 September 2014 Accepted 17 November 2014

Accepted manuscript posted online 21 November 2014

Citation Pan Z, Ma J, Dong W, Song W, Wang K, Lu C, Yao H. 2015. Novel variant serotype of *Streptococcus suis* isolated from piglets with meningitis. *Appl Environ Microbiol* 81:976–985. doi:10.1128/AEM.02962-14.

Editor: H. L. Drake

Address correspondence to Huochun Yao, yaohch@njau.edu.cn, or Chengping Lu, lucp@njau.edu.cn.

Z.P. and J.M. contributed equally to this article.

Supplemental material for this article may be found at <http://dx.doi.org/10.1128/AEM.02962-14>.

Copyright © 2015, American Society for Microbiology. All Rights Reserved.

doi:10.1128/ALM.02962-14

TABLE 1 Bacterial strains and cell lines used in this study

Strain or cell designation	Characteristic or function	Reference
<b>Strains</b>		
P1/7	European classical highly virulent strain, isolated from a pig dying from meningitis	21
9801	Virulent strain of serotype 2 isolated from a pig that died with acute septicemia, China, 1998	22
CZ130302	A novel variant serotype Chz of <i>S. suis</i> which caused acute meningitis in piglets, China, 2013	This study
CZ110902	Serotype Chz, clinical isolate JiangSu province, China, 2011	This study
HN136	Serotype Chz, clinical isolate HeNan province, China, 2006	This study
AH681	Serotype Chz, clinical isolate AnHui province, China, 2006	This study
<b>Cells</b>		
HEp-2	Human laryngeal cancer epithelial cell line, widely used to evaluate the pathogenicity of <i>S. suis</i> isolates	19
bEnd.3	Mouse brain microvascular endothelial cell line	This study

plated on Todd-Hewitt agar (THA) containing 7.5% (vol/vol) sheep blood at 37°C.

**Identification of bacteria.** Regular bacterial isolation was performed. The isolate was identified as *S. suis* using the Vitek 2 system (bioMérieux Vitek, Inc., Hazelwood, MO). The isolates were also confirmed as *S. suis* by 16S rRNA gene sequencing and *gdh*-specific PCR (Table 2) (11, 16). The capsule of *S. suis* CZ130302 was observed by transmission electron microscopy (see Fig. S1B in the supplemental material).

Phylogenetic relationships of *Streptococcus* spp. based on a 552-bp segment of the *cpn60* gene were determined by following the procedures outlined by Hill et al. (11). A ClustalW alignment with default parameters was used with 552-bp nucleic acid sequences. Similarly, sequencing analyses of *sodA* and *recN* were performed. The phylogenetic tree was constructed with the MEGA (v.5.0.3) software package using the neighbor-joining method, with P-distance, complete gap deletion, and bootstrapping ( $n = 500$ ) parameters.

**Agglutination tests.** Serological typing was carried out by agglutination performed as described earlier (17). The serotyping antiserum produced by rabbits was prepared by reported methods. All reference serotypes were tested for reactivity with CZ130302 antiserum. Correspondingly, the reference antisera of serotypes 1, 1/2, and 2 to 34 were used to agglutinate the variant CZ130302. Positive results were recorded when a strong reaction was obtained within 1 min. The judgment standards are shown in Fig. 1.

**Multiplex PCR.** The serotyping primers were designed based on the sequences of capsule loci (*cps*), which were described in earlier reports (13, 14). Using the multiplex PCR system, four reactions were developed to detect all serotypes of *S. suis*. Furthermore, a cross-hybridization experiment was performed to screen the new specific gene in CZ130302. Primers for *cps chzM* were designed for monitoring known serotypes and clinical isolates that were nontypeable (Table 2). All primers were produced by Life Technologies and dissolved in Tris-EDTA (TE) buffer.

**Genetic typing analyses of the *cps* gene cluster.** The complete genome sequence of *S. suis* strain CZ130302 was determined by Solexa pyrosequencing at BGI (Shenzhen, China), and the *cps* gene cluster was obtained. Maps of the new strain gene cluster were constructed manually in

the VECTOR NTI program. Visual representation of the alignments using nucleotide similarities (tblastx) of all *cps* gene clusters was carried out with the Artemis comparison tool (ACT) (18). Conserved Wzy polymerase, Wzx flippase, and glycosyltransferase genes as the serotype-specific genes were analyzed by MEGA (v.5.0.3).

**MLST.** All the isolates in this study were typed using multilocus sequence typing (MLST). The seven housekeeping genes (*dpr*, *mutS*, *cpn60*, *thrA*, *recA*, *aroA*, and *gki*) were amplified by PCR, and internal fragments sequences were obtained as described previously (5). For each isolate, the allele numbers and sequence types (STs) were defined by analysis of the allele sequences in the MLST database (<http://ssuis.mlst.net/>). The results were analyzed by eBURST (version 3).

**Assessment of pathogenicity of *S. suis* CZ130302 in mouse infection model.** The BALB/c mouse infection model (19, 20) was used to compare the virulence of the new serotype isolate with that of two known virulent serotype 2 *S. suis* strains, P1/7 and 9801 (21, 22). A total of  $5 \times 10^7$  CFU/mouse of each strain was injected intraperitoneally (10 mice per strain) to obtain the survival curve. The groups were observed throughout a 7-day period, and survival condition was recorded every day. The blank-control group was injected with sterile phosphate-buffered saline (PBS). The mice were observed for 7 days until survival rates were steady. A total of  $2 \times 10^7$  CFU/mouse ( $\sim 10 \times$  the 50% lethal dose [ $LD_{50}$ ]) of *S. suis* CZ130302 was injected intraperitoneally into 50 mice. Five symptomatic mice were selected for euthanization and dissection every 24 h. Bacteria were isolated from the hearts, kidneys, lungs, brains, and urine homogenate by plating 10-fold serial dilutions on THA. The number of bacteria colonizing the organs of the mice during systemic infection was obtained.

**Adhesion assays with HEp-2 and bEnd.3 cells.** In accordance with the bacterial colonization capacity *in vivo*, we used the human laryngeal carcinoma cell line HEp-2 and mouse brain microvascular endothelial cells (bEnd.3) as in the models of bacterial colonization (19, 20, 23) and meningitis (24, 25) *in vitro*, respectively. The adherence assays were performed as previously described (26). To release all bacteria, the monolayers were disrupted by adding sterile water for HEp-2 cells or 0.01% Triton X-100 for bEnd.3 cells after digestion with trypsin.

TABLE 2 Primers used for PCR amplification

Primer	Sequence (5'-3')	Product size (bp)	$T_m$ (°C)	Comment
16S-rRNA-F	AGAGTTTGATCGTGGCTCA	1,500	55	Domain-specific 16S primers
16S-rRNA-R	TACGGTTACCTTGTACGACTT			
gdh-F	CCATGGACAGATAAAGATGG	688	54	Primers for <i>S. suis</i> identification
gdh-R	GCAGCGTATTCTGTCAAACG			
Chz-M-F	AATGAATAAGGAACCTTGAACCTA	424	59.8	Constructed in this study
Chz-M-R	CGTATCATCTGTATTAGCTAAA			

<sup>a</sup>  $T_m$ , melting temperature.

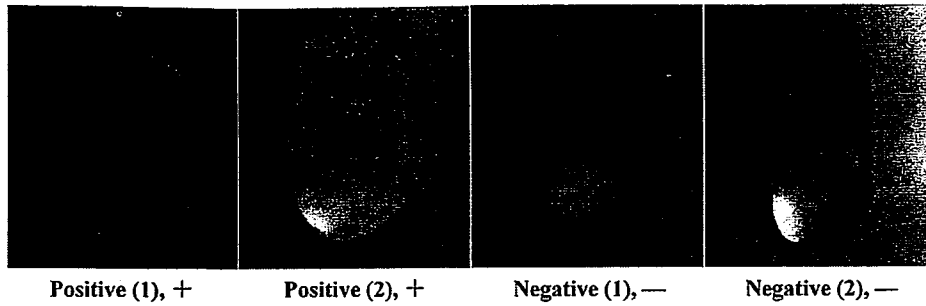


FIG 1 Judgment standards of the agglutination assay.

**Cytotoxicity assays.** In order to further confirm the ability to cause meningitis, the cytotoxic effect of bacteria was evaluated along with bEnd.3 cell adhesion by lactate dehydrogenase (LDH) measurement using the CytoTox 96 nonradioactive cytotoxicity assay (Promega

Corporation, USA) (27, 28). The percent cytotoxicity was calculated as  $[(\text{sample OD}_{490} - \text{bacterial spontaneous OD}_{490} - \text{cell spontaneous OD}_{490}) / (\text{cell maximum OD}_{490} - \text{cell spontaneous OD}_{490})] \times 100$ , where  $\text{OD}_{490}$  is optical density at 490 nm. LDH release was measured

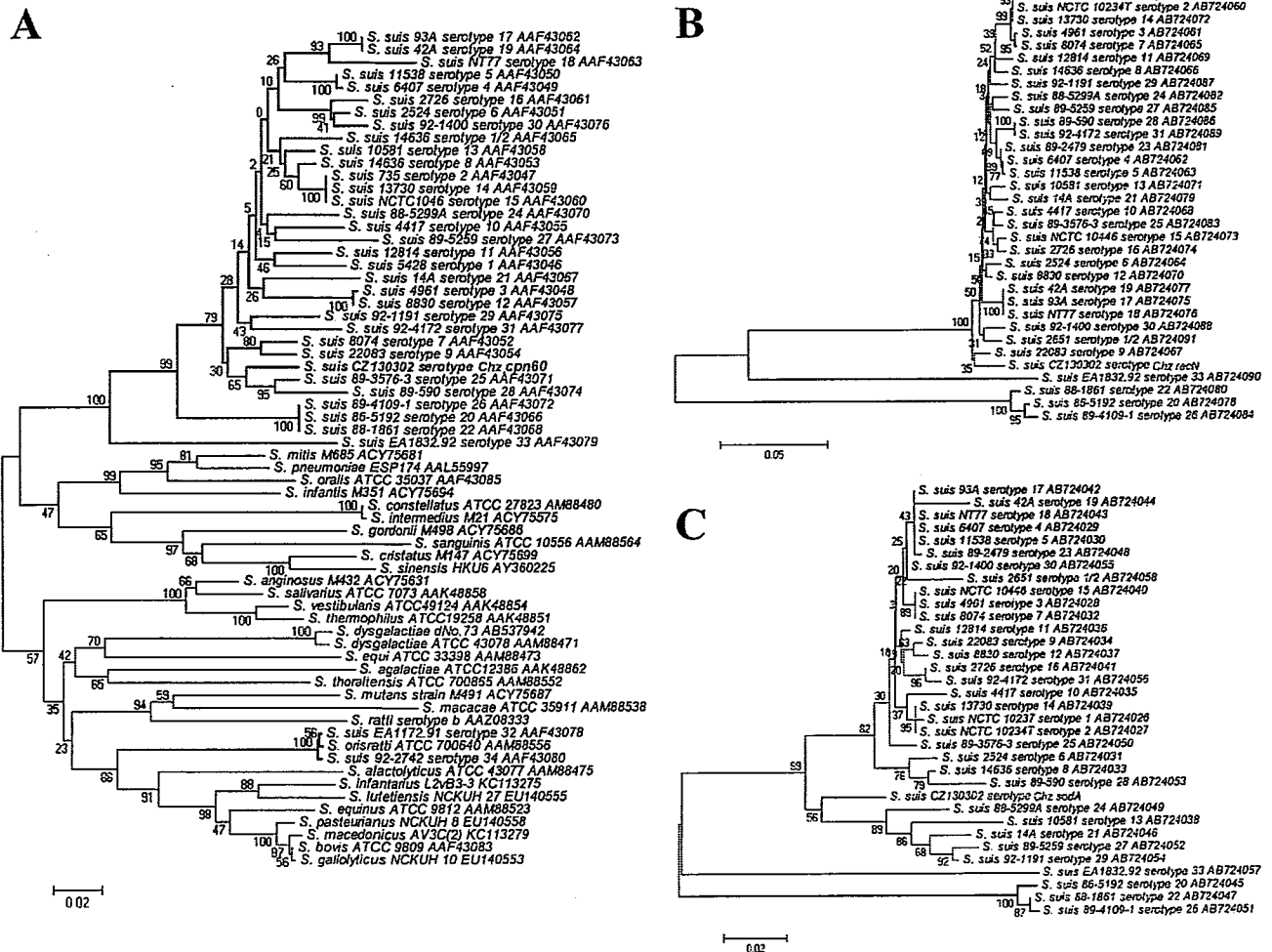


FIG 2 Phylogenetic analysis of three key genes in *Streptococcus*. (A) Phylogenetic relationships of most *Streptococcus* spp. based on a 552-bp segment of the *cpn60* gene. The tree was constructed with the MEGA (v.5.0.3) software package using the neighbor-joining method, with P-distance, complete gap deletion, and bootstrapping ( $n = 500$ ) parameters. Accession numbers for sequences used in this analysis are shown after the strain names. The *cpn60* segments of *S. suis* strains are highlighted with red branches, and the red type indicates the *cpn60* segment from *S. suis* serotype Chz. The *cpn60* segments of previous *S. suis* serotypes 32 and 34 and *S. orisratti* are highlighted with blue branches and red type. (B) Phylogenetic relationships of 35 serotypes of *S. suis* based on a 1,056-bp segment of the *recN* gene. The red type indicates the *recN* segment from *S. suis* serotype Chz. The *recN* segments of previous *S. suis* serotypes 20, 22, 26, and 33 are highlighted with blue branches and type. (C) Phylogenetic relationships of 35 serotypes of *S. suis* based on a 409-bp segment of the *sodA* gene. The red type indicates the *sodA* segment from *S. suis* serotype Chz. The *sodA* segments of *S. suis* serotypes 20, 22, 26, and 33 are highlighted with blue branches and type.

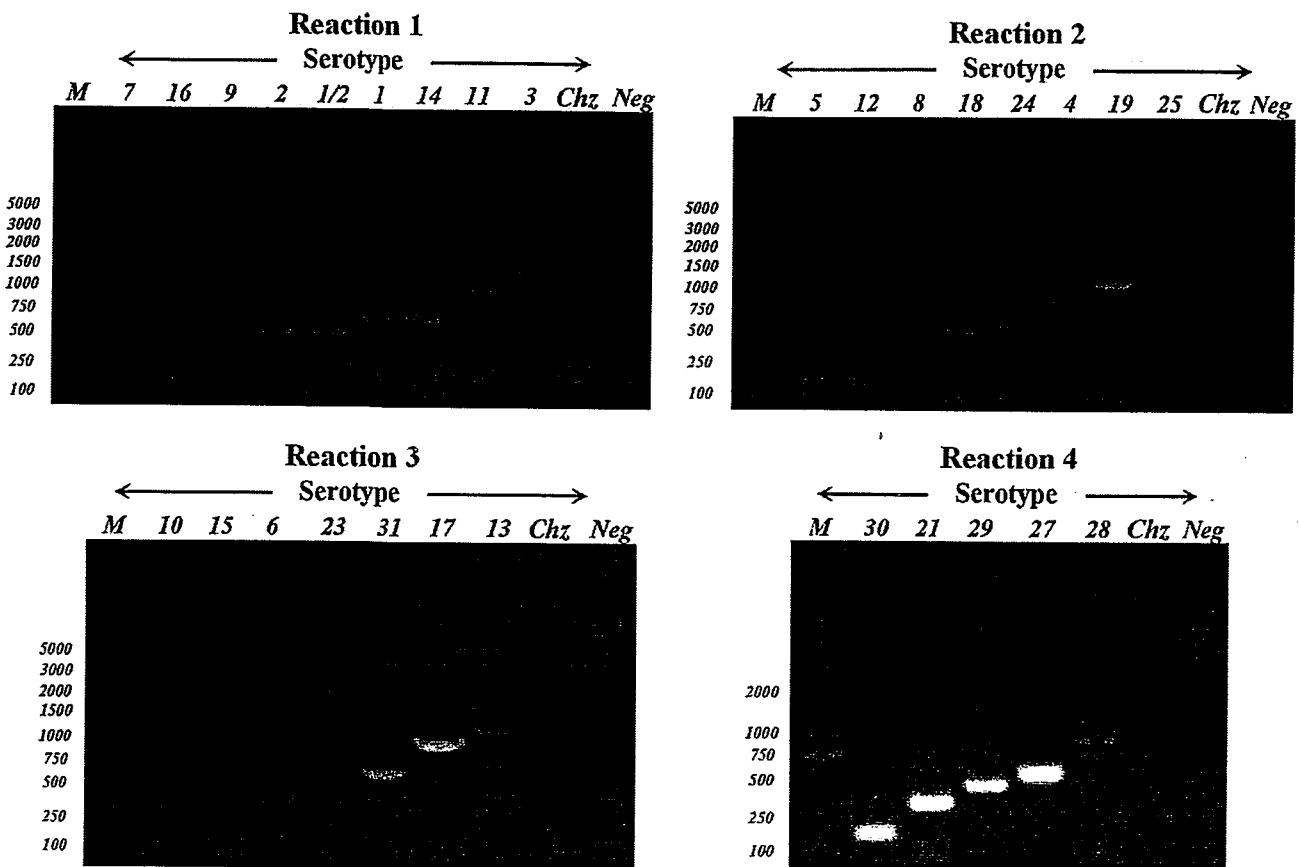


FIG 3 Multiplex PCR (4 reaction sets) products of *S. suis* new serotype CZ130302 and 29 reference strains. PCR products were electrophoresed on a 1.5% (wt/vol) agarose gel, stained with GoldView, and photographed under UV light. Serotypes are indicated above the lanes. Lanes M, 5,000-bp DNA ladder markers (Biomed, Beijing, China); sizes (bp) are indicated on the left.

after different durations of incubation (1 h to 4 h) at a bacterium-cell ratio of 1:1 at 37°C.

**Statistical analysis.** Statistical analysis for *in vitro* and *in vivo* experiments was carried out using Prism 5 (GraphPad Software, La Jolla, CA). One-way analysis of variance (ANOVA) was used in the analysis of the cell adherence assay results. Student's *t* tests were applied for comparison of serum IgG levels, and mouse survival data were analyzed by the Kaplan-Meier estimation method (29). A difference with a *P* value of <0.05 was considered significant, and a *P* value of <0.01 was considered greatly significant.

**Nucleotide sequence accession number.** For meningitis-associated *S. suis* isolate CZ130302, a *cps* cluster sequence of 28,481 bp was obtained. The DNA sequence was deposited in GenBank under accession number KJ669337.

## RESULTS

**Isolation and identification of bacteria.** The significant beta-hemolytic zones were created by piglet meningitis-associated strain CZ130302 (see Fig. S1A in the supplemental material). The capsule of *S. suis* CZ130302 was observed by transmission electron microscopy (see Fig. S1B). Further identification of the organism as *S. suis* was confirmed at the OIE Reference Laboratory for Swine Streptococcosis in Nanjing Agricultural University by the Vitek 2 system (bioMérieux Vitek), the result of which was completely consistent with *S. suis* (see Fig. S2). 16S rRNA gene sequencing was

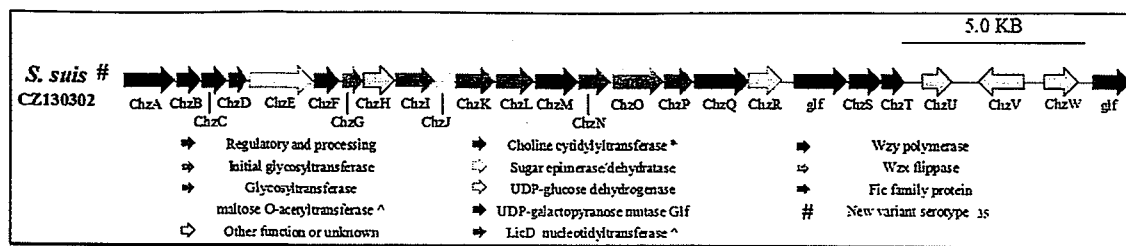
also performed; the results showed >99% homology with the *S. suis* European classical strain P1/7 (1,524/1,528 bases) and Chinese epidemic strain SC84 (1,523/1,528 bases).

Phylogenetic relationships of the *cpn60*, *recN*, and *sodA* genes in all serotypes were demonstrated in cladograms (Fig. 2). In a phylogenetic tree of partial *cpn60*, *S. orisratti* and *S. suis* serotypes 32 and 34 are located in a group including *S. equinus*, *S. alactolyticus*, and so on, while strain CZ130302 and all other serotypes of *S. suis* are found together in a separate and distinct cluster (Fig. 2A). Likewise, the phylogenetic trees of *sodA* and *recN* showed that serotypes 20, 22, 26, and 33 located outside a clade formed by 29 other serotypes and strain CZ130302 (Fig. 2B and C). These result indicated that serotype Chz was a veritable emerging serotype of *S. suis*.

**Agglutination tests.** Agglutination tests of isolate CZ130302 showed negative reactions with all 33 serotypes. Correspondingly, the reversed agglutination tests between the existing *S. suis* serotypes and the new serotyping antiserum produced by rabbits showed no strong positive result for any of the 33 serotype reference strains (see Table S1 in the supplemental material).

**Identification of serotypes by multiplex PCR.** Specific PCRs for the 33 known serotypes were performed, and they confirmed a negative result for the novel variant CZ130302 (Fig. 3). Every se-

**A**



**B**

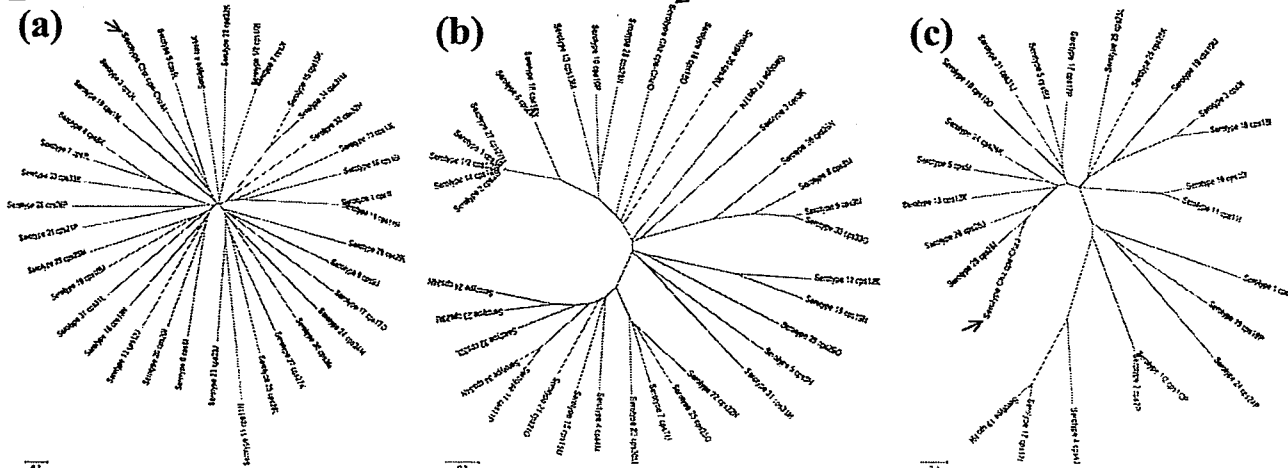


**FIG 4** The *cps* cluster of strain CZ130302 and its key genes. (A) Schematic diagram of the genetic organization of the *S. suis* serotype Chz strain CZ130302 *cps* gene cluster. Genes encoding conserved domain proteins are represented by the same colors. White arrows refer to other genes in the *cps* gene clusters that were not identified as part of the conserved core described by Okura et al. (12). The direction of the arrows indicates the direction of transcription. The color key for the functional classes of genes in the *cps* cluster is shown at the bottom. (B) Sequence relationship of Wzy, Wzx, and acetyltransferase of all *S. suis* serotypes. Three neighbor-joining trees (bootstrap  $n = 1,000$ ; Poisson correction) were constructed based on the ClustalW alignments of the Wzy, Wzx, and acetyltransferase amino acid sequences from all of *S. suis* serotypes. Wzy, Wzx, and acetyltransferase from *S. suis* strains CZ130302 are indicated by red arrows.

rotype reference strain was used as a positive control. The results indicated that no serotype-specific genes of known serotypes were found in strain CZ130603, whose *cps* gene cluster was highly differential.

**The *cps* cluster of strain CZ130302.** The CZ130302 CP genes are named *chzA*-*chzW*, corresponding to the regulation portions (*cpsA*-*cpsW*) of the chromosome (*cps* gene cluster portions) in *S. suis* (Fig. 4A) (12). In order to identify whether this strain represented an emerging serotype of *S. suis*, genetic analysis of whole *cps* gene clusters of all serotypes was performed in this study. The results of comparative genomics showed that the *cps* gene cluster of CZ130302 lacked homology with the sequences of other known strains; no *cps* cluster has been seen to lack homology to other such sequences previously (Fig. 5). The novel serotype shares homologous *wzg*, *wzd*, *wze*, and *wzh* sequences with all known serotypes of *S. suis* in their *cps* gene clusters, whereas it contains other unique key genes from *chzI* (7,735 bp) to *chzW* (28,481 bp) (Fig. 5; see also Table S2 in the supplemental material), such as the polymerase (*wzy*), flippase (*wzx*), glycosyltransferase, and acetyltransferase genes (Fig. 4B).

Some of the CZ130302 *cps* genes were predicted to encode modifying enzymes (such as acetyltransferase [*chzI*], nucleotidyltransferase [*chzP*], choline phosphate cytidylyltransferase [*chzQ*], UDP-glucose dehydrogenase [*chzR*], and phosphocholine cytidylyltransferase [*chzT*]), which are involved in the biosynthesis and

addition to other components on CPs (such as glycerol and choline) (Fig. 4A; see also Table S2 in the supplemental material). The novel *S. suis* *cps* gene cluster also has a disrupted gene encoding a protein in the transposase family (*chzW*) in the 3' region, similar to most of the *cps* gene clusters. The *cps* gene cluster of the new serotype has a >65% specific sequence, which guides the synthesis of the characteristic capsule of isolate CZ130302 (see Table S2).

**Development of novel serotype-specific PCR.** We selected oligonucleotide primers within the *cps chzM* gene to generate specific amplicons of 424 bp according to the cross-hybridization results. A total of 45 nontypeable strains of *S. suis* isolated from China were used to check the *cps chzM* gene; 3 (HN136, AH681, and CZ110902) of them showed 424-bp bands. Agglutination tests of two isolates (HN136 and CZ110902) showed classical positivity with the CZ130302 antiserum (see Table S3 in the supplemental material). The sequencing results for their *cps chzM* genes showed >99% homology with the *cps* gene of reference strain CZ130302. The results demonstrate that they all belong to this novel serotype.

**MLST typing.** All 4 isolates of the novel serotype were characterized using MLST. Two isolates were classified as ST 383 and showed strong pathogenicity in the piglet and BALB/c mouse models (see Table S4 in the supplemental material). Avirulent strain HN136 was classified as ST 264, and AH681 was ST 475.

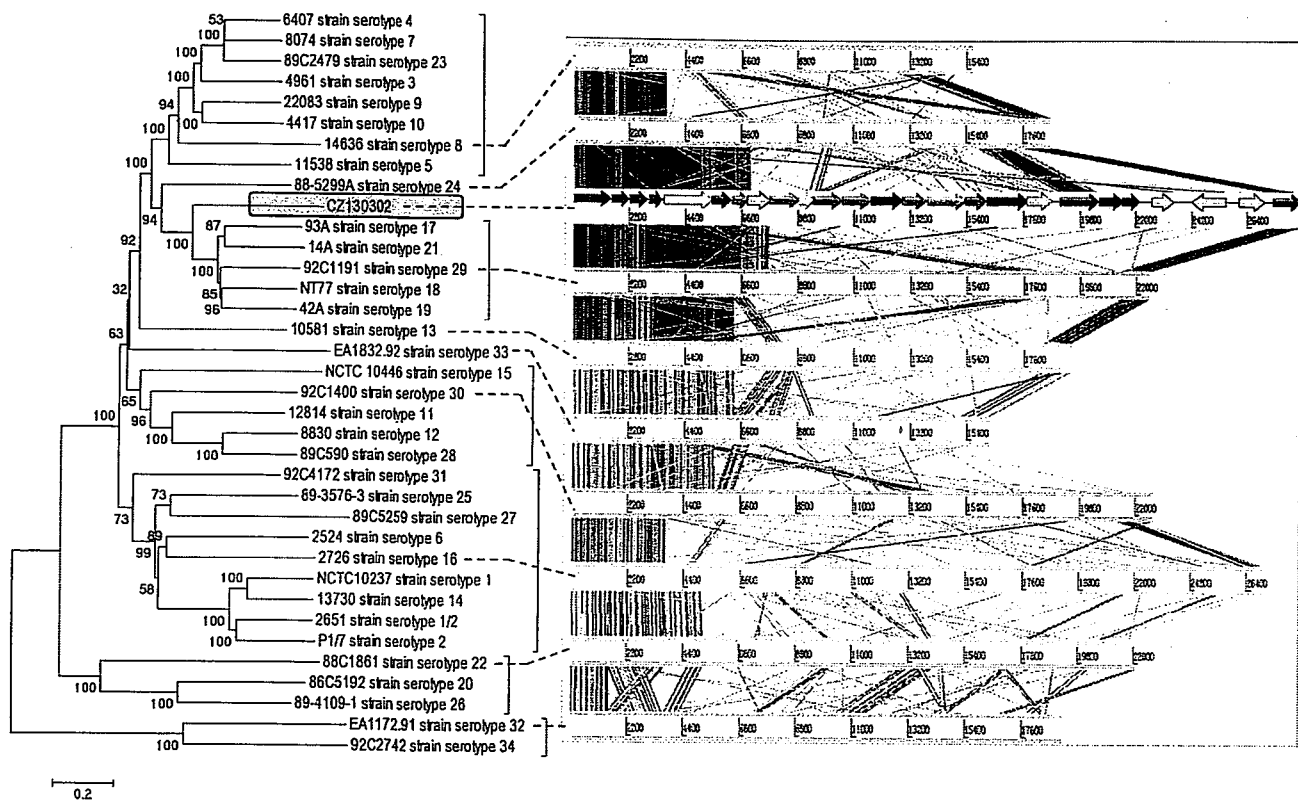


FIG 5 Comparative genome alignments of 35 *cps* gene clusters. The color key for the functional classes of genes and relevant information is the same as shown in Fig. 6A. Phylogenetic relationships of the *cps* gene clusters were obtained using a neighbor-joining tree (bootstrap  $n = 1,000$ ) based on a ClustalW alignment of the complete cluster sequences. Visual representation of the alignments using nucleotide similarities (tblastx) of the *cps* gene clusters as determined with the Artemis comparison tool (ACT) (18).

None of these three STs could be grouped in any clonal complexes (CC) according to eBURST analysis (Fig. 6).

**Evaluation of pathogenicity of the novel serotype strains in the BALB/c mouse model.** The mouse model has been demonstrated to be a useful tool for evaluating the virulence of *S. suis*. The mortality of BALB/c mice was observed for 7 days after the challenge. The survival curve for strain CZ130302 was significantly lower than for strains P1/7, 9801, and HN136 ( $P < 0.01$ ) (Fig. 7A). These results confirmed that strain CZ130302 showed high virulence and pathogenicity in the BALB/c mouse model. However, strain HN136 was avirulent in this study (Fig. 7A; see also Table S4 in the supplemental material).

**Strong virulence of the isolate CZ130302 associated with acute meningitis.** The novel serotype isolate CZ130302 caused a large outbreak of piglet meningitis in eastern China. This strong pathogenicity of meningitis was reproduced successfully in the BALB/c mouse model. More than 60% (19/30) of mice infected with CZ130302 ( $5 \times 10^5$  CFU/mouse) showed neurological symptoms (see Video S1 in the supplemental material), and many survivors had sequelae, including tetraplegia, paraplegia, neck-crooking, circling, etc. The density of CZ130302 was able to reach  $1 \times 10^8$  CFU/g in the brains and kidneys of dying mice 3 days after challenge, with  $1 \times 10^5$  CFU/g or less in other organs (Fig. 7B). The pathological observation of brain tissue showed obvious abscess and bleeding (Fig. 8). These results demonstrated that isolate CZ130302 had a strong capacity to cause meningitis in BALB/c mice.

**High virulence of cerebral infection verified by host cell adhesion assay.** The capacities of adhesion to host cells were compared among the CZ130302, 9801, and P1/7 strains under the same conditions. As shown in Fig. 9A, the bEnd.3 cell adhesion for strains P1/7, 9801, and CZ130302 was significantly higher than for HN136 ( $P < 0.01$ ) (Fig. 9A). The HEP2 cell adhesion for strain CZ130302 was significantly lower than for strain P1/7 ( $P < 0.01$ ) and not significantly different from that of strain 9801 (Fig. 9A). These results suggested that strain CZ130302 had stronger capacity than strains HN136 in the adhesion of HEP2 and bEnd.3 cells, with a bit weaker capacity for strain P1/7. These findings confirmed the notion that the pathogenesis of new isolate CZ130302 might be associated with bacterial colonization in respiratory tract and brain tissue.

**Strain CZ130302 can damage bEnd.3 cells.** A multiplicity of infection (MOI) of 1 bacterium/cell ( $2 \times 10^5$  CFU/well) was chosen to study the kinetics of cytotoxicity by *S. suis*. Maximal cytotoxic levels were observed at the third hour of bacterium-cell contact (Fig. 9B). The kinetics of cell damage fell between 60% and 80% (Fig. 9B). These results suggested that strain CZ130302 was able to kill mouse brain microvascular endothelial cells (bEnd.3) due to bacterial colonization in the brain tissue.

## DISCUSSION

*S. suis* is increasingly recognized as a significant zoonotic agent. Increasing awareness of *S. suis* infection is expected to help coun-

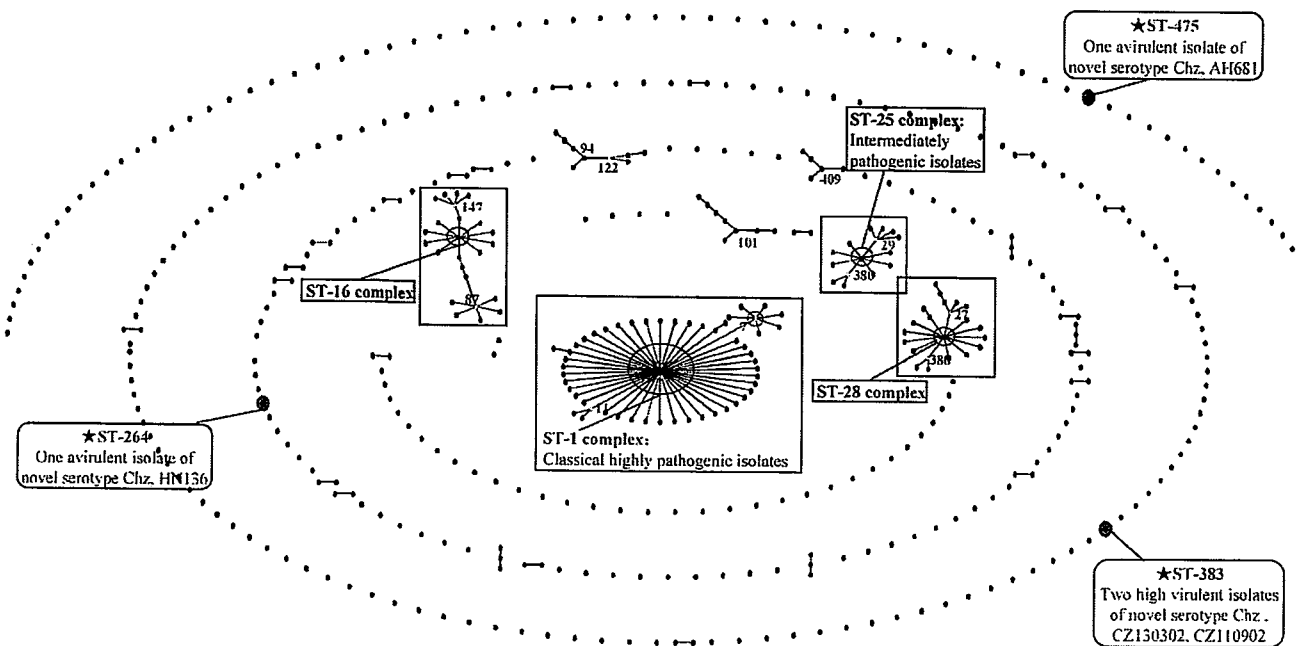


FIG 6 eBURST diagram of the *S. suis* population. Population snapshots of *S. suis* of related STs within the entire *S. suis* MLST database were constructed. Each ST is represented as a dot. Two dots separated by one node represent a single-locus variation between two STs (a single-locus variant). The STs positioned centrally in the clonal complex (CC) are primary founders (blue) or subgroup founders (yellow). STs in purple circles are those identified in this study. For clarity, labels of STs have been removed, except related STs and founders in CCs. Some STs are labeled with blue boxes to emphasize their importance. The eBURST diagram does not show the genetic distance between unlinked STs and CCs.

ter animal or human streptococcosis. In this study, obvious neurological symptoms were observed in piglets infected by strain CZ130302, such as walking in circles and single-side neck crooking. The mouse model also replicated the classical symptom. Previous studies have shown that meningitis was mainly caused by serotypes 2, 9, and 14 (30–32), of which the presenting features were generally similar to those of pyogenic meningitis caused by other bacteria. Acute meningitis caused by a novel variant sero-

type has never been reported previously. This potentially unrecognized hazard of the swine industry is demonstrated by this study.

Serological typing is the foundation of *S. suis* serotyping (17, 33). The antiserum of the novel serotype prepared can provide reliable and original results for identification of this novel serotype. PCR typing assays provide a fast and cost-effective way to determine the serotypes of isolates. The multiplex PCR method

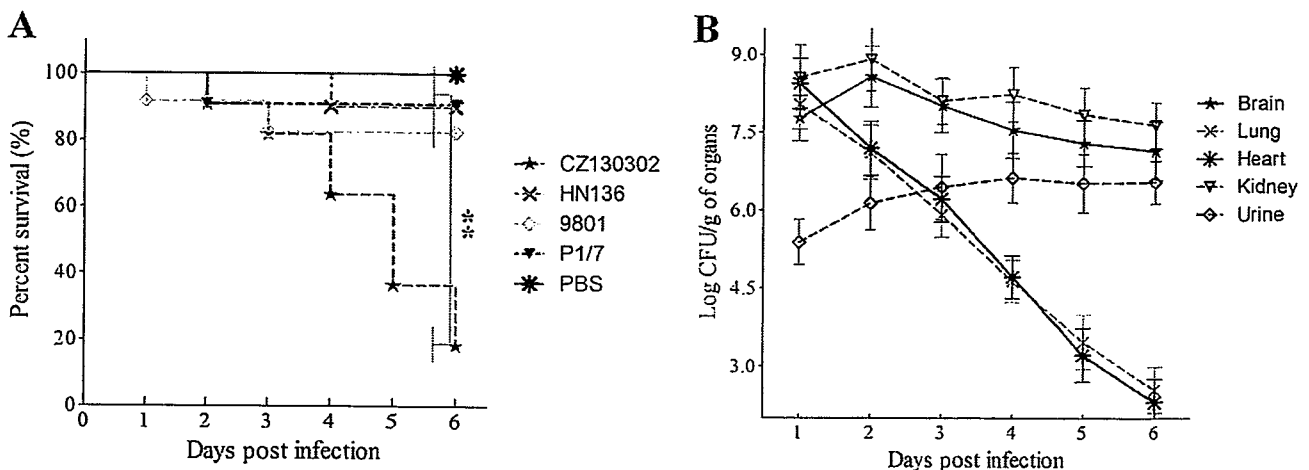


FIG 7 Challenge studies in the BALB/c mouse model and cell adhesion assay. (A) Mortality curve of lethal challenge with *S. suis* strains. A total of  $5 \times 10^7$  CFU/mouse of each strain was injected intraperitoneally (10 mice per strain) to obtain the survival curve. The groups were observed throughout a 7-day period, and survival condition was recorded every day. (B) A total of  $2 \times 10^7$  CFU/mice ( $\sim 10 \times \text{LD}_{50}$ ) of *S. suis* CZ130302 was injected intraperitoneally into 50 mice. Five symptomatic mice were euthanized to perform reisolation of *S. suis* every 24 h by plating 10-fold serial dilutions on THA (\*,  $P < 0.01$ ; †,  $P < 0.05$ ).

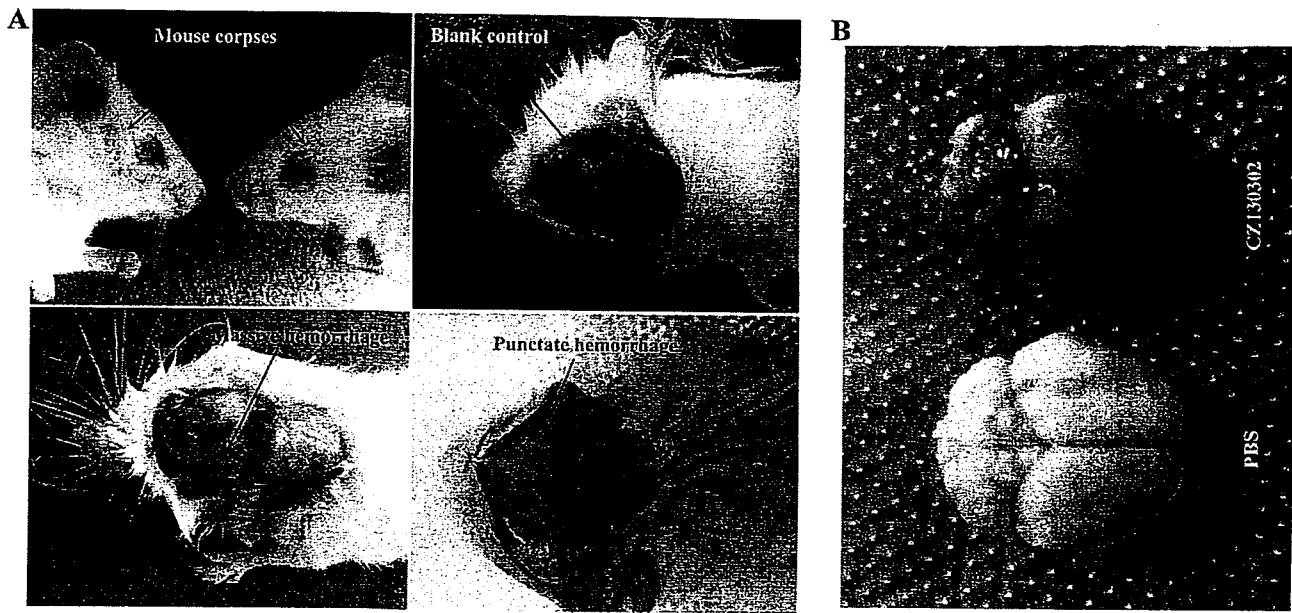


FIG 8 Autopsy images of mouse brain.

has been developed in recent years (13, 14, 34); the specific *cps* genes are planned for use in typing. This gene cluster strongly supports the results of agglutination assays and avoids the false positivity of naked-eye observation in the agglutination test. Inevitably, cross-antigenicity happened between the novel antiserum and some serotypes (serotypes 15, 13, 26, 6, 19, 24, and 25). For increased assurance, we designed the *cps chzM* gene primers to differentiate this novel serotype from all exciting serotypes. Three positive strains were searched from the 45 nontypeable *S. suis* strains stored in our laboratory. These positive strains were from different areas and periods, but they were all recently isolated strains from eastern China.

MLST has been widely used to study genetic diversity, population structure, and molecular epidemiology in *S. suis* (5).

None of the three STs of the novel serotype was linked with any highly virulent STs by virologists, whereas ST 383 isolates were strongly associated with high pathogenicity in an animal model (35, 36). Additionally, the complete sequence of the *cps* locus of CZ130302 was obtained in subsequent research. Capsular polysaccharides are an extremely diverse range of molecules that may differ not only by monosaccharide units but also in how these units are joined together (37). CPs of all *S. suis* serotypes are synthesized by the *Wzx/Wzy* pathway, which recognizes common oligosaccharide structures conserved in the different repeat units (12).

The results of this study demonstrate that strain CZ130302 belongs to a novel serotype (Chz) of *S. suis*, based on sequencing of the *cps* gene cluster, PCR, and agglutination typing. MLST analysis

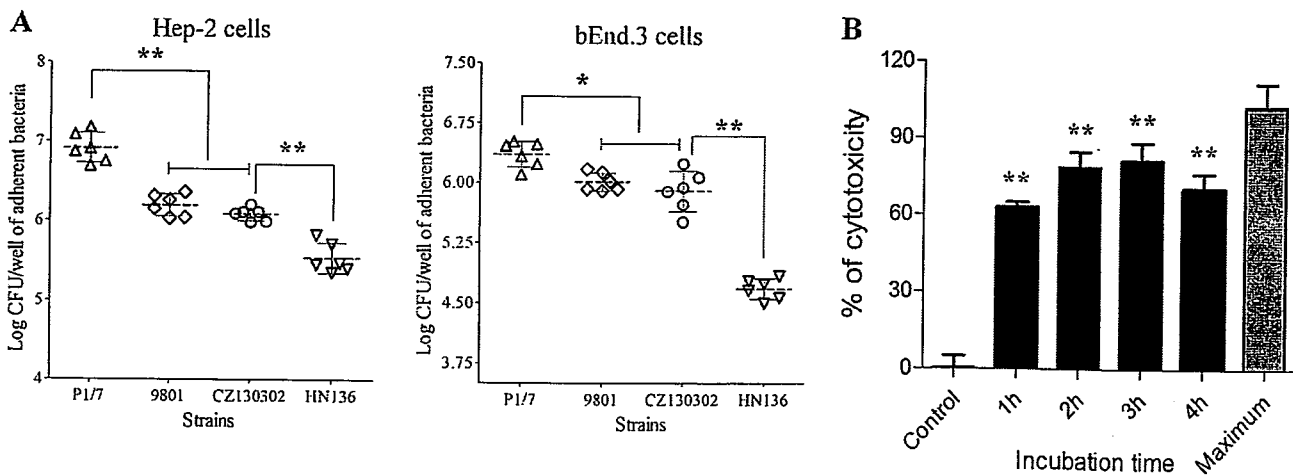


FIG 9 Cell adhesion and cytotoxicity assay. All assays were run in triplicate. Statistical significance was determined by Student's *t* test (\*\*,  $P < 0.01$ ; \*,  $P < 0.05$ ). (A) The assessment of cell adhesion ability of *S. suis* serotype Chz. Virulent strain CZ130302 shows a strong capacity of adhesion to bEnd.3 and HEp2 cells (MOI, 100). (B) Assessment of the cytotoxicity of strain CZ130302. An MOI of 1 bacterium/cell ( $2 \times 10^5$  CFU bacteria/well) was chosen to study the kinetics of cytotoxicity by *S. suis*. Strain CZ130302 was able to significantly damage mouse brain microvascular endothelial cells (bEnd.3).



and Wzx/Wzy phylogenetic tree profiling also prove to be useful in establishing the serotype.

#### ACKNOWLEDGMENTS

This research was supported by the Special Fund for Public Welfare Industry of the Chinese Ministry of Agriculture (2013003041), the 948 Major Project and Industry Project from the Chinese Ministry of Agriculture (2014-S11), and a project funded by the Priority Academic Program Development of Jiangsu Higher Education Institutions (PAPD).

#### REFERENCES

- Fittipaldi N, Segura M, Grenier D, Gottschalk M. 2012. Virulence factors involved in the pathogenesis of the infection caused by the swine pathogen and zoonotic agent *Streptococcus suis*. *Future Microbiol* 7:259–279. <http://dx.doi.org/10.2217/fmb.11.149>.
- Perch B, Kristjansen P, Skadhauge K. 1968. Group R streptococci pathogenic for man. Two cases of meningitis and one fatal case of sepsis. *Acta Pathol Microbiol Scand* 74:69–76.
- Demar M, Belzunce C, Simonnet C, Renaux A, Abboud P, Okandze A, Marois-Crehan C, Djossou F. 2013. *Streptococcus suis* meningitis and bacteremia in man, French Guiana. *Emerg Infect Dis* 19:1545–1546. <http://dx.doi.org/10.3201/eid1909.121872>.
- Zalas-Wieczek P, Michalska A, Grabczewska E, Olczak A, Pawlowska M, Gospodarek E. 2013. Human meningitis caused by *Streptococcus suis*. *J Med Microbiol* 62:483–485. <http://dx.doi.org/10.1099/jmm.0.046599-0>.
- King SJ, Leigh JA, Heath PJ, Luque I, Tarradas C, Dowson CG, Whatmore AM. 2002. Development of a multilocus sequence typing scheme for the pig pathogen *Streptococcus suis*: identification of virulent clones and potential capsular serotype exchange. *J Clin Microbiol* 40:3671–3680. <http://dx.doi.org/10.1128/JCM.40.10.3671-3680.2002>.
- Suankratay C, Intalaporn P, Nunthapisud P, Arunyingmongkol K, Wilde H. 2004. *Streptococcus suis* meningitis in Thailand. *Southeast Asian J Trop Med Public Health* 35:868–876.
- Takamatsu D, Wongsawan K, Osaki M, Nishino H, Ishiji T, Tharavitkul P, Khantawa B, Fongcom A, Takai S, Sekizaki T. 2008. *Streptococcus suis* in humans, Thailand. *Emerg Infect Dis* 14:181–183. <http://dx.doi.org/10.3201/eid1401.070568>.
- Yu H, Jing H, Chen Z, Zheng H, Zhu X, Wang H, Wang S, Liu L, Zu R, Luo L, Xiang N, Liu H, Liu X, Shu Y, Lee SS, Chuang SK, Wang Y, Xu J, Yang W. 2006. Human *Streptococcus suis* outbreak, Sichuan, China. *Emerg Infect Dis* 12:914–920. <http://dx.doi.org/10.3201/eid1206.051194>.
- Mai NT, Hoa NT, Nga TV, Linh le D, Chau TT, Sinh DX, Phu NH, Chuong LV, Diep TS, Campbell J, Nghia HD, Minh TN, Chau NV, de Jong MD, Chinh NT, Hien TT, Farrar J, Schultz C. 2008. *Streptococcus suis* meningitis in adults in Vietnam. *Clin Infect Dis* 46:659–667. <http://dx.doi.org/10.1086/527385>.
- Palmieri C, Varaldo PE, Facinelli B. 2011. *Streptococcus suis*, an emerging drug-resistant animal and human pathogen. *Front Microbiol* 2:235. <http://dx.doi.org/10.3389/fmicb.2011.00235>.
- Hill JE, Gottschalk M, Brousseau R, Harel J, Hemmingsen SM, Goh SH. 2005. Biochemical analysis, cpn60 and 16S rDNA sequence data indicate that *Streptococcus suis* serotypes 32 and 34, isolated from pigs, are *Streptococcus orisratti*. *Vet Microbiol* 107:63–69. <http://dx.doi.org/10.1016/j.vetmic.2005.01.003>.
- Okura M, Takamatsu D, Maruyama F, Nozawa T, Nakagawa I, Osaki M, Sekizaki T, Gottschalk M, Kumagai Y, Hamada S. 2013. Genetic analysis of capsular polysaccharide synthesis gene clusters from all serotypes of *Streptococcus suis*: potential mechanisms for generation of capsular variation. *Appl Environ Microbiol* 79:2796–2806. <http://dx.doi.org/10.1128/AEM.03742-12>.
- Kerdsin A, Akeda Y, Hatrongjit R, Detchawna U, Sekizaki T, Hamada S, Gottschalk M, Oishi K. 2014. *Streptococcus suis* serotyping by a new multiplex PCR. *J Med Microbiol* 63:824–830. <http://dx.doi.org/10.1099/jmm.0.069757-0>.
- Liu Z, Zheng H, Gottschalk M, Bai X, Lan R, Ji S, Liu H, Xu J. 2013. Development of multiplex PCR assays for the identification of the 33 serotypes of *Streptococcus suis*. *PLoS One* 8:e72070. <http://dx.doi.org/10.1371/journal.pone.0072070>.
- Wang K, Sun X, Lu C. 2012. Development of rapid serotype-specific PCR assays for eight serotypes of *Streptococcus suis*. *J Clin Microbiol* 50:3329–3334. <http://dx.doi.org/10.1128/JCM.01584-12>.
- Okwumabua O, O'Connor M, Shull E. 2003. A polymerase chain reaction (PCR) assay specific for *Streptococcus suis* based on the gene encoding the glutamate dehydrogenase. *FEMS Microbiol Lett* 218:79–84. <http://dx.doi.org/10.1111/j.1574-6968.2003.tb11501.x>.
- Higgins R, Gottschalk M, Boudreau M, Lebrun A, Henrichsen J. 1995. Description of six new capsular types (29–34) of *Streptococcus suis*. *J Vet Diagn Invest* 7:405–406. <http://dx.doi.org/10.1177/104063879500700322>.
- Carver TJ, Rutherford KM, Berriman M, Rajandream MA, Barrell BG, Parkhill J. 2005. ACT: the Artemis Comparison Tool. *Bioinformatics* 21:3422–3423. <http://dx.doi.org/10.1093/bioinformatics/bti553>.
- Si Y, Yuan F, Chang H, Liu X, Li H, Cai K, Xu Z, Huang Q, Bei W, Chen H. 2009. Contribution of glutamine synthetase to the virulence of *Streptococcus suis* serotype 2. *Vet Microbiol* 139:80–88. <http://dx.doi.org/10.1016/j.vetmic.2009.04.024>.
- Wichgers Schreuf PJ, Rebel JM, Smits MA, van Putten JP, Smith HE. 2011. TroA of *Streptococcus suis* is required for manganese acquisition and full virulence. *J Bacteriol* 193:5073–5080. <http://dx.doi.org/10.1128/JB.05305-11>.
- Allen AG, Bolitho S, Lindsay H, Khan S, Bryant C, Norton P, Ward P, Leigh J, Morgan J, Riches H, Easty S, Maskell D. 2001. Generation and characterization of a defined mutant of *Streptococcus suis* lacking suily-sin. *Infect Immun* 69:2732–2735. <http://dx.doi.org/10.1128/IAI.69.4.2732-2735.2001>.
- Ju CX, Gu HW, Lu CP. 2012. Characterization and functional analysis of atl, a novel gene encoding autolysin in *Streptococcus suis*. *J Bacteriol* 194:1464–1473. <http://dx.doi.org/10.1128/JB.06231-11>.
- Vanier G, Segura M, Friedl P, Lacouture S, Gottschalk M. 2004. Invasion of porcine brain microvascular endothelial cells by *Streptococcus suis* serotype 2. *Infect Immun* 72:1441–1449. <http://dx.doi.org/10.1128/IAI.72.3.1441-1449.2004>.
- El-Assaad F, Wheway J, Mitchell AJ, Lou J, Hunt NH, Combes V, Grau GE. 2013. Cytoadherence of *Plasmodium berghei*-infected red blood cells to murine brain and lung microvascular endothelial cells in vitro. *Infect Immun* 81:3984–3991. <http://dx.doi.org/10.1128/IAI.00428-13>.
- Huang SH, Wang L, Chi F, Wu CH, Cao H, Zhang A, Jong A. 2013. Circulating brain microvascular endothelial cells (cBMECs) as potential biomarkers of the blood-brain barrier disorders caused by microbial and non-microbial factors. *PLoS One* 8:e62164. <http://dx.doi.org/10.1371/journal.pone.0062164>.
- Wertheim HF, Nghia HD, Taylor W, Schultz C. 2009. *Streptococcus suis*: an emerging human pathogen. *Clin Infect Dis* 48:617–625. <http://dx.doi.org/10.1086/596763>.
- Behl K, Davis JB, Lesley R, Schubert D. 1994. Hydrogen peroxide mediates amyloid beta protein toxicity. *Cell* 77:817–827. [http://dx.doi.org/10.1016/0092-8674\(94\)90131-7](http://dx.doi.org/10.1016/0092-8674(94)90131-7).
- Segura M, Gottschalk M. 2002. *Streptococcus suis* interactions with the murine macrophage cell line J774: adhesion and cytotoxicity. *Infect Immun* 70:4312–4322. <http://dx.doi.org/10.1128/IAI.70.8.4312-4322.2002>.
- Langová K, Gallo J. 2010. Is Kaplan-Meier statistics the most appropriate tool for survivorship measurement of outcomes in orthopaedics? *Acta Chir Orthop Traumatol Cech* 77:118–123. (In Czech.)
- Fowler HN, Brown P, Rovira A, Shade B, Klammer K, Smith K, Scheftel J. 2013. *Streptococcus suis* meningitis in swine worker, Minnesota, USA. *Emerg Infect Dis* 19:330–331. <http://dx.doi.org/10.3201/eid1902.120918>.
- Wu Z, Zhang W, Lu C. 2008. Comparative proteome analysis of secreted proteins of *Streptococcus suis* serotype 9 isolates from diseased and healthy pigs. *Microb Pathog* 45:159–166. <http://dx.doi.org/10.1016/j.micpath.2008.04.009>.
- Haleis A, Alfa M, Gottschalk M, Bernard K, Ronald A, Manickam K. 2009. Meningitis caused by *Streptococcus suis* serotype 14, North America. *Emerg Infect Dis* 15:350–352. <http://dx.doi.org/10.3201/eid1502.080842>.
- Gottschalk M, Higgins R, Jacques M, Beaudoin M, Henrichsen J. 1991. Characterization of six new capsular types (23 through 28) of *Streptococcus suis*. *J Clin Microbiol* 29:2590–2594.
- Kerdsin A, Dejsirilert S, Akeda Y, Sekizaki T, Hamada S, Gottschalk M, Oishi K. 2012. Fifteen *Streptococcus suis* serotypes identified by multiplex

- PCR. *J Med Microbiol* 61:1669–1672. <http://dx.doi.org/10.1099/jmm.0.048587-0>.
35. Ye C, Bai X, Zhang J, Jing H, Zheng H, Du H, Cui Z, Zhang S, Jin D, Xu Y, Xiong Y, Zhao A, Luo X, Sun Q, Gottschalk M, Xu J. 2008. Spread of *Streptococcus suis* sequence type 7, China. *Emerg Infect Dis* 14:787–791. <http://dx.doi.org/10.3201/cid1405.070437>.
36. Zhu W, Wu C, Sun X, Zhang A, Zhu J, Hua Y, Chen H, Jin M. 2013. Characterization of *Streptococcus suis* serotype 2 isolates from China. *Vet Microbiol* 166:527–534. <http://dx.doi.org/10.1016/j.vetmic.2013.06.009>.
37. Roberts IS. 1996. The biochemistry and genetics of capsular polysaccharide production in bacteria. *Annu Rev Microbiol* 50:285–315. <http://dx.doi.org/10.1146/annurev.micro.50.1.285>.



面向 21 世纪的课程教材  
Textbook Series for 21st Century

# 兽医微生物学实验指导

第二版

姚火春 主编

兽医专业用

中国农业出版社

兽医微生物学实验指导/ 姚火春主编. —2 版. —北京: 中国农业出版社, 2002. 2 (2007. 1 重印)

面向 21 世纪课程教材

ISBN 978 - 7 - 109 - 07337 - 1

I. 兽... II. 姚... III. 兽医学: 微生物学 - 实验 - 高等学校 - 教学参考资料 IV. S852.6 - 33

中国版本图书馆 CIP 数据核字 (2006) 第 143456 号

中国农业出版社出版

(北京市朝阳区农展馆北路 2 号)

(邮政编码 100125)

责任编辑 武旭峰

北京通州皇家印刷厂印刷

新华书店北京发行所发行

1980 年 10 月第 1 版

2002 年 3 月第 2 版

2012 年 6 月第 2 版北京第 11 次印刷

开本: 787mm×960mm 1/16

印张: 8.5

字数: 145 千字



中国科学院图书馆 第五版 动物植物  
 全国高等学校教材 第五版 动物植物



中国科学院图书馆 第五版 动物植物

# 兽医微生物学

Veterinary Microbiology 第五版

陆承平 主编



本书可作为高等院校动物医学专业及相关专业的教材，也可供从事兽医工作的技术人员参考。

中国农业出版社